MEKELLE UNIVERSITY

COLLEGE OF NATURAL AND COMPUTATIONAL SCIENCES

DEPARTMENT OF CHEMISTRY

MSc thesis

On

Detoxification Effect of Rosemary Leaf Powder on Repeatedly Deep-Fried Hayat Palm Oil for Potato Chip Production

Prepared By: -

ASSEFA MIESHO GEBRE ID № CNCS/PR169367/12

Under the supervision of

Advisor: Prof. ABRAHA GEBREKIDAN (PhD)
Co-advisor: KALAYOU HILUF (PhD)

January, 2025

Mekelle, Tigray

DECLARATION

I, Assefa Miesho Gebre, declare that this Thesis on "***Detoxification Effect of Rosemary Leaf Powder on Repeatedly Deep-Fried Hayat Palm Oil for Potato Chip Production"***, is my original work for the MSc degree in Analytical chemistry. It has not been submitted elsewhere, and all sources are acknowledged. This research was conducted under the supervision of Professor Abraha Gebrekidan (Advisor) and Dr. Kalayou Hiluf (Co-advisor), Department of Chemistry, College of Natural and Computational Science, Mekelle University in the academic year 2025.

ASSEFA MIESHO GEBRE	____________________	____________________
Post Graduate Student	Signature	Date

As Thesis research advisors, we at this moment certify that we have read and evaluated this Thesis prepared, under our guidance, by **Assefa Miesho Gebre** Entitled: ***Detoxification Effect of Rosemary Leaf Powder on Repeatedly Deep-Fried Hayat Palm Oil for Potato Chip Production***. We recommend that the thesis be accepted as fulfilling the criteria of the MSc thesis requirement.

Prof. ABRAHA G/KIDAN (PhD)	____________________	____________________
Advisor's name	Signature	Date
KALAYOU HILUF (PhD)	____________________	____________________
Co-Advisor name	Signature	Date

ACKNOWLEDGMENT

I would like to express my deepest gratitude to my Almighty God for providing me with the strength throughout my work. I am sincerely thankful to Mekelle University for giving me the chance to study for my Master's degree in Analytical Chemistry and for supporting my research financially. My deepest appreciation goes to my advisors, Prof. Abraha Gebrekidan (PhD) and Kalayou Hiluf (PhD), for their vital guidance, constructive feedback, and continuous support throughout my thesis work. I am also grateful to Adwa College of Teacher's Education and Educational Leadership for the opportunity they gave me to pursue my master's degree. Special thanks to my friends for sharing their insights and providing encouragement along the way.

Finally, I would like to express my gratitude to my generous family and all those who contributed, both morally and financially, to success my academy journey. Thank you from the bottom of my heart!

TABLE OF CONTENT

DECLARATION i
ACKNOWLEDGMENT ii
TABLE OF CONTENT iii
LIST OF FIGURES vii
LIST OF TABLES viii
LIST OF ABBRIVATIONS ix
ABSTRACT xi
CHAPTER-ONE 1
1. INTRODUCTION 1
  1.1. Background of the Study 1
  1.2. Statement of the Problem 2
  1.3. Objective of the Study 3
    1.3.1. General objective 3
    1.3.2. Specific Objectives 3
  1.4. Research Questions 3
  1.5. Significant of the Study 4
  1.6. Scope of the Study 4
CHAPTER-TWO 5
2. LITERATURE REVIEW 5
  2.1. Overview of Palm Oil 5
  2.2. Palm Oil and its Nutritional Standard Value 6
  2.3. Potato Chips 7
  2.4. Repeated Deep Frying of Palm Oil 7
  2.5. Factors affecting Palm oil quality 8
    2.5.1. Decomposition of Palm Oil during Frying 8

2.5.1.1. Hydrolysis 8
2.5.1.2. Oxidation 9
2.6. Health Impact of Repeated Deep-Frying PO 11
2.7. Therapeutic Applications of Rosemary 12
2.8. Reaction of Antioxidant with free radical and heavy metal 13
2.9. Physico-chemical measurement of Fried PO 15
2.9.1. Physical Parameters 15
2.9.2. Chemical Titration Methods 19
2.10. Conjugated Diene of fried palm oil 22
2.11. Application of Spectroscopy 23
2.11.1. General Concept of UV-Visible 23
2.11.2. General Concept of AAS 25
2.11.3. General Concept of GC-MS 26
CHAPTER-THREE 28
3. MATERIALS AND METHODS 28
3.1. Study Area 28
3.2. Sampling Technique 29
3.3. Chemicals 29
3.4. Apparatus 30
3.5. Instruments 30
3.6. Preparation of Rosemary Leaf Extract 30
3.7. Determination of Total Polyphenol in Rosemary 32
3.8. Repeated Deep Frying HPO Procedure 32
3.9. Physical Parameter Analysis of HPO Using Apparatus Methods 34
3.9.1. Measurement of Moisture Content Using Oven Method 34

3.9.2. Specific Gravity Measurement 34
3.9.3. Refractive Index Measurement 34
3.9.4. pH 35
3.9.5. Viscosity Measurement 35
3.10. Chemical Parameter Analysis of HPO Using Titration Method 36
3.10.1. Determination of peroxide value (PV) 36
3.10.2. Determination of Iodine Value (IV) using Hanus Method 36
3.10.3. Determination of Acid Value (AV) 37
3.10.4. Determination of Saponification Value (SV) 37
3.11. Characterization of FHPO and FHPOR Samples 38
3.11.1. Conjugated Di-ene Value Analysis 38
3.11.2. Heavy Metal Analysis 38
3.11.3. GC-MS Analysis of FHPO and FHPOR 40
3.12. Data Analysis 41
CHAPTER-FOUR 42
4. RESULTS AND DISCUSSION 42
4.1. Extraction Yields of Rosemary 42
4.2. Total polyphenol Content in Rosemary 42
4.3. Effect of Rosemary on Repeatedly Deep-Fried Cycles of HPO 43
4.4. Measurement of Physico-chemical parameters of HPO 43
4.4.1. Physical parameters of fried HPO 44
4.4.2. Chemical Parameter of Fried HPO 47
4.5. Characterization of Fried Hayat Palm Oil 51
4.5.1. Conjugated diene value Analysis using UV-visible 51
4.5.2. Chemical Composition of Rosemary 52

4.5.3. Chemical Composition of Fatty Acid in Fried Hayat Palm Oil 54

4.5.4. Heavy Metal Content in Fried Hayat Palm Oil 57

CHAPTER-FIVE 60

5. CONCLUSION AND RECOMMENDATION 60

5.1. CONCLUSION 60

5.2. RECOMMENDATION 61

REFERENCE 62

Appendix 84

LIST OF FIGURES

Figure 1: The hydrolysis of triacylglycerol in the presence of water produces free fatty acids and diacylglycerols. 9

Figure 2: The mechanism of the oxidation of triacylglycerol Via free radical mediation produces initiation, propagation, and termination. 11

Figure 3. Mechanism of triacylglycerol free radical scavenging by antioxidants 14

Figure 4: Metal chelation mechanism phenolic antioxidants. 15

Figure 5: Quercetin binds to a metal (oxidant) to form a complex ring-like structure. 15

Figure 6: The oxidation reaction of unsaturated fatty acids in triglyceride. 19

Figure 7: Chemical Reactions Involved in the IV Estimation of Oils through Hanus Method. ... 20

Figure 8: Lipids, such as linoleic acid, form a peroxyl radical ($LOO^\bullet$) in the presence of O_2. 22

Figure 9: Map of Study Area. 28

Figure 10: Maceration process to prepare rosemary leaf powder 31

Figure 11: Repeated deep-fried Hayat palm oil procedure. 33

Figure 12: GAE calibration curve for determination of total polyphenol content in RE. 84

Figure 13: Typical GC-MS total ion mass chromatograms showing the volatile chemicals found in the 99.8% methanolic extracts for extracted rosemary leaves at room temperature. ... 96

Figure 14: MS (m/z) ratio fragment for (2R,3R,4aR,5S,8aS)-2-Hydroxy-4a,5-dimethyl-3-(prop-1-en-2-yl) octahydronaphthalen-1(2H)-one(C15H24O2) Compound. 96

Figure 15: Typical GC-MS total ion mass chromatograms showing the volatile chemicals found in FHPOR at room temperature. 96

Figure 16: Typical GC-MS total ion mass chromatograms showing the volatile chemicals found in FHPO at room temperature. 97

Figure 17: Calibration graphs for all six heavy metals analyzed by AAS. 99

LIST OF TABLES

Table 1: Structures and common fatty acids found in the triglycerides of palm oil. 5
Table 2: List of standard reference methods for palm oil. 6
Table 3: Advantage and limitations of GC-MS. 27
Table 4: Result analysis of physical parameters of FHPO and FHPOR. 44
Table 5: Result analysis of chemical parameters of FHPO and FHPOR. 48
Table 6: Result analysis of the CDV of FHPO and FHPOR using a UV-visible spectrometer. .. 52
Table 7: The chemical composition of methanolic extract of rosemary leaves powder analyzed by GC-MS. 53
Table 8: Summarizes the percentage peak areas and retention times for the total fatty acid result from GC-MS (FHPOR). 55
Table 9: Summarizes the percentage peak areas and retention times for the total fatty acid result from GC-MS (FHPO). 56
Table 10: Result analysis of some selected heavy metals of FHPO and FHPOR using atomic absorption spectroscopy (AAS). 57
Table 11: Method Validation Parameters for heavy metals in FHPO and FHPOR Using AAS .. 59
Table 12: Calculation on total amount of polyphenol from gallic acid calibration line 84
Table 13: Moisture content data record using dry digital oven method for FHPO & FHPOR 85
Table 14: Specific gravity data record using pycnometer for FHPO & FHPOR.......................... 87
Table 15: Refractive index value data record using refractometer for FHPO & FHPOR 88
Table 16: pH value data record using digital PH meter for FHPO & FHPOR............................. 89
Table 17: Viscosity data record using digital viscometer for FHPO & FHPOR 90
Table 18: Peroxide value data record using titration methods for FHPO & FHPOR................... 91
Table 19: Iodine value data record using titration methods for FHPO & FHPOR....................... 92
Table 20: Acid value data record using titration methods for FHPO & FHPOR 93
Table 21: Saponification value data record using titration methods for FHPO & FHPOR.......... 94
Table 22: Result analysis of CDV for FHPO & FHPOR using UV-Visible spectrometer........... 95
Table 23: Result of heavy metals for FHPO & FHPOR using AAS spectrometer....................... 97

LIST OF ABBRIVATIONS

HPO	Hayat palm oil
PO	Palm Oil
FHPO	Fried Hayat Palm Oil without Rosemary
FHPOR	Fried Hayat Palm Oil with Rosemary
UV-visible	Ultraviolet-visible spectroscopy
ANOVA	Analysis of Variance
EU	European Union
nm	nanometer
AAS	Atomic Absorption spectroscopy
FFA	Free fatty acid
ISO	International Organization for Standardization
AOCS	American Oil Chemists’ Society
IOC	International Olive Council
FAO	Food and Agricultural Organizations
WHO	World Health Organizations
AOAC	Association of Official Analytical Chemists
ASTM	American Society for Testing and Materials
N	Normality
ppm	part per million
FAs	Fatty acids
Ƞ	Dynamic viscosity
V	Kinematic viscosity
W	Weight
C	Concentration
mPa.s	meter pascal per second
ρ	Density
g	gram
rpm	rotation per minute
Me^{n+1}	Metal ion

Df	Dilution factor
RI	Refractive index
CDV	Conjugate Diene Value
IV	Iodine value
PV	Peroxide value
SV	Saponification value
AV	Acid Value
FAME	Fatty acid methyl ester
RE	Rosemary extraction
TPC	Total polyphenol content
FCR	Folin-Ciocâlteu reagent
NIST	National institute of standards and technology
cP	Centipoise or pascal-seconds
LOD	Limit of Detection
LOQ	Limit of Quantification
CDLA	Conjugated Diene of Linoleic Acid
GA	Gallic acid

ABSTRACT

Deep-frying with vegetable oils, particularly Hayat palm oil (HPO), is widespread activity in Tigrai; Northern Ethiopia. However, frequently frying with HPO can generate harmful chemicals to health. Therefore, the purpose of this study was to assess the detoxification effect of rosemary leave powder on HPO used for the preparation of potato chips. Different frying cycles (1st, 3rd, 5th, 7th, and 9th) with and without rosemary powder were employed for frying 500 g of row potato at 180 ^{o}C in 2L of Hayat palm oil at different doses of 100,150, 200, 250, and 300 mg/kg rosemary powder for 20 min. Oil samples were taken at 1st, 3rd, 5th, 7th, and 9th frying days. The result of the analyzed physical parameters such as moisture content for fried Hayat palm oil without rosemary (FHPO) was found in the ranges of 0.73 to 1.265% while fried Hayat palm oil with rosemary (FHPOR) varied from 0.19 to 0.538% and specific gravity from 0.8906 to 0.9226% for FHPO and 0.8868 to 0.9121% for FHPOR. The refractive index for FHPO was also recorded from 1.459 to 1.547, but FHPOR was obtained in the ranges of 1.453 to 1.459. The pH values were recorded between 4.058 to 4.57 for FHPO and 4.68 to 5.814 for FHPOR. In addition, the viscosity value also ranged from 73.635 to 88.415 cP for FHPO and 48.214 to 63.741 cP for FHPOR. Among the chemical parameters analyzed, peroxide values ranged from 10.167 to 14.578 meqO_2/kg oil for FHPO and 6.463 to 9.8 meqO_2/kg oil for FHPOR, iodine values from 57.34 to 53.54 g of I_2/100g oil for FHPO, and from 45.55 to 50.465 g of I_2/100g oil for FHPOR, acid values from 0.935 to 5.61mg KOH/g oil for FHPO and from 0.186 to 0.7922 mg KOH/g oil for FHPOR, saponification values from 204.5431 to 208.508 mg KOH/g oil for FHPO and 157.129 to 203.977 mg KOH/g oil for FHPOR, conjugated diene values from 3.079 to 4.374 % for FHPO and 0.2869 to 0.6432% for FHPOR. Statistical analyses using one-way ANOVA and Tukey's test revealed significant differences ($p < 0.05$) across all studied physical and chemical parameters. GC-MS analysis also confirmed the removal of harmful chemicals such as alcohol, epoxide, ketone, and CDLA from FHPOR while oleic acid present, indicating that the oil had not decomposed. The level of heavy metal concentrations in FHPOR were found within the permissible limits (Pb: 0.01, Fe: 0.10, Cu: 0.10, Cd: 0.01, As: 0.01, Hg: 0.01) mg/100g, while FHPO exhibited higher levels (Pb: 0.10, Fe: 0.02, Cu: 0.11, Cd: 0.12, As: 0.11, Hg: 0.10) mg/100g. In conclusion, the incorporation of rosemary leaf powder into deep-frying practices significantly enhances the chemical profile of HPO by reducing toxicant chemicals and improving its oxidative stability. Generally, the present study showed the potential of rosemary as a natural additive for healthier cooking methods and improved oil quality.

***Keywords**: Hayat palm oil, frying, rosemary leaf powder, potato chips, heavy metals*

CHAPTER-ONE

1. INTRODUCTION

1.1. Background of the Study

Vegetable oils are an important part of the human diet; (Osunrinade *et al*., 2020). Among these, Hayat Palm Oil (HPO) is widely used as a cooking oil in Asia and Africa (Edo *et al*., 2022). Although HPO is cheap and commonly used, it contains saturated palmitic acid methyl ester, which is not as healthy as unsaturated oils of oleic and linoleic acid methyl ester (Gu *et al*., 2020). The process of frying with oil results in the formation of harmful compounds through chemical reactions like hydrolysis, oxidation, and polymerization (Esfarjani *et al*., 2019). These compounds adversely affect the quality and stability of the oil, impacting its physical appearance, and nutritional value (Jurid *et al*., 2020).

Furthermore, the presence of heavy metals in cooking oil, which can transfer from fryer equipment (Heshmati *et al*., 2020), such as Fe, Hg, Cd, Pb, Cu, and As, can accelerate the oxidation of unsaturated bonds in lipids, leading to produce toxic reaction products (Adeyeye *et al*., 2022). Repeated deep frying also causes the formation of secondary compounds like fatty acids, alcohol (hydroxyl), aldehyde, ketone, and epoxides which are more reactive compounds (Zhang *et al*., 2024). Consuming fried foods or rancid oils containing these harmful compounds at high dose can pose various health risks, including obesity (Pougoue *et al*., 2023), cardiovascular diseases, diabetes, cancer, and neurodegenerative diseases (Mahiran *et al*., 2023; Sikdar *et al*., 2021).

Therefore, due to health issues monitoring of oil quality is paramount to avoid the use of poor quality or contaminated oil while repeatedly frying HPO to prepare chips. Some researchers have studied the harmful effects of frying potato chips in palm oil without removing the contaminated oil (Omojola *et al*., 2020). According to Jurid *et al*., (2020), recycled palm oil is prepared by frying potato strips for up to five cycles, assessed with quality of color, density, viscosity, moisture, peroxide value, and iodine value. Based on the analysis of the rapid decomposition of peroxides and the unsaturation of the oil at high temperatures, it becomes rancid and toxic to humans. Therefore, rancid oil should be discarded after the first use. On the other hand, Moufakkir *et al.*, (2023) investigated the effect of rosemary extract in soybean oil which slow down the oxidation process effectively. Thus, rosemary extract powder (RE) ensures the high stability of soybean oil against oxidation and a longer shelf life. In addition, Borsato *et al*., (2020) studied a biodiesel samples containing Cr^{3+}, Co^{2+}, Fe^{2+}, and Fe^{3+} ions analyzed with rosemary extract and the extract was also found to be more stable than without the extract indicating that rosemary extract can hold on free radicals in biodiesel.

This research aims to address the gap in exploring the impact of rosemary leaf powder on the physicochemical properties of palm oil and the nutritional quality of potato chips, particularly in Tigrai Region of Ethiopia, where chip is widely consumed. In this Region, chip is typically fried using repeatedly reused oil, without the addition of rosemary, which may contribute to the accumulation of harmful toxicants. The study focuses on evaluating rosemary extract as a natural antioxidant to mitigate these toxicants. Accordingly, different parameters were analyzed including specific gravity, moisture content, pH, viscosity, refractive index, peroxide value, acid value, iodine value, saponification value, conjugated diene value, and some selected heavy metals (Cu, Fe, As, Hg, Cd, Pb), to assess both the quality and contamination levels of the oil.

For this purpose, different analytical and spectroscopic techniques, such as gas chromatography-mass spectrometry (GC-MS), ultra-visible spectrometry (UV), and atomic absorption spectrometry (AAS) were employed to evaluate the physicochemical parameters and heavy metals in fried HPO. Therefore, the primary objective was to mitigate the toxicity associated with repeated deep frying of HPO by incorporating rosemary extract as an antioxidant. In Addition, it was aimed to assess oil quality and contamination levels by comparing them against the national and international standards.

1.2. Statement of the Problem

Reusing oil for frying is a common practice in household cooking, particularly in the production of potato chips, which often involves frying with HPO at higher temperatures. This repeated use of oil leads to lipid peroxidation, resulting in the formation of harmful compounds that alter the oil's physicochemical properties (Nanayakkara *et al*., 2020). The fried potato chips mostly contain over 20% oil from the frying process (Yusof & Mohamad, 2019). Consequently, these secondary toxicant compounds can contribute to carcinogenicity (Duguma & Abebaw, 2020).

In recent years, oils have become commonly used for frying foods such as potato chips, and are increasingly consumed in Tigrai, Ethiopia. Among these foods, potato chips are being fried in large quantities and sold to consumers on the streets of cities. In each city many vendors of the

Tigrai Region, particularly in the cities of Mekelle, Adigrat, Axum, and Shire, about 25 women make for living by preparing and selling chips, fried in recycled oil for up to three weeks without discarding and without use of rosemary, posing significant health risks due to the accumulation of toxic substances. Despite its occurrence, no research has been conducted in this region on mitigating the toxic effects of palm oil using rosemary.

To address this issue, the solution is the use of rosemary leaf powder, a natural antioxidant, to slow lipid oxidation in frequently used frying oils. While synthetic antioxidants are commonly added to frying oils, they degrade at high temperatures and may pose health risks (Gao *et al*., 2022). In contrast, rosemary extract could prove a safer, natural alternative. This aims to explore the potential of rosemary leaf powder in reducing the harmful effects of repeatedly used HPO during the frying of potato chips (Ujong *et al*., 2023), to improve public health and promote safer cooking practices in Tigrai.

1.3. Objective of the Study

1.3.1. General objective

- ✓ To evaluate the detoxification effect of rosemary leaf powder on frequently fried HPO for potato chip preparation using titration and characterization methods

1.3.2. Specific Objectives

- ✓ To determine the physicochemical parameters of fried HPO in the presence of rosemary leaf powder
- ✓ To characterize the chemical composition, conjugated diene value (CDV), and level of heavy metals content in frequently fried HPO with and without rosemary leaf powder using GC-MS, UV-visible, and AAS, respectively.
- ✓ To compare and contrast the effects of frying HPO with and without rosemary, under standard limits of ISO, AOCS, FAO, AOAC, WHO, SON, and Codex Values.

1.4. Research Questions

Based on the above objectives, this study aimed to answer the following research questions.

- ✓ What was the absorbance of conjugated diene value (CDV) of fried HPO with and without rosemary leaf powder?

- ✓ What were the levels of heavy metal concentrations (Hg, Cd, Cu, Fe, Pb & As) presented in fried HPO before and after treatment using rosemary leaf powder?
- ✓ Did the levels of physicochemical parameters and heavy metal content decrease their toxicity after the addition of rosemary leaf powder when compare to standard limit?

1.5. Significant of the Study

This study is significant for addressing health concerns related to the use of repeatedly deep-fried HPO in potato chip preparation. By developing a detoxification method using rosemary leaf powder, the research aims to reduce lipid peroxidation in the oil, thereby improving the safety and quality of potato chips. The findings are expected to contribute to practical strategies for mitigating health risks associated with deep-fried foods.

1.6. Scope of the Study

This study focused on the detoxification of repeatedly deep-fried HPO used in potato chip production with rosemary leaf powder. The research aimed to determine the optimal concentration of leaf powder, assess detoxification efficiency through titration and characterization methods, and evaluate the physico-chemical parameters of the detoxified oil. Due to constraints in time, budget, and equipment, the study was conducted in Axum city, and intended to represent other cities in the Tigrai Region. The assessment specifically concentrated on the physicochemical properties of fried batches (1st,3rd, 5th, 7th, 9th) for both FHPO and FHPOR, as well as selected heavy metals (Hg, Cd, Cu, Fe, Pb & As) in reused HPO.

CHAPTER-TWO

2. LITERATURE REVIEW

2.1. Overview of Palm Oil

Palm oil, a widely used vegetable oil extracted from the mesocarp of the oil palm tree (*Elaeis guineensis*), consists mainly of triglycerides formed from fatty acids and glycerol, with about 95% of its composition being fatty acids (Puji *et al*., 2024). It contains essential fatty acids crucial for optimal health (Asikin *et al*., 2023) and is notable for its high vitamin E content, particularly γ-tocotrienol, a potent antioxidant (Sulaiman *et al*., 2022). Palm oil has a balanced fatty acid profile, with linoleic (10–11%), oleic (39-40%) and palmitic acid (44–45%) as the main unsaturated and saturated fatty acids, which are listed in Table 1, respectively (Izuddin *et al*., 2023).

Its rich orange color is attributed to high levels of α- and β-carotene, which comprise over 80% of its carotenoid content (Jadhav *et al*., 2022). Physically, palm oil is semi-solid at room temperature and soluble in solvents like ethanol and n-hexane, which are commonly used in extraction (Liu, 2020). Its versatility allows for applications in baking, frying, detergents, cosmetics, and medicine (Cavalcanti *et al*., 2022). Additionally, palm oil contains oleic and linoleic fatty acids, which may lower bad cholesterol and reduce heart disease (Stavila, *et al*., 2023).

However, oils rich in polyunsaturated fatty acids like palm oil are more prone when compared to those rich in mono- or saturated fats (Ahmed *et al*., 2023), highlighting the importance of considering its stability alongside health benefits in both industrial and nutritional contexts (Yılmaz *et al*., 2023).

Table 1: Structures and common fatty acids found in the triglycerides of palm oil.

Fatty acid	**Structure**	**Reference**
Palmitic acid (C16:0)	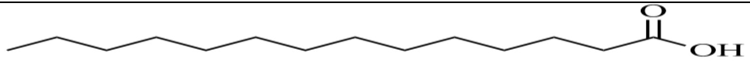	(Shotts *et al*., 2021)
Oleic acid (C18:1)	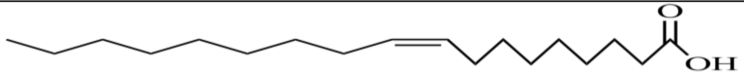	
Linoleic acid (C18:2)	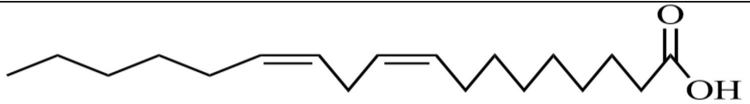	

2.2. Palm Oil and its Nutritional Standard Value

The quality of palm oil, a widely utilized vegetable oil in food and other applications, is assessed using several parameters, including physicochemical parameters, and some selected heavy metals which are listed in Table 2.

Table 2: List of standard reference methods for palm oil.

№	**Physicochemical parameters**	**Recommended value**	**validated methods by**	**Reference**
1	Moisture at 105 ^{0}C	< 0.2 % maximum in (% m/m)	ISO 662:2016; AOCS Ca 2d-25	(Hishamuddin *et al*, 2020; Purnama, *et al.*, 2020)
2	Acid value	0.6 mg max of KOH/g oil	ISO 660:2009; AOCS Cd 3d-63	
3	Peroxide value	10milliequivalents max of active O_2 per kg of oil	ISO 3960:2017, BS 684-2.14:2001, AOCS Cd 8b.90 AOAC 965.33	
4	Saponification	195-205 mg KOH per g oil	ISO 3657:2013; AOCS Cd 3-25	
5	Refractive index (RI 40 ^{0}C)	1.454 – 1.456	ISO 6320:2017; AOCS Cc 7-25: AOAC 921.08	
6	pH	5-7	Standard Organization of Nigeria (SON)	(Edo *et al.*, 2022)
7	Iodine value	45–55 (g I_2/100 g oil)	ISO 3961	(Purnama *et al.*, 2020)
			Codex Values	(MacArthur, *et al.*, 2021)
8	CDV	< 2.5 %	Codex values	(Chbani, *et al.*, 2023)
9	Specific gravity at 50 ^{0}C	0.891–0.899	WHO/FAO	(Negash, *et al.*, 2019)
10	Viscosity	50-60 cP	WHO standard	(Adelagun *et al.*, 2023)
№	**Heavy metal**	**Permissible Limit**	**validated methods by**	**Reference**
1	Lead (Pb)	Maximum 0.05 mg/g	(FAO/WHO JECFA)	(Lin *et al.*, 2024)
2	Iron (Fe)	maximum 1.5 mg/g	CODEX STAN 193-1995	(Al-Akayleh *et al.*, 2024)
3	Copper (Cu)	maximum 0.1 mg/g		

4	Cadmium (Cd)	Maximum 0.05 mg/g	(JECFAFAO/WHO.,2019)	(Wathum, 2021)
5	Arsenic (As)	Maximum 0.01 mg/g	WHO	(Enemuor *et al*., 2021)
6	Mercury (Hg)	Maximum 0.05 mg/g	FAO/WHO	(Code, 2021)

2.3. Potato Chips

Potato scientifically referred to as *Solanum tuberosum*, is a highly valuable and commonly consumed source of carbohydrates. Their nutritious value and adaptability make them one of the most popular foods in the world (Yaghi *et al.*, 2022). It is a great supply for human nutrition as a source of energy. Their dry weight is mostly made up of starch, with the remaining 60–80% being made up of carbohydrates. Potatoes are not only a good source of carbohydrates but also a full protein source (Tolessa *et al*., 2019). Potatoes provide high-quality protein, despite having a comparatively low protein content when compared to other dietary crops. Despite being low in fat, it is still rich in vital nutrients. They have potassium, vitamin C, and vitamin B6 among other vitamins and minerals. The Food and Agriculture Organization (FAO) reports that potatoes rank as the world's fourth most important crop and play a vital role in the world's food supply (Beals, 2019). Made by deep-frying sliced potatoes in vegetable oil to a temperature higher than the boiling point of water (180°C), potato chips are a widely consumed snack across the globe. Because the water in the potatoes evaporates during the frying process, the end product has more than 20% oil, mostly from the frying process (Yusof & Mohamad, 2019).

2.4. Repeated Deep Frying of Palm Oil

Foods can be fried using various vegetable oils, with palm oil being a popular option in Ethiopia due to its favorable frying qualities and low cost (Chathiran *et al*., 2024). (Mahmud *et al*., 2023), among frying oils, palm oil stands out for its distinct fatty acid makeup and high smoke point of 230 ˚C. However, the increased use of palm oil raises concerns about the long-term health effects of its frequent use. Research indicates heating palm oil at different frying cycles can accelerate the oxidation of fatty acids, leading to the degradation of beneficial components, like α-tocopherol and γ-tocotrienol, compared to other types of oil (Amsalu *et al*., 2020). Essential fatty acids, especially those in the omega-6 family, are crucial for maintaining cell integrity and controlling physiological processes, such as inflammation, reproduction, and heart health. During deep-frying, these fatty acids can break down, producing off-putting aromas (Demgne *et al*., 2023).

Deep-frying involves submerging food in hot oil at a recommended maximum temperature of 180°C (Patil *et al*., 2023; Yılmaz *et al*., 2023). However, repeated deep frying causes oil to oxidize, leading to the formation of hydroperoxides and a range of hazardous secondary compounds, such as alcohols, aldehydes, ketones, acids, and epoxides (Erickson *et al*., 2023).

2.5. Factors affecting Palm oil quality

The quality of frying oil is influenced by various factors, including the frying temperature, frying time, the presence of heavy metals, equipment used in frying, the type of oil used in frying, the presence of additives, and the structure of the fried food are the main factors affecting these reactions (Yildiz *et al*., 2024; Yılmaz *et al*., 2023). Repeated deep frying can lead to issues such as stickiness, foaming, darkening, and the overall degradation of the oil. For instance, fryer metals made from copper or iron can accelerate the oxidation process of the frying oil (Madhujith & Sivakanthan, 2019).

2.5.1. Decomposition of Palm Oil during Frying

Chemical reactions such as oxidation, hydrolysis, and polymerization occur when oil is heated during frying. These reactions change the physicochemical properties of the oil (Sikdar *et al*., 2021).

2.5.1.1. Hydrolysis

Hydrolysis of Esters in diglycerol and fatty acids forms the basis of fats and oils, with triglycerides being tri-esters composed of three fatty acids linked to a glycerol molecule. During frying, water/moisture, steam, and oxygen cause chemical reactions in both the oil and food, leading to the hydrolysis of triglycerides into diglycerides, mono-glyceride, glycerol, and free fatty acids as shown in Figure 1 (Yadav *et al*., 2023). Water acts as a weak nucleophile, attacking the ester bonds in triglycerides, which increase the concentration of FFAs as critical indicators of oil quality. As food is cooked, the interaction between water and oil accelerates hydrolysis, particularly with short-chain fats (Abeshu, 2023). The hydrolysis process is influenced by factors such as oil temperature, the area contacts between oil and water, and the presence of moisture, with glycerol partially evaporating at a temperature of 150 ^{0}C. The resulting FFAs can impact off-flavors and degrade the oil's stability and quality, making it unsuitable for further frying (Mathew, 2021).

Therefore, monitoring the FFA content, typically between 0.05% to 0.08%, is essential for assessing frying oil quality. Ultimately, the breakdown products of hydrolysis not only accelerate oxidation but also shorten the oil's fry life (Abeshu, 2023).

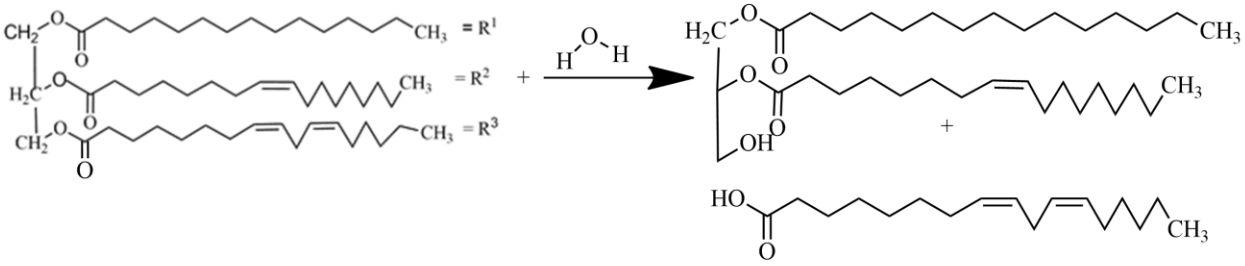

Figure 1: The hydrolysis of triacylglycerol in the presence of water produces free fatty acids and diacylglycerols (Erickson *et al*., 2023).

2.5.1.2. Oxidation

Edible oils, like palm oil, undergo autoxidation during frying due to the reaction between oxygen and unsaturated fatty acids, producing various products (Chew, 2021). This process involves lipid radical-initiated chain reactions, particularly at frying temperatures between 150 and 190°C, which promote peroxide formation and the oxidation products' subsequent polymerization processes (Fatima *et al*., 2023). The energy needed to release hydrogen depends on the fatty acids present, especially from allylic carbons near double bonds, leading, to the production of conjugated dienes as a stabilizing mechanism as shown in Figure 2 (Chew, 2021).

The initiation begins when unsaturated fatty acids (RH) lose hydrogen adjacent to double bonds, forming highly reactive carbon radicals ($R^\bullet$) due to exposure to high temperature, light, humidity, or metal ions (Flores *et al*., 2021). Heavy metals like Fe^{3+} and Cu^{2+}, can catalyze this oxidation, generating alkyl and peroxyl radicals, which produce non-volatile compounds such as aldehydes and ketones (Zaghi *et al*., 2019). This process results in the production of polymers and darker-colored oils as frying cycles and temperatures increase (Haider *et al*., 2023).

During propagation, lipid radicals ($ROO\bullet$) abstract hydrogen from RH, forming new radicals and hydroperoxides (ROOH), which can further decompose into secondary oxidation products like alcohols, and shorter-chain carboxylic acids (Valle *et al*., 2024). The resulting compounds can undergo reactions like aldol-condensation and polymerization, negatively impacting oil quality parameters such as viscosity and acid value (Amran *et al*., 2022).

In the termination phase, radicals can self-interact to form non-radical species, including dimers or trimers of oxidized lipids (ROOR). Notably, deep-frying oil generates toxic secondary compounds, including epoxides (C-O), hydroxyls (-OH), and ketones (C=O), which are potentially harmful (Grootveld, 2022). Free radical chain reaction R-O• with unsaturated fatty acid to form epoxide, hydroxy, and ketone (Zhang *et al*., 2024). Hydroxyl compounds such as hydroperoxides are linked to inflammation and oxidative stress in the body (Stavila *et al*., 2023). The epoxidation process occurs directly at the double bond of fatty acids, producing hydroxy and carbonyl glycerides, with linoleic acid primarily forming di-epoxides and oleic acid mono-epoxides (González *et al*., 2021).

Imitation: $\mathrm{RH} + \mathrm{HO}^{\bullet} \rightarrow \mathrm{R}^{\bullet}$ Eq (1)
$\mathrm{R}^{\bullet} + \mathrm{O2} \rightarrow \mathrm{ROO}^{\bullet}$ Eq (2)
$\mathrm{Me}^{\mathrm{n}+} + \mathrm{ROO}^{\bullet} \rightarrow \mathrm{Me}^{\mathrm{n}+1} + \mathrm{RO}^{\bullet} + \mathrm{OH}^{\bullet}$ Eq (3)
$\mathrm{Me}^{\mathrm{n}+1} + \mathrm{ROOH} \rightarrow \mathrm{Me}^{\mathrm{n}+} + \mathrm{ROO}^{\bullet} + \mathrm{H}^{\bullet}$ Eq (4)
Propagation: $\mathrm{RH} + \mathrm{ROO}^{\bullet} \rightarrow \mathrm{R}^{\bullet} + \mathrm{ROOH}$ Eq (5)
Termination: $\mathrm{R}^{\bullet} + \mathrm{R}^{\bullet} \rightarrow \mathrm{R} - \mathrm{R}$ Eq (6)
$\mathrm{R}^{\bullet} + \mathrm{ROO}^{\bullet} \rightarrow \mathrm{ROOR}$ Eq (7)
$\mathrm{ROO}^{\bullet} + \mathrm{ROO}^{\bullet} \rightarrow \mathrm{ROOR} + \mathrm{O}_2$ Eq (8)

Where RH represents to linoleic acid, $\mathrm{R}^{\bullet}$= free radical (alkyl), $\mathrm{RO}^{\bullet}$=alkoxyl radical, $\mathrm{ROO}^{\bullet}$ = peroxyl-radical, and ROOH = hydroperoxide (Valle *et al*., 2024; Amran *et al*., 2022).

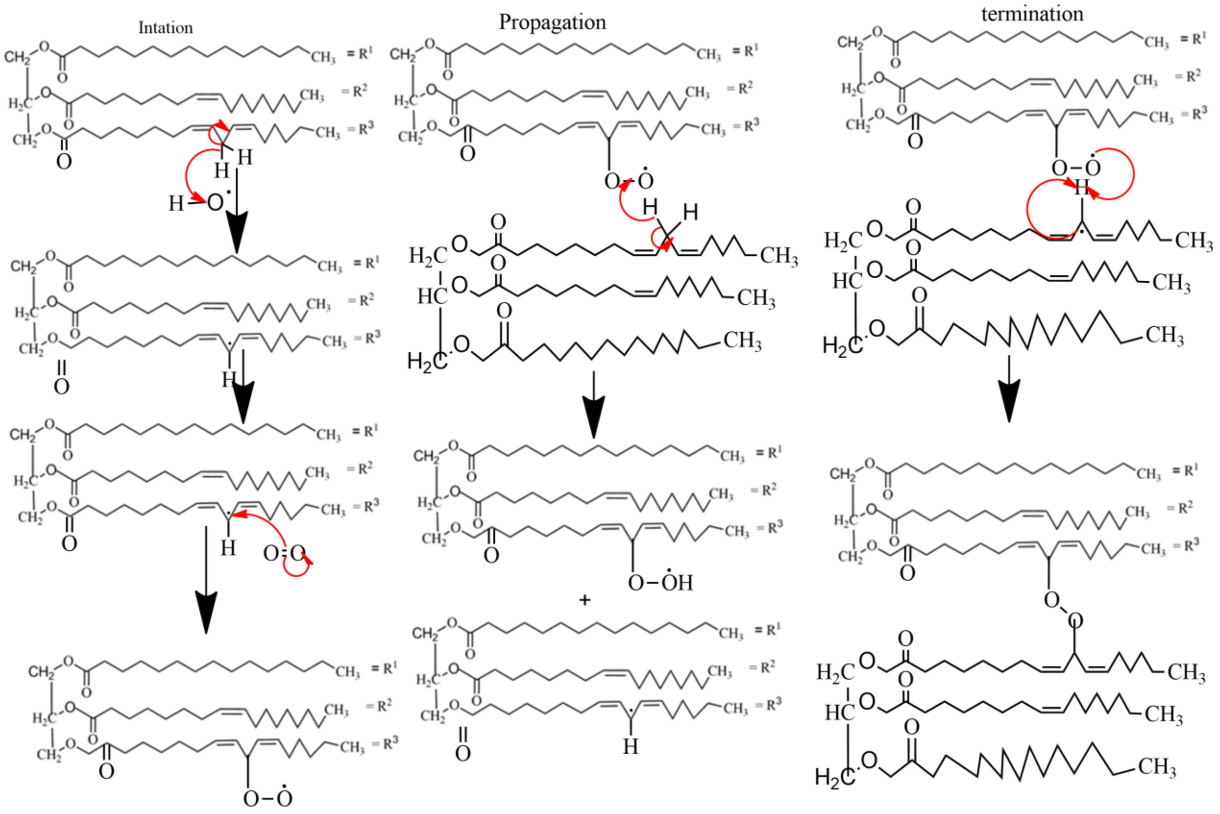

Figure 2: The mechanism of the oxidation of triacylglycerol Via free radical mediation produces initiation, propagation, and termination (Erickson *et al*., 2023).

2.6. Health Impact of Repeated Deep-Frying PO

Consumers are choosing deep-fried foods like potato chips due to their appealing qualities, including palatability, color, flavor, and texture (Ujong *et al*., 2023). Nevertheless, this cooking method generates harmful byproducts such as peroxides, ketones, aldehydes, alcohols, free radicals, and epoxide which can lead to rancid tastes and odors from oxidation at n-6 double bonds (Mohammadi *et al*., 2021). Repeated frying can introduce anti-nutritional properties, particularly through substances like epoxides, which are associated with potential health risks, including genotoxicity, skin irritation, respiratory issues, and carcinogenic effects (Dangal *et al*., 2024). Harmful ketones, such as acrolein can cause carcinogenic, liver and kidney damage, neurological problems, and metabolic abnormalities (Lozano *et al*., 2022). Long-term exposure to oxidized lipids can produce free radicals, increasing the risk of chronic diseases, like cancer, inflammatory disorders, and heart problems (Dangal *et al*., 2024). Frequent consumption of fried foods (four or more times a week) is associated with serious health problems such as cancer, heart disease, type

2 diabetes, premature aging, obesity, pancreatitis, and gastrointestinal disorders (Alexandre *et al*., 2022; Valle *et al*., 2024).

Additionally, fried foods may contain heavy metals like lead (Pb), iron (Fe), copper (Cu), cadmium (Cd), arsenic (As), and mercury (Hg), which can damage vital organs, including the kidneys, brain, liver, skin, and heart (Abdullahi *et al*.,2023). The presence of these heavy metals is linked to adverse health outcomes such as immune suppression, chemical sensitivity, breast cancer, reduced sperm count, and infertility. Ultimately, the consumption of rancid oil from frying is associated with elevated cholesterol, pancreatitis, gastrointestinal issues, lung damage, cancer, cardiovascular disease, type 2 diabetes, accelerated aging, and obesity (Ukwo, 2024).

2.7. Therapeutic Applications of Rosemary

The quality and nutritional content of frying oil can deteriorate with repeated use, negatively impacting health (Jurid *et al*., 2020). To enhance oxidation stability, antioxidants are added, with natural options like barley, sage, and rosemary preferred over synthetic alternatives due to their efficacy and health benefits. Extracts from cinnamon and rosemary, particularly rosemary (*Rosmarinus officinalis*) have been shown to extend the shelf life of palm oil (Nanayakkara *et al*., 2020). Rosemary extract, obtained through solvent maceration with acetone, water, ethanol, and methanol is rich in phenolic compounds such as flavonoids, diterpenoids, triterpenoids, and lignans (Alexandre *et al*., 2022).

These phenolic compounds possess strong antioxidant properties, the ability to scavenge free radicals, and metal chelators, which can help prevent diseases like cancer, diabetes, neurological diseases, and cardiovascular diseases (Jeruto *et al*., 2024). Rosemary extract also contributes to the prevention of food's color, flavor, and nutrition content (Girish *et al*., 2023). Its application spans various industries, including food, cosmetics, and perfumes, where it aids in product preservation, oil stabilization, and flavor enhancement (Zheng, *et al*., 2019). The European Union (EU) recognizes rosemary extract (E392) as safe and effective food preservation, while synthetic antioxidants butylated hydroxy anisole (BHA), butylated hydroxytoluene (BHT), and tert-butylhydroquinone (TBHQ), are limited due to potential toxicity (Fotiadou *et al*., 2024; Sarmah *et al*., 2020).

Research indicates that rosemary extract added at 200 mg/kg, is more effective than synthetic antioxidants in reducing the deterioration of soybean during frying (180 ˚C and 2 h) (Li *et al*., 2023). In another study found by Guo *et al*., (2023), the optimal level of rosemary extract (RE) for storage stability ranges from 50–200 mg/kg, demonstrating efficacy compared to synthetic antioxidants alternatives and stability at high temperatures (190-240 °C) (Gao *et al*., 2022). Rosemary's primary antioxidants and particularly effective at scavenging free radicals and halting oxidation chain reactions, such as delaying or stopping its propagation stage (Ginsburg & Maleky, 2020). Furthermore, increasing ethanol concentration and extraction time can enhance polyphenol content in rosemary, reaching a maximum of 24.14 mg GAE/g, achieved using 80% ethanolic solution at 70 ˚C for 60 min (Vella & Laratta, 2023). The medicinal properties of rosemary are attributed to its bioactive compounds, including caffeic acid, rosmarinic acid (RA), ursolic acid (UA), carnosic acid (CA), and carnosol, along with essential minerals like calcium (Ca), phosphorus (P), potassium (K), sodium (Na), iron (Fe) and zinc (Zn) (Makhamra, 2023: Nik *et al*., 2022). In addition to findings by Zhao *et al*., (2020) and Ayoola *et al*., (2020), methanolic extracts of rosemary leaf powder contain phenolic antioxidants that are effective scavengers of free radicals. These compounds demonstrate various biological activities, including antimicrobial agents, antiviral activities, antifungal, and antibacterial. They also have potential applications as pesticides, cancer drugs, food additives, and herbicides such as 2,4-Di-tert-butylphenol (2,4-DTBP). Another significant compound is (2R,3R,4aR,5S,8aS)-2-Hydroxy-4a,5-dimethyl-3-(prop-1-en-2-yl) octahydronaphthalen-1(2H)-one also known as Santalcamphor. This compound likely exhibits antioxidant properties due to its hydroxyl group (-OH), which enables it to participate in antioxidant mechanisms by scavenging free radicals.

2.8. Reaction of Antioxidant with free radical and heavy metal

Polyphenolic compounds are vital antioxidants that can compact oxidative damage in food through various mechanisms. They primarily function as hydrogen donors, metal ion chelators, free radical scavengers, and singlet oxygen quenchers (Lee *et al*., 2020). Specifically, polyphenols neutralize free radicals via two main processes: hydrogen atom transfer and electron transfer. In hydrogen atom transfer, an antioxidant (AH) donates a hydrogen atom to a free radical (R•), a more stable radical (A•) and a reduced free radical (RH), thereby halting the formation of toxic lipids peroxides as shown in Figure 3. ($R\bullet + AH \rightarrow RH + A\bullet$) (Viana *et al*., 2022). After deep-fried, polyphenolic compounds continue to exert antioxidative effects by capturing harmful aldehydes, delaying polymerized triacylglycerols (TAGs) formation, and stopping the oxidation chain reactions (Viana *et al*., 2022).

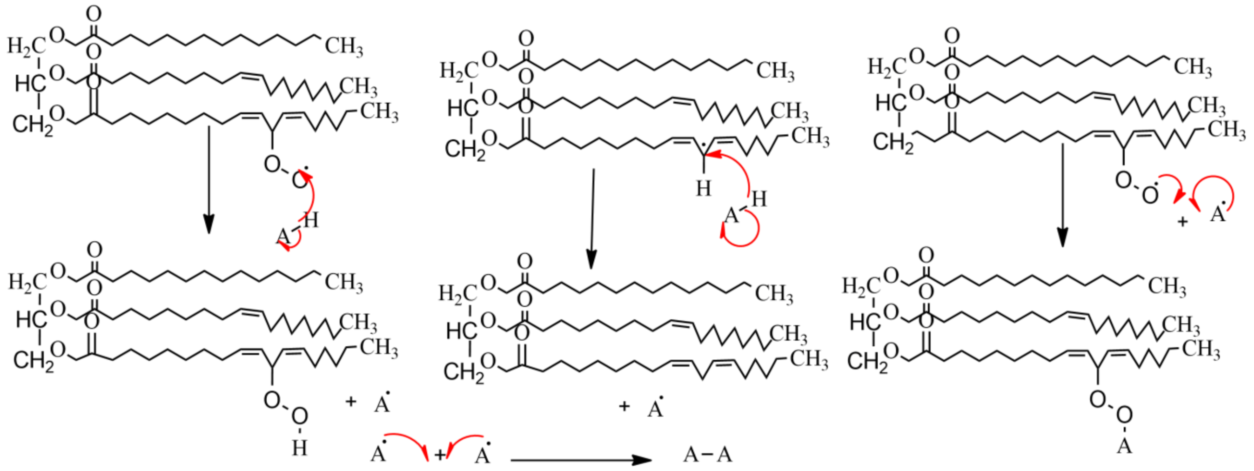

Figure 3. Mechanism of triacylglycerol free radical scavenging by antioxidants

Electron transfer involves the antioxidant providing an electron to the free radical, stabilizing it, and preventing further oxidative damage as shown in Figure 4 and 5 (Nieto *et al*., 2023). Additionally, they chelate metal ions such as Fe^{2+}, Fe^{3+}, Cu^{2+}, and Cu^{+}, forming stable complexes that inhibit metal-catalyzed oxidation (Wang *et al*., 2023). The chelating ability of phenolic compounds extends to various transition metal ions, such as Hg, Pb, Cu, Zn, Cd, Ni, Fe, As, and Sb, especially in their anion form (Pirzadah, *et al*., 2019). Furthermore, phenolic compounds stabilize free radicals through resonance delocalization, preventing them from attacking stable molecules. Common types of phenolic compounds including volatile oils, flavonoids, phenolic acids, and phenolic di-terpenes, with their antioxidant effectiveness influenced by the arrangement of hydroxyl (OH) groups around the aromatic ring (Ginsburg & Maleky, 2020). In the molecular structure, complexation takes place with the C-3 and C-5 hydroxyl groups as well as the di-hydroxyl groups in the B ring (Bouizgma *et al*., 2023). Overall, due to their diverse mechanisms metal ion chelation, radical scavenging, and stabilization polyphenolic compounds are excellent antioxidants, playing a significant role in maintaining food quality and extending shelf life (Wang, *et al*., 2023).

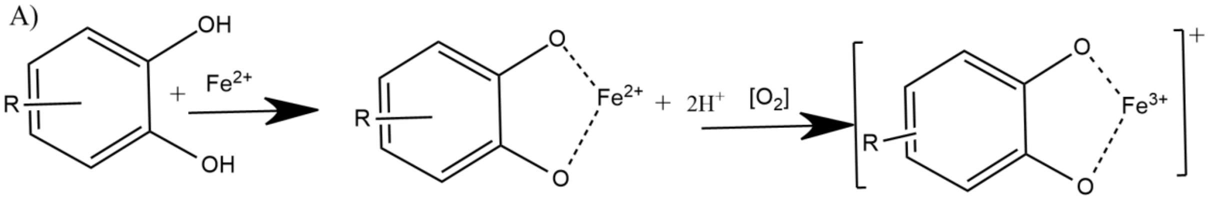

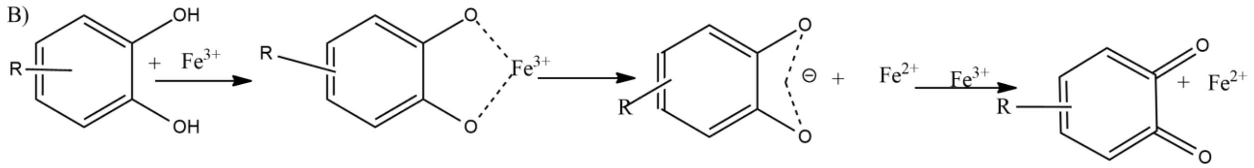

Figure 4: Metal chelation mechanism phenolic antioxidants.

A) coordination of Fe^{2+} by polyphenols and subsequent electron transfer reaction in the presence of oxygen generating the Fe^{2+} polyphenol complex: B) coordination of Fe^{3+} by polyphenols, subsequent iron reduction and semi Quinone of formation (partially oxidized polyphenol), and reduction of Fe^{3+} to form a Quinone (fully oxidized polyphenol) species and Fe^{3+}; R=H or OH (Wang *et al.*, 2023).

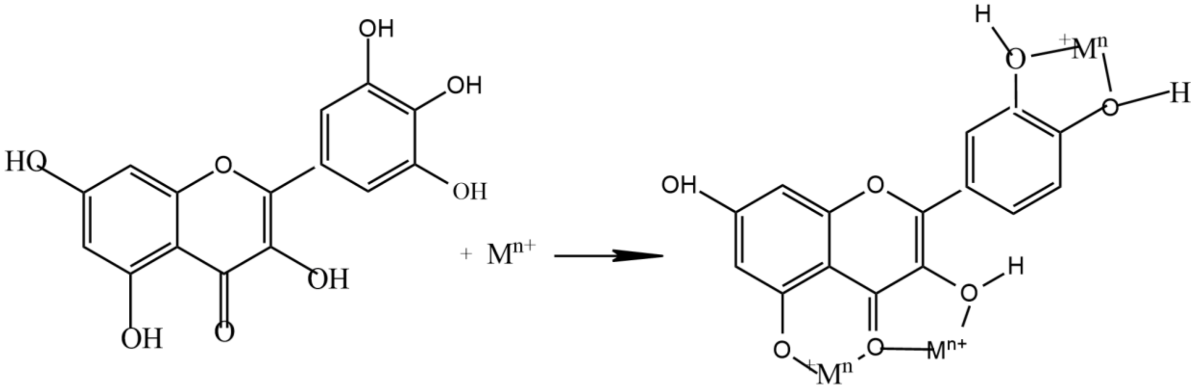

Figure 5: Quercetin binds to a metal (oxidant) to form a complex ring-like structure (Beya *et al.*, 2021).

2.9. Physico-chemical measurement of Fried PO

2.9.1. Physical Parameters

The degradation of frying oil can be monitored through various physical measurement techniques that assess indicators such as refractive index, pH, moisture content, viscosity, and specific gravity. These parameters provide immediate insights into the frying oil's quality and are quick and easy to measure (Abiodun *et al.*, 2020).

2.9.1.1. pH value

The pH of fresh vegetable oils typically ranges from 5 to 7, reflecting their weak acid. However, during frying, the pH decreases due to the hydrolysis of triglycerides into free fatty acids (FFAs) and glycerol, which influences the oil's acidity. This reduction in pH can also on the specific food being fried (Edo *et al*., 2022). Oils with low pH values are often rancid and unsafe for consumption, as the degradation of long-chain fatty acids into short-chain compounds produces highly acidic byproducts that contribute to a rancid taste. Both raw and fried oil can be measured using the AOAC (1984) method, employing a pH meter calibrated at pH 4 and 7. Samples are prepared by mixing oil with hot distilled water and cool in a cold-water bath to 25˚C (Bikila *et al*., 2020). A higher acidity level indicates a significant breakdown of fatty acids frying, consistent with findings by (Benmeziane *et al*., 2024), who reported decreased pH values in soybean and corn oil due to FFA release during repeated frying, catalyzed by vapors, oxygen, and water from the fried potato.

2.9.1.2. Refractive index (n_D^{30} or RI)

Refractive index (RI) is a crucial property that indicates how light passes through a material, offering insights into its chemical composition and oil quality during multiple frying cycles (Ahmed *et al*., 2021). Several factors influence the RI of frying oils, including molecular weight, fatty acid chain length, degree of unsaturation, and degree of conjugation. The RI is determined using the AOCS method (1989) with a digital refractometer set to room temperature. Research indicates that longer fatty acid chains and a higher degree of unsaturation increase the RI. For instance, the RI values for edible palm oil range from 1.454 to 1.456 (Flores *et al*., 2021). To obtain accurate results, it is necessary to determine the refractive index at a specified calibration temperature using the appropriate formula:

$$\boxed{R = R^1 + K(T^1 - T)} \qquad \text{Eq. (9)}$$

Where R=Refractometer reading reduced to specified temperature T °C, R^1=Reading at T^1 °C, K=constant 0.000365 for fats and 0.000385 for oils (usually 40°C) (Ayouaz *et al*., 2022).

2.9.1.3. Moisture content

Moisture is transferred from food to oil during frying, resulting to water loss from the food and an increase in the oil's moisture content, which affects various physicochemical properties (Liyansan *et al*., 2022; Yildiz *et al*., 2024). the quality of palm oil for deep frying is determined by its initial characteristics, high-grade palm oil exhibiting low free fatty acids and moisture content, very low levels of contaminants, and an excellent bleachability index (Mahmud *et al*., 2023). The moisture content of the oil is measured by the mass lost when the sample is heated to a specific temperature (105 ± 10 °C) (Nizam & Mahmud, 2021). Excess moisture can contaminate the oil, increasing FFAs, and causing flavor loss and rancidity (Yusof & Mohamad, 2019). Continued frying raises moisture content due to oxygen exposure and excess water transfer from potatoes to oil, potentially leading to hydrolytic rancidity (Moufakkir *et al*., 2023). High moisture levels are linked to chemical reactions such as polymerization, oxidation, and accelerating degradation and forming harmful substances (Alzaa *et al*., 2021; Dodoo *et al*., 2022). For example, in a study of palm oil, Initial moisture content increased from 0.08% to 0.61% after the third frying cycle, attributed to moisture transfer from the potato chips to the oil (Anwar *et al*., 2024). The moisture content of the oil affects the frying process, with high levels leading to foaming and splattering, while prolonged frying further, the oil becomes more saturated with moisture, degrading its quality and flavor. The relationship between the initial moisture content of the food and the oil content is significant, influencing both oil absorption and the overall frying outcome (Yadav *et al*., 2023). The mass (g) of the dried oil sample was then calculated by subtracting the mass of oil plus crucible after heating from the mass of oil plus crucible before heating (Kamanula *et al*., 2022). The moisture content of oil is calculated according to the equation:

$$\boxed{\%\ \text{Moisture content} = \left(\frac{w_2 - w_3}{w_2 - w_1}\right) \text{X}\ 100\ \%} \qquad \text{Eq. (10)}$$

where, W_1 = Weight of container (g), W_2 = Weight of container and sample before drying (g), W_3 = Weight of container and sample after drying (g).

2.9.1.4. Relative density or specific gravity

The quality and purity of edible oils are significantly influenced by their specific gravity, which measures the density of a material relative to water (Ahmed *et al*., 2021). Specific gravity reflects of oil the mass per unit volume of oil and is used as an indicator of purity, determined through a gravimetric method that compares the weight of oil to an equivalent volume of water (Ondo *et al*., 2021). Factors like the fatty acid composition and storage temperature affect oil density, with specific gravity expressed without units. longer fatty acid chains correlate with higher molecular mass while increasing temperature generally results in lower specific gravity. According to Codex (2017), palm oil has a relative density ranging from 0.891 to 0.899 at 25 °C. The increase in densities with frying cycles is attributed to the formation of higher molecular-weight polar compounds due to polymerization reactions during repeated frying (Chowdhury, 2023). This increase depends on factors like temperature, the number of frying cycles, and the composition of the samples used, as noted by Nduka *et al*., (2021), who observed a progressive increase in the density of refined, bleached, and deodorized palm oil (RBDPO) from the first to the fifth cycle involving potatoes. The degradation during frying due to hydrolysis, oxidation, and polymerization affects the compound. A high specific gravity often indicates lower oil content, whereas a low specific gravity suggests higher purity, implying that oil with high specific gravity contains fewer impurities (Iloamaeke *et al*., 2024). Specific density is calculated as:

$$\boxed{\text{Specific gravity} = \frac{w_1 - w_2}{w_2 - w_0}} \qquad \text{Eq. (11)}$$

Where, W_0 = weight of dry empty density bottle, W_1 = weight of density bottle + oil, and W_2 = weight of density bottle + distilled water (Maduako *et al*., 2022).

2.9.1.5. Viscosity

Oil viscosity quantifies how resistant to shear or flow and is measured according to ASTM D2270 (Pathmasiri & Perera, 2020). It can be expressed as kinematic viscosity (v) and dynamic viscosity (η) measured using a Brookfield dial reading viscometer with a big cylindrical spindle number 02 (Daniel *et al*., 2021). Low viscosity indicates low flow resistance, while high viscosity signifies greater flow resistance. Temperature affects viscosity; high temperature improves molecular mobility and reduces viscosity. Additionally, the unsaturation of fatty acids decreases viscosity due to double bonds making bonding more rigid and rotation between C-C bonds more active (Sikdar *et al*., 2021).

Viscosity stability serves as an indicator of oxidative stability, measured at a shear rate of 0-100 s^{-1} (Jadhav *et al*., 2022). Direct readings of the dynamic viscosity value (mPa.s or Pa. s, or pascal second) were obtained from the viscometer, which was kept at a steady 25°C (Zhou *et al*., 2024). In the previous study, Saleh *et al*., (2021), observed results between fresh and in-use oil, in-use oil showed higher viscosity than fresh oil, with increased frying cycles. This increase is linked to polymerization and fatty acid length, indicating oil degradation. For instance, viscosity rises from 48.4 cP at the 5th frying cycle to 68.76 cP at the 20th cycle (Assefa *et al*., 2024). Higher viscosity results from the accumulation of polymeric compounds and affects how adherers to fried foods

(Yadav *et al*., 2023). The recommended maximum viscosity range is 50 to 60 cP (Adelagun *et al*., 2023). kinematic viscosity mathematically expressed as meter square per second ($mPa.s/m^2/s$) as:

$$\boxed{\text{Kinematic Viscosity of oil (v)} = \frac{\eta oil}{\rho oil}} \qquad \text{Eq. (12)}$$

Where: η_{oil} is dynamic viscosity (mPa.s or Pa.s), while ρ_{oil} is density at a constant temperature of 25°C (0.899-0.92 g/ml) (Redzuan *et al*., 2023).

2.9.2. Chemical Titration Methods

2.9.2.1. Peroxide value (PV)

The peroxide value (PV) measures the formation of peroxide or hydro-peroxide compounds during the initial oxidation of fats or oils, (Rahman, *et al*., 2023) serving as an essential indicator of freshness, rancidity, and shelf life. According to Codex (2017) and IOC (2019b), the maximum PV for palm oil is 10 meq O_2/kg of oil. Hydro peroxides, primarily oxidation products, break down at 180°C, producing both volatile and non-volatile secondary products. Lipid oxidation follows three main steps: initiation, propagation, and termination (Yusof & Mohamad, 2019). When unsaturated fatty acids oxidize, unstable peroxide molecules form, subsequently reacting to produce ketones and aldehydes, leading to rancidity. This process occurs when oxygen reacts with fatty acid double bonds in triglycerides, resulting in peroxide formation (Figure 6).

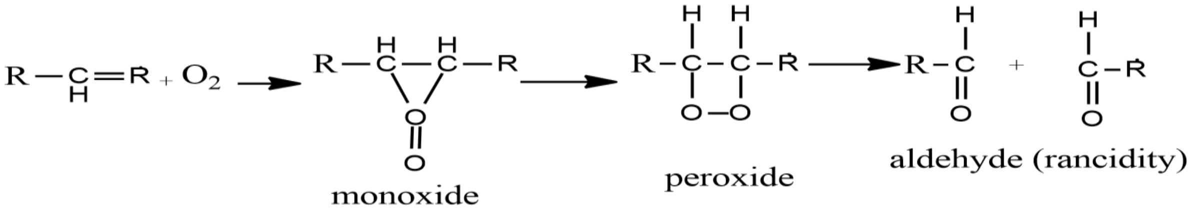

Figure 6: The oxidation reaction of unsaturated fatty acids in triglyceride (Fajriati *et al*., 2023).

A lower PV indicates better oil quality, measured by the iodine produced from the reaction of peroxides with iodide ion

$2I^- + H_2O + HOOH \rightarrow HOH + 2OH^- + I_2$………………………. ………………………. Eq.(13)

The base produced in this reaction is absorbed by the excess acetic acid present. The released iodine is titrated with sodium thiosulfate.

$2S_2O_3^{2-} + I_2$ (purple) $\rightarrow S_4O_6^{2-} + 2I^-$ (colorless)……… ……………………………………Eq.(14)

(Asouzu *et al*., 2023; Daniel *et al*., 2024).

$$\boxed{PV = \frac{Vs \times N \times 1000}{\text{Weight of sample (g)}}} \quad \text{Eq. (15)}$$

where, Vs= volume of $Na_2S_2O_3$ for sample, w= weight of sample (g) and N= 0.01N concentration of $Na_2S_2O_3$ (Liyansan *et al*., 2022).

2.9.2.2. Iodine value (IV)

The iodine value (IV) measures the degree of unsaturation or the average number of double bonds in the fatty acids of fats and oils (Multari *et al*., 2019). It is defined as the grams of iodine that can be added to 100 grams of oil. This value serves as an assessment of the oil's stability against oxidation, with a lower value indicating enhanced stability during storage. The analysis entails dissolving a precise quantity of fat or oil in a solvent and reacting it with an excess of iodine or another halogen that reacts with the carbon-carbon double bonds. Higher iodine values indicate a greater extent of unsaturation. With prolonged frying time, the iodine value tends to decrease due to sharp oxidation rates. The Hanus method is commonly utilized to determine the iodine value, involving titration with sodium thiosulfate as the titrant and starch as the indicator. This analytical method facilitates the formation of di-iodo alkanes through a chemical reaction (Flores *et al*., 2021). Any excess unreacted IBr reagent is subsequently converted to molecular iodine by treatment with KI. Then, the IV is estimated from the difference of this value from that obtained for blank and using the below reaction in Figure 7.

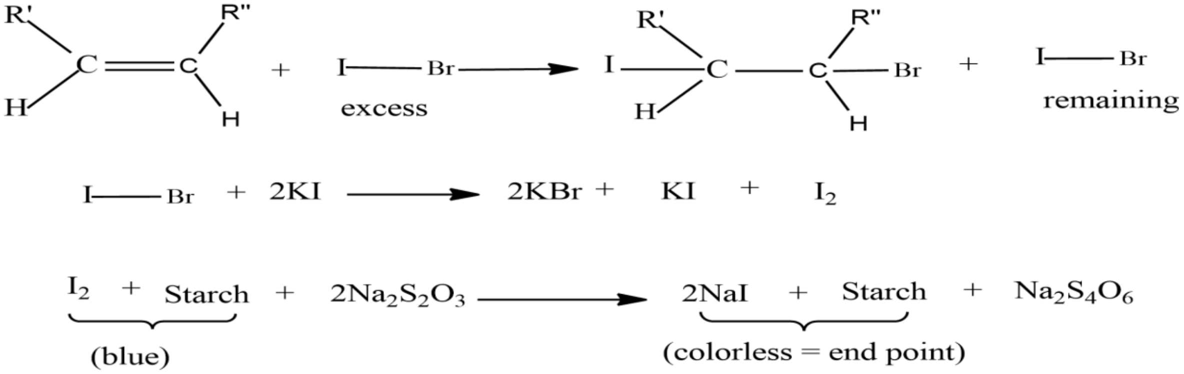

Figure 7: Chemical Reactions Involved in the IV Estimation of Oils through Hanus Method (Pulassery *et al*., 2022).

Iodine value (IV) was calculated using the expression; Blank titration was also performed: -

$$\boxed{IV = \frac{12.69 \, x \, N \, x \, (V_2 - V_1)}{W}} \quad \text{Eq. (16)}$$

Where, N = normality of sodium thiosulphate ($Na_2S_2O_3$), V_2 = volume of $Na_2S_2O_3$ solution in mL used for sample, V_1 = volume of $Na_2S_2O_3$ solution in mL used for bank, W = weight of sample in grams 12.69 = used to convert from Eq (16). thiosulphate to grams of iodine. (M_W of iodine is 126.9) (Yusof & Mohamad, 2019).

2.9.2.3. Acid value (AV)

The quantity of fatty acids that have been hydrolyzed from triacylglycerol or generated as a result of rancidity is indicated by the acid value, sometimes referred to as the free fatty acid value. It is defined as the amount of potassium hydroxide, expressed in milligrams, required to neutralize the free acids found in one gram of fat or oil (Omozuwa *et al.*, 2023). The acid value is used to determine whether the oil is suitable for ingestion and how rancid it is. It is commonly stated as palmitic, oleic, and linoleic acid and is expressed as a percentage of free fatty acids. Triglycerides hydrolyze and produce free fatty acids as byproducts. Fry oil undergoes a hydrolysis reaction that raises the amount of free fatty acids. These acids are made up of small molecules that can be volatile or break down at high temperatures, which lowers the amount of free fatty acids (Liu, 2020). Using phenolphthalein as an indicator, titration with sodium hydroxide or potassium hydroxide is frequently used to determine the free fatty acid concentration. Determination of free fatty acids (FFAs) content using the equation:

$$\boxed{\text{Acid value } \left(\text{mg}\frac{\text{KOH}}{\text{g}}\right) = \frac{(\text{Vs}-\text{Vb})\text{x M x } 56.1}{\text{w}}} \qquad \text{Eq. (17)}$$

where Vs and V_b are volumes of titrant used for the sample and blank, respectively. M is the molarity of the titrant solution and W is the weight of the sample (in g) (Munir *et al.*, 2021; Patil *et al.*, 2023).

2.9.2.4. Saponification value (SV)

The saponification value is a measurement that indicates the amount of alkali required to saponify a given quantity of fat or oil. It is expressed in milligrams of potassium hydroxide (KOH) needed to saponify 1 gram of the sample. Saponification is the process of treating triglycerides with alkali, resulting in the breakdown of the triglycerides into glycerol and fatty acids (Flores *et al.*, 2021). The saponification value provides a rough indication of the molecular weight of the fat or oil. A lower saponification value suggests a lower average molecular weight of the fatty acids or a lower number of ester bonds. This value can be used to assess the purity of fats or oils. According to Codex (2017), the saponification index for palm oil falls within the range of 195 to 205 mg KOH/g oil. The saponification index is determined through an experimental process involving the reaction of palm oil with a specific amount of potassium hydroxide (KOH) and subsequent titration with HCl (Maduako *et al*., 2022). The Saponification value (SV) calculated using the expression given below:

$$\boxed{SV = \frac{(\mathrm{Vs} - \mathrm{Vb}) \text{ x M x } 56.1}{\mathrm{w}} \text{ x } 100} \qquad \text{Eq. (18)}$$

Where, Vs = sample titer value, Vb = blank titer value, M = molarity of the HCl, and 56.1 = molecular weight of KOH (Miyuranga *et al*., 2023).

2.10. Conjugated Diene of fried palm oil

Repeatedly frying of palm oil leads to the formation of hydro-peroxides, indicated by the absorbance at 230 nm, while the breakdown of these hydroperoxides into secondary oxidation products of linoleic acid is noted at 230 nm (Mechqoq *et al*., 2021). During lipid oxidation, electrons transfer from a non-conjugated to a conjugated position, forming conjugated double bonds in fatty acids, particularly in polyunsaturated fatty acids like linoleic acid, which contain methylene-interrupted dienes as shown in Figure 8. unlikely hydroperoxides derived from oleic acid, which have a single double bond, those from polyunsaturated fats include conjugated dienes in their structure (Shahidi & Yeo, 2020).

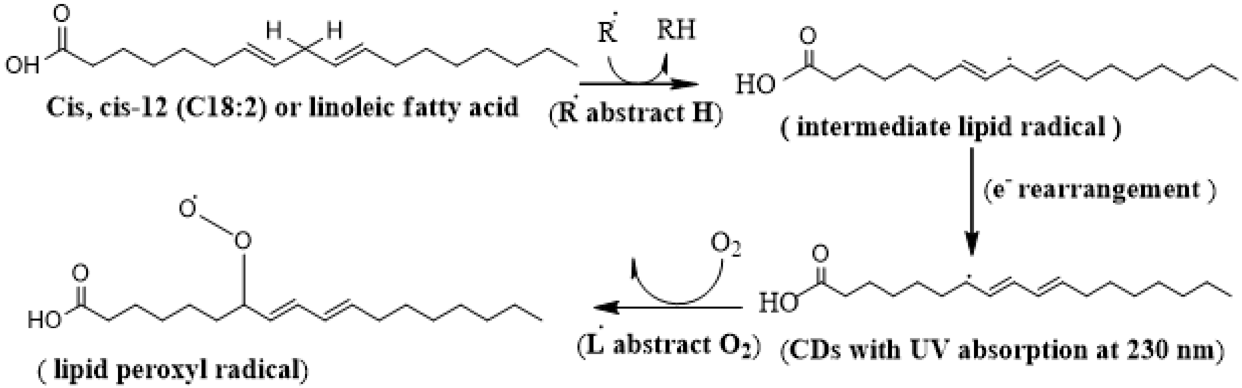

Figure 8: Lipids, such as linoleic acid, form a peroxyl radical ($LOO^{\bullet}$) in the presence of O_2 (Christodoulou *et al*., 2022; Kaseke *et al*., 2021).

The conjugated dienes in palm oil imply oxidative deterioration (Salama *et al*., 2020). When evaluating the quality of polluted palm oil, UV-Vis spectrometer analysis has the advantages of being quick, requiring little sample volume, not requiring chemical reagents, and not being affected by color changes or chemical interactions (Fonseca *et al*., 2021). Oil samples are suitably diluted in solvents like n-hexane or iso-octane/cyclohexane before the examination. The CDV calculated as extinction values （E_1%) using following equation;

$$\boxed{\mathrm{E1\%} = [\frac{A\lambda_{s}230}{bc}]} \qquad \text{Eq. (19)}$$

Where Aλs is the absorbance of the sample, b is the path length of the cuvette, and c= concentration of sample used for absorbance measurement in (g/100 mL) (Pereira *et al*., 2020).

2.11. Application of Spectroscopy

Spectroscopic techniques are widely used to detect defects in fried palm oil due to their number of advantages, including non-destructive analysis, elimination of hazardous chemicals and minimal sample preparation, cost- and time-effectiveness, high reliability, and reproducibility. These benefits make them particularly effective for identifying defects in vegetable oils (Maouardi *et al*., 2023).

2.11.1. General Concept of UV-Visible

UV-Visible spectrometry has progressed from the early spectroscopes of 1860 to modern instruments widely used since the 1960s (Carpentieri & Domenici, 2024). This analytical technique measures light absorption in the UV and visible ranges for qualitative and quantitative analysis, particularly in detecting pollutants in cosmetics, food safety, and textiles (Arce-Saldaña *et al*., 2023). Grounded in Lambert-Beer law, it relates absorbance to concentration and optical path thickness (Guo *et al*., 2020). A monochromator converts polychromatic light into monochromatic light, allowing quantification based on absorbed light intensity (Tanwar *et al.*, 2024). Measurement begins with a baseline from a solvent blank, followed by the sample to assess changes in transmitted light (Voss *et al*., 2024). Configuration may include single-beam and double-beam designs, affecting accuracy and stability (Nandiyanto *et al.*, 2023). UV-visible analysis is frequently used to evaluate the quality of spoiled oils, such as palm oil, detecting photon emission or absorption in the 200–800 nm range. This non-destructive technique provides insights into physicochemical changes due to oxidation when foods high in proteins and carbohydrates are repeatedly fried (Jolayemi & Mritala, 2020). It can also determine free fatty acid content, with high FFA levels indicating poor oil quality, making this test significant (Arafat *et al*., 2021).

2.11.1.1. Single Beam UV-Vis Spectrophotometer

Single beam UV-visible spectrometer, such as the Agilent Technologies Cary 60, is tailored for lipid analysis (Conrad *et al*., 2024). It emits UV and visible light, which is separated by a monochromator to select wavelengths typically between 200-800 nm (Abiodun *et al*., 2024). The sample compartment holds a 1cm cuvette containing the oil sample, ensuring a clear optical path. The detector measures transmitted light intensity, converting it into an electrical signal (Abed *et al*., 2023). The instrument features a single light source (flash deuterium lamp from 190 to 400 nm or a tungsten lamp for visible light from 400 to 800 nm), which limits its suitability for source additivity tests (Vallbona *et al*., 2024). The data acquisition system processes the signal for real-time absorbance readings, aided by a baseline correction mechanism for accuracy. Control software manages settings and analysis, presenting results through a user interface (Jaffar *et al*., 2024). A cooling system may also maintain stable temperatures during measurements. These components collectively enable precise absorbance measurements, essential for assessing oil oxidative stability in quality control and research (Berger & Trunschke, 2021).

2.11.1.2. Double Beam UV-Vis Spectrophotometer

The double beam UV-visible spectrophotometer, such as the England UV3114503, enhances analytical capabilities for lipid analysis, including the measurement of polyphenol compounds formed with Folin-Ciocâlteu (FC) reagent, detected at 760 nm (Fabjanowicz *et al*., 2024). This instrument features two optical paths, one for the sample and the other for the reference allowing real-time comparisons and improved accuracy. The light sources typically include a deuterium lamp for UV from 190 to 400 nm or a tungsten lamp for visible light from 400 to 800 nm. Light passes through a monochromator to select the desired wavelength before interacting with the sample in the cuvette, while the reference path contains a blank or solvent. The detector measures light intensity from both paths to calculate absorbance based on intensity deference, which the data acquisition system processes (Nandiyanto *et al*., 2023). The control software manages operational parameters, conducts baseline corrections, and generates absorbance values, facilitating data interpretation and reporting. This design supports precise measurements and stability, making it suitable for quality control and research in lipid analysis and other fields (Carpentieri & Domenici, 2024). Following Lambert-Beer law, the instrument converts polychromatic light into monochromatic light, measuring absorbance proportional to analyte concentration (Nhivekar *et al*., 2022). Measurement involves first determining blank intensity with a solvent, and then analyzing the sample's light absorption to calculate concentration changes (Poh *et al*., 2020).

2.11.2. General Concept of AAS

The Atomic Absorption Spectrophotometer is designed for the precise measurement of heavy metals through interconnected components. The hollow cathode lamp serves as a light source, emitting specific wavelengths that excite electrons in the target metals (Sevillano-Morales *et al*., 2023). The nebulizer converts the liquid sample into a fine aerosol, enhancing sample introduction into the flame. In the flame system, fired by acetylene and an oxidant, this aerosol is atomized, vaporizes the sample and dissociates metal compounds into free atoms (Sulthana *et al*., 2024). A monochromator isolates the relevant wavelength, ensuring only related light reaches the detector, which measures light intensity and converts it into an electrical signal proportional to the metal concentration (Pasias *et al*., 2021). The data acquisition system processes these signals to calculate absorbance and determine concentration, while control software facilitates calibration and data reporting. A cooling system may also be included to maintain consistent performance. Together, these components provide accurate and reliable measurements of heavy metals, making AAS essential for environmental monitoring and quality control (Slota *et al*., 2023).

Vegetable oils naturally contain trace amounts of metals, which can accelerate oxidation when present in higher concentrations. These metals may originate from soil, fertilizers, pesticides, and frying equipment, significantly impacting oxidation stability and oil quality (Lin *et al*., 2024). To analyze these minerals, a wet digestion method is commonly employed using a digestion furnace (HYP-1040; Xianjian, Shanghai, China) and heated at 370 ˚C for 4 h, with H_2O_2 added (Sun *et al*., 2021). This method involves a mixture or aqua regia of nitric acid (HNO_3) and hydrochloric acid (HCl) to decompose organic matter, separating target analytes from the matrix and eliminating organic substances that could interfere with subsequent analysis. This step is crucial for ensuring accurate and reliable results in the analysis of metals in vegetable oils (Asrade & Ketema, 2023).

AAS is the most widely used technique for heavy metal analysis. Because of its sensitivity, specificity, simplicity and accuracy. The amount of energy absorbed is proportional to the concentration of the element in the sample. The digested sample was analyzed for the spectrophotometer (Asrade & Ketema, 2023). The value of the dilution factor (DF), required as input to calculate the heavy metal concentration, was determined using the following formula:

$$\boxed{\mathrm{DF}\ (\frac{\mathrm{L}}{\mathrm{kg}}) = \frac{\mathrm{V(L)}}{\mathrm{W(kg\ )}}} \qquad \text{Eq. (20)}$$

where V refers to the volume of a diluted digested sample read from a volumetric flask while W represents the weight of a material sample. Subsequently, the heavy metal final concentration in the original sample will be computed using the following formula:

$$\boxed{\mathrm{C}\left(\mathrm{ppm\ or}\,\frac{\mathrm{mg}}{\mathrm{L}}\right) = \mathrm{AAS\ reading}\ \left(\frac{\mathrm{mg}}{\mathrm{L}}\right)\mathrm{XDF}\ \left(\frac{\mathrm{L}}{\mathrm{kg}}\right)} \qquad \text{Eq. (21)}$$

where C refers to the actual concentration while the AAS corrected concentration was obtained from the calibration curve (Tek & Ng, 2024). The level of metal content was calculated by using the formula:

$$\boxed{\mathrm{Metal\ content}\ \left(\frac{\mathrm{mg}}{\mathrm{100g}}\right) = \frac{\mathrm{C\ x\ V}}{\mathrm{W}}} \qquad \text{Eq. (22)}$$

Where, W = Weight of sample in (g), V=Volume of extract (ml), C = Concentration of sample solution (µg/ml) (Mohammed & Saleem, 2023).

2.11.3. General Concept of GC-MS

Chromatography is a technique that separates components in a mixture based on their partitioning behavior between mobile and stationary phases (Bajo-Fernández *et al.*,2024). Gas chromatography introduced by James and Martin in 1952, is specifically designed for separating, identifying, and quantifying volatile chemicals with boiling points up to 350 ^{o}C or 400 ^{o}C (Ferraz-Almeida *et al.*, 2020). In GC, the mobile phase is gas, while the stationary phase is liquid or solid. The process begins with the injection of the sample into an injector, where it is vaporized and transported through a column filled with the stationary phase by an inert gas (Fabjanowicz *et al.*, 2024). As the sample composition exits the column, they are detected and recorded as a sequence of peaks, each corresponding to a specific component and its retention time (Williams *et al.*, 2021). The various components of the sample are separated and eluted at different and specific times, which is referred to as retention time. GC-MS is a crucial tool for identifying and quantifying organic compounds in environmental samples, and it has advantage and disadvantage as shown in Table 3 (Joia & Muhammad, 2023). The fatty acids composition in oils can be calculated from individual peaks expressed as % of total fatty acids using the formula:

$$\boxed{\%\ \text{fatty acid} = \frac{\text{each peak area}}{\Sigma\ \text{total peak area}}\ \text{X}\ 100\ \%} \qquad \text{Eq. (23)}$$

(Korede *et al*., 2024)

Mass spectrometry is an analytical method that determines the mass-to-charge ratio of ions, is employed to identify new compounds and characterize known components. When combined with gas chromatography, GC-MS is considered the standard for analyzing lipids, components of FFAs, drug metabolites, and environmental contaminants. (Kaisan *et al*., 2021).

Table 3: Advantage and limitations of GC-MS.

Analytical techniques	**Advantage**	**Limitation**	**Reference**
GC-MS	Provide better resolution and separation for peaks Lower limit of detection (LOD) Provide rich information of qualitative and quantitative analysis of sample Robustness Offer greater sensitivity and specificity High reproducibility	Massive and lengthy sample preparation (hydrolysis and derivatization of sample) Destructive method Time consuming for sample analysis Incapable of compounds that are non-volatile, polar, or thermally labile Identified compounds have to be in a mass spectral library/ database for identification purposes	(Tan *et al*., 2022).

GC-MS-gas chromatography-mass spectrometer:

CHAPTER-THREE

3. MATERIALS AND METHODS

3.1. Study Area

The research was conducted in Axum, a city in the Central Zone of the Tigrai Region, Northern Ethiopia. Axum is located approximately 1043 Km far from Addis Ababa and 249 Km from Mekelle via Adigrat as shown in Figure 9. Its geographical coordinates are approximately 38° 44' 50.244" E longitude and 14° 8' 2.5152" N latitude, with an elevation of 2,131m above sea level. Various Woredas and agricultural production areas surround Axum. Notably, potatoes are grown in the May Ngus irrigation area, which is close to Axum.

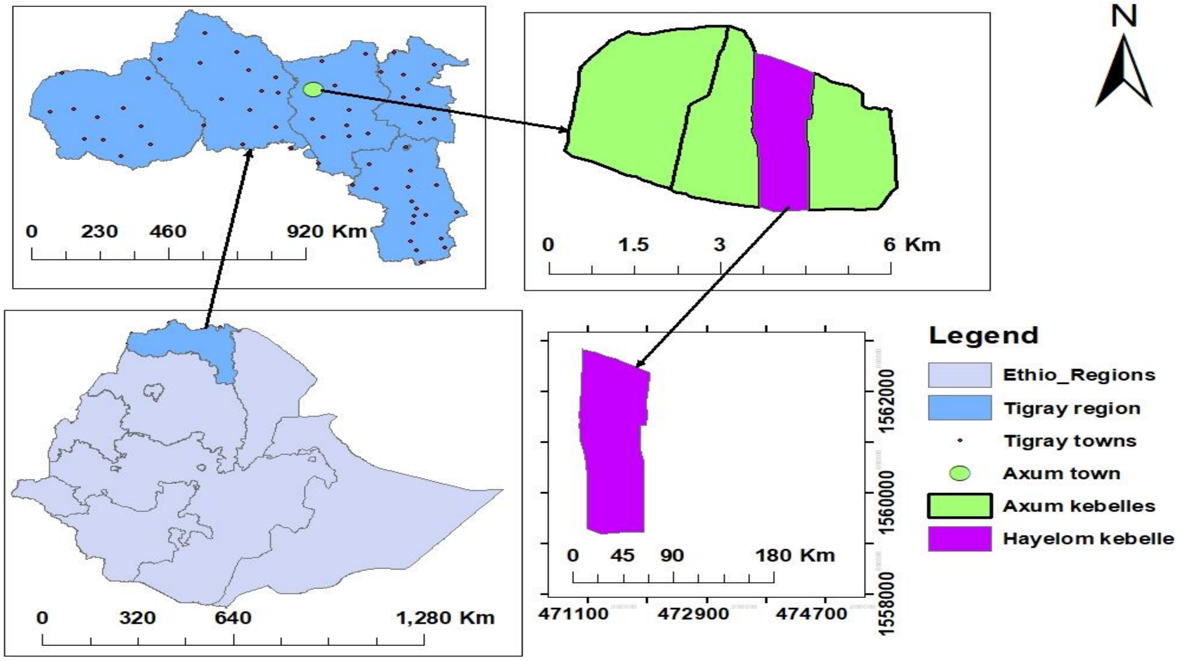

Figure 9: Map of Study Area.

3.2. Sampling Technique

HPO samples were randomly taken from Axum city road market and analyzed their physicochemical parameters and some selected heavy metals from the repeatedly deep-frying (HPO) at high-temperature directly from the sellers found near the bus station. 500g of potatoes were taken for each fried cycle at constant temperature (180 °C) which was controlled using a thermostat collected at the same time interval of 20 min and the same volume of oil (2L). For this purpose, two types of samples were prepared: one with fried HPO without rosemary powder (FHPO), and the other fried HPO with rosemary powder using different amounts (100, 150, 200, 250, 300 mg/kg) (FHPOR), respectively. To prevent, contamination in each fried cycle the chips fryer machine was washed with soap and distilled water and made ready for the next time. Sample collection was done for two weeks from January 1-15, 2016 E.C. Accordingly, 1.8, 1.7, 1.5, 1.4, and 1L of frying oils were collected from each fried cycle for each consecutive day which was fried at 20, 60, 100, 140, 180 min of time interval from the final fry. Samples were labeled as FHPO for every fried cycle (1st, 3rd, 5th, 7th, 9th) and FHPOR also labeled as (1st, 3rd, 5th, 7th, 9th). To ensure sample integrity, samples were packaged in plastic bags and covered with aluminum foil to prevent photodegradation. The samples were then transported to Mekelle University for further analysis.

3.3. Chemicals

HNO_3 (68%; Chem Corp Industries, USA), H_2SO_4 (99.8%; Sulfa Chem Ltd., Germany), CH_3Cl (99%; Chloro Chem Solutions, India), $HClO_4$ (70%; Acid Tech Manufacturing, Japan), KI (99%; Iodine Innovations, USA), CH_3COOH (99%; Acetate Chemical Co., Brazil), $Na_2S_2O_3$ (94.6%; Thio Chemicals Inc., UK), HCl (37%; Hydro Chem solutions, China), KOH (99.5%; KOH Dynamics, Australia), CH_3OH (99.8%; Methanol Makers, Canada), phenolphthalein Indicators (Indicator Solutions, France), CCl_4 (99%; CCl_4 Industries, Mexico), KBr (99.9%; Bromide Technologies, South Korea), I_2 (99.5%; Iodine Resources, India), H_2O (Pure Water Co., USA standard in APF), H_2O (Distillation Solutions, Messebo Cement Factory), starch solution 99.4% (Starch Chem Corp., Netherland), H_2O_2 (35%; Peroxide Chem, Italy), Folin-Ciocâlteu reagent, (HPLC) grade (Reagent Masters, USA), Standard Gallic Acid 99.5% extra pure (Pure Lab Chemicals, Switzerland), Na_2CO_3 (98%; Carbonate Chemicals Ltd., UK), Na_2SO_4 (99%; Sulfate

Solutions, France), $C_4H_{10}O$ (99.7%; Ether Chem, USA), petroleum ether 95% (Petro Solvents Inc., Saudi Arabia), C_6H_{10} (Indian, HPLC grade solvent 99.9%; Cyclo Solvent Ltd), C_6H_{14} (98.84%; Hexane Technologies, Canada), pH 4 and 7 standard buffers (Buffer Solutions Inc., Germany), acetone (99%) (Acetone Solutions, USA), and Whatman № 42 filter paper (Whatman International, UK) were used during the study.

3.4. Apparatus

Digital analytical balance made in Korea serial №: 15641875, digestive furnace model (HYP-1040; Xinjian, Shanghai, China), rosemary blender or grinder model IKA Grinding Mill A11, 2mm size mesh or sieve, Heidolph Laborota 400 vacuum rotary, laboratory fume hood, Conical flasks, beakers, watch glass, pipette, Volumetric flask, Crucible, oven model 30-1060, desiccator, HANNA meter model (HI-5522 pH meter), burette, BIOBASE SY-2L4H water baths , funnel, digital refractometer serial №:BU16127, electrical centrifuge model U8V-2, stainless steel metal fryer, thermostat to control the fryer’s temperature, brook field viscometer model (MA 023434666, 1031, USA), Erlenmeyer flask, magnetic stirrer made in UK serial №: R000104942, vacuum filtration, cuvette, pycnometer/density or corked bottle, reagent bottles and test tubes were used during the study.

3.5. Instruments

UV-visible spectrophotometer (Agilent Technologies Cary 60 UV-Vis, SER №: MY15410011 manufactured in Malaysia), UV-visible spectrophotometer (ENGLAND, SER №: UV3114503), atomic absorption spectrophotometer (50B AAS Varian Country), and gas chromatography-mass spectrometer (GC-MS) (Agilent, England GC7890B /USA MSD5977) were used for characterization of fried HPO with and without rosemary leaf powder.

3.6. Preparation of Rosemary Leaf Extract

Rosemary (*Rosmarinus officinalis L.*) leaves were properly cleaned with tap water and then distilled water and dried in an oven at room temperature (25° C) for ten days, it reached a consistent weight. The leaves were processed into a fine powder using grinder. Then, the powder samples were sieved through a 2mm screen placed in polyethylene bags, and kept at room temperature storage (Pontillo *et al*., 2021).

128.538 g of powdered rosemary and 1289 mL of 99.8% methanol were combined for maceration in the ratio of 1:10 (1g rosemary to 10 mL methanol). The mixture was carefully placed into a 5000 mL beaker and macerated for three days at room temperature while being constantly shaken with a magnetic stirrer. After that, it was macerated for three days. Then, the extracts were filtered through Whatman №-42 filter paper in a vacuum pump filtration system. The extract was placed in vacuum rotary evaporator to remove methanol solvent at 64.7°C (Hussein *et al*., 2022). Hence, the extraction process was carried out for the maceration of rosemary (Amalraj *et al*., 2022). A total of 21.538 g extracted powder (which is a light brown or dark green color) was collected during the process, labeled as rosemary leaf extracts (RE), and kept in a brown bottle or dark vial in a refrigerator at 4°C was collected as in Figure 10 (Tohma *et al*., 2021; Zeraat *et al*., 2023).

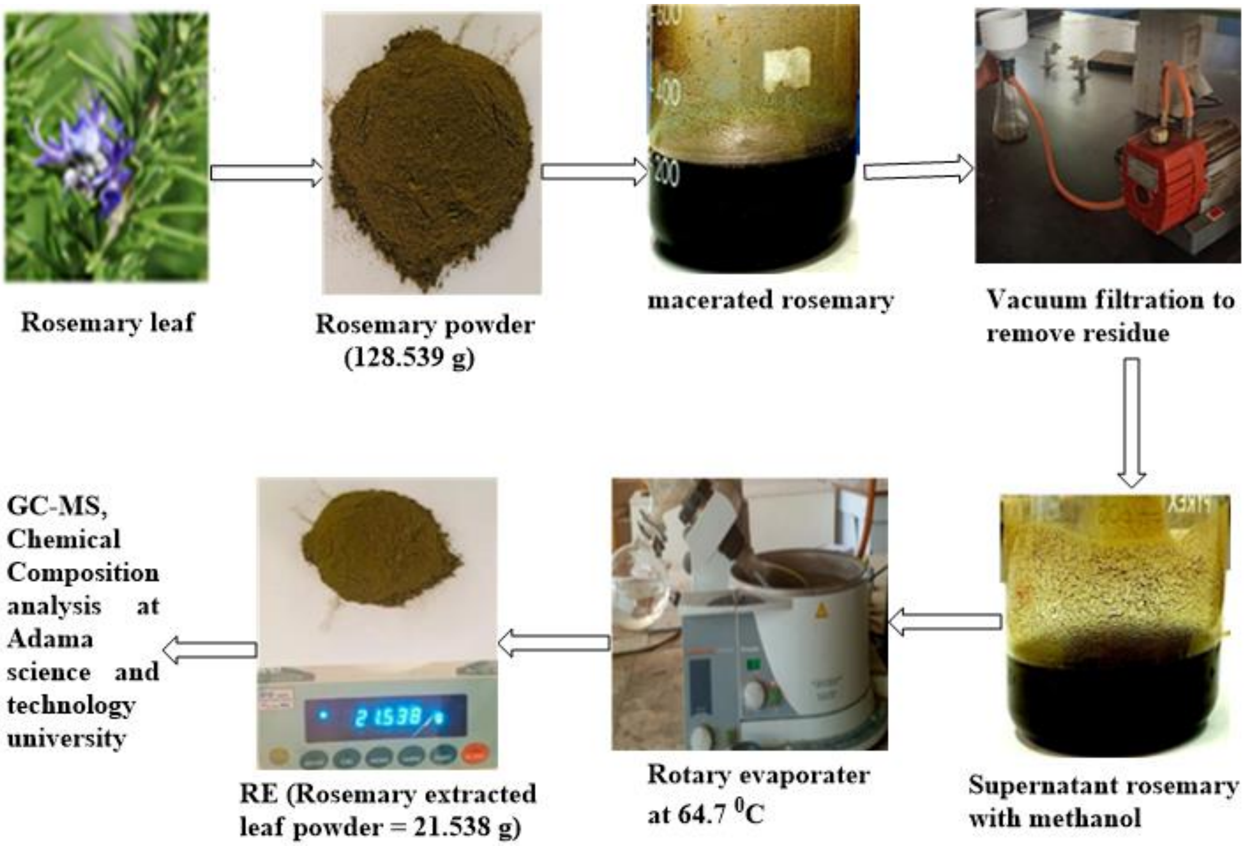

Figure 10: Maceration process to prepare rosemary leaf powder

3.7. Determination of Total Polyphenol in Rosemary

A 250 mL volumetric flask containing 10 g of rosemary powder was used for the Folin-Ciocâlteu reaction. Following that, 100 mL of the Folin-Ciocâlteu reagent (1:10 v/v in deionized water) was added, and the mixture was left to react for 5 min at room temperature. Next, 80mL of saturated Na_2CO_3 solution (6-7.5% w/v) was added, and the solution was diluted with deionized water to the appropriate level. The mixture was allowed to settle at room temperature for 90 min, covered with aluminum foil, and placed in dark place (Cheng *et al*., 2022).

In a 250 mL volumetric flask, 25 g of Gallic acid was dissolved in 250 mL of methanol (99.8%), and serial dilutions were carried out at concentrations of 10, 20, 30, 40, and 50 µg/mL. A blank solution was made with 20 mL of Na_2CO_3, 5 mL of methanol, and 5 mL of the Folin-Ciocâlteu reagent. The prepared solutions were allowed to settle at room temperature for 8 min. To each solution, 3mL of saturated Na_2CO_3 solution was added, and the mixture was shaken for 3 min. From this, 1 mL, 2 mL, 3 mL, 4 mL, and 5 mL of each RE, blank, and Gallic acid equivalent (GAE) standard solution were taken for serial dilution, and deionized water was added to get the final solution up to the 1000 mL mark of the volumetric flask. The mixture was then allowed to develop its color for 90 min at room temperature in a dark condition (Shaziya *et al*., 2022).

Finally, a UV-vis spectrophotometer was used to measure the absorbance at a wavelength of 765 nm using a 2 mL glass cuvette. The absorbance of the blank sample was subtracted from the absorbance results for each concentration of the extracts. The standard curve produced by GAE was used to calculate the sample's Gallic acid content (Mohammed & Saleem, 2023).

3.8. Repeated Deep Frying HPO Procedure

A 6 L household stainless steel frying pan without a cover was used for this experiment. The frying process was carried out for 25 consecutive total fried cycles, with each frying time consisting of 20 min of frying following the same procedures. Samples for analysis were taken from the last frying session on the (1st, 3rd, 5th, 7th, and 9th) number of fried cycles as in Figure 11 (Nduka *et al*., 2021).

In total fried cycles, 12.5 kg potato in 10 L of HPO was used i.e.; in the 1st method, 500 g in 2 L, 1.5 kg in 2 L, 2.5 kg in 2 L, 3.5 kg in 2 L, and 4.5 kg in 2 L of FHPO labeled as the 1st, 3rd, 5th, 7th, and 9th number of fried cycles, respectively. For each frying process, 500 g of potatoes were peeled, washed, and cut into thick, evenly sized-pieces using a mechanical cutter. The potatoes were washed with distilled water before frying and cleaned with a tidy white dress to remove water from the potato to decrease the hydrolysis reaction. In the first method, the potatoes were placed in an electric fryer containing each 2 L of oil, and the temperature was set to 180°C for 20 min to initiate frying (Ceylan & Baştürk, 2023). This method served as the control without any additive of rosemary antioxidant (FHPO) (Hussain, 2020).

In the 2nd method, the process was similar to the first method, but the only difference was the addition of rosemary leaf powder. Different doses of rosemary leaf powder (100 mg/kg, 150 mg/kg, 200 mg/kg, 250 mg/kg, and 300 mg/kg) were added in each 2L of oil before frying on the (1st, 3rd, 5th, 7th and 9th) number of fried cycles, respectively. At the end of each frying method, the fryer was turned off after the last batch of fries. The remaining fried oil samples were collected and filtered through Whatman №-42 filter paper to remove any residue or debris. These samples were then stored in dark brown bottles and labeled as FHPO and FHPOR for each fried cycle of the 1st, 3rd, 5th, 7th, and 9th, and stored at-4°C until further analysis of their physicochemical properties, and some selected heavy metal contents (Plaskova & Mlcek, 2023).

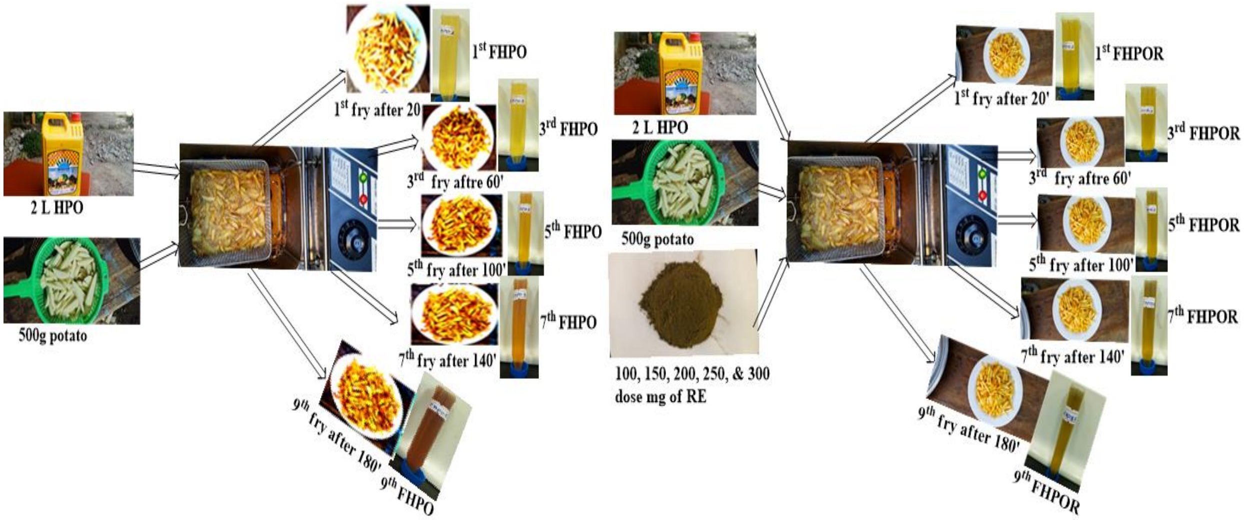

A) FHPO B) FHPOR

Figure 11: Repeated deep-fried Hayat palm oil procedure. A) FHPO & B) FHPOR have the same (time interval, amount of potato, volume of oil, and same temperature (180 ^{O}C), but different variable doses of rosemary leaf powder were taken.

3.9. Physical Parameter Analysis of HPO Using Apparatus Methods

After collecting the samples for analysis, samples were subjected to centrifugation at 4200 rpm for 15 min, which was used to separate any solid particles from the oil. For further purification, a filtration process was employed with vacuum filtration using Whatman №-42 filter paper, and the supernatant samples. This filtration method was used to ensure that the purified oil was used for subsequent titration and characterization (Irfan *et al*., 2020).

3.9.1. Measurement of Moisture Content Using Oven Method

To determine the moisture content of FHPO and FHPOR samples from each final frying cycle, the standard oven drying method was used with a slight modification (AOAC, 2000). The process involved weighing an empty crucible and adding 10 g of FHPO of the 1st, 3rd, 5th, 7th, and 9th number of fried cycles. The sample was then dried in an oven at 105°C for 1 h or until a constant weight was obtained. After cooling in the desiccator, the crucible was reweighed. The same procedure was followed to obtain the weight of the last FHPOR sample from each of the fried cycles (1st, 3rd, 5th, 7th, and 9th) number of fried cycles. This analysis was conducted three times (Liyansan *et al*., 2022).

3.9.2. Specific Gravity Measurement

To determine the specific density of the oil, a density bottle also known as a pycnometer 25 mL or standard weight 24.8 mL, was used. The sample of HPO was melted and filtered through filter paper to remove any impurities. A clean and dry corked bottle with a capacity of 25 cm^3 was weighed (W_0). Then, the empty bottle was filled up to the mark with the last fried time FHPO and FHPOR samples from each of the fried cycles (1st, 3rd, 5th, 7th, and 9th), corked, and weighed again to obtain (W_1) for each sample. After washing, drying, and reweighing the bottle, it was filled with distilled water (W_2) to replace the oil. This process was repeated three times (Aslam *et al*., 2021).

3.9.3. Refractive Index Measurement

As per AOAC (2000) guidelines, the refractive index was measured using an automatic digital refractometer serial №: BU16127 at room temperature. Before taking the readings, the first sample was melted and filtered to remove impurities. The prism of the instrument was cleaned with

distilled water and acetone. Calibration was done using distilled water at a temperature of 25°C to ensure uniformity. The prism was cleaned again with acetone and dried (Okoro *et al*., 2023).
Then after, a few drops of FHPO and FHPOR samples from the last frying cycle (1st, 3rd, 5th, 7th, and 9th) several fried cycles were separately placed on the prism, closed, and their respective values were recorded. This analysis was repeated three times (Aslam *et al*., 2021).

3.9.4. pH

The pH value of the oil sample was measured using a digital pH meter. With a slight modification, samples were diluted with hot distilled water (1:10 ratio). A 10 g portion of the sample from FHPO and FHPOR was mixed separately in 100 mL of distilled water for 60 s using a magnetic stirrer. The mixture was filtered through a Whatman №-42 filter paper to obtain a clear filtrate for pH measurement (Hasanah *et al*., 2024). The pH meter was first calibrated with pH 4 and 7 standard buffers by dissolving one capsule in 100 mL of distilled water. The pH of the sample was determined by dipping the electrode of a pH meter into the mixture. After calibrating the pH meter, then filling a clean and dry 50mL from FHPO and FHPOR of the last fried cycle (1st, 3rd, 5th, 7th, and 9th), respectively samples into a separate beaker, the pH value was recorded in triplicates (Frances *et al*., 2023).

3.9.5. Viscosity Measurement

The viscosity of the oil sample was determined using a viscometer as per the specifications of the instrument. The viscometer was set up at room temperature with a spindle number 02, which falls within the recommended range. To calibrate the viscometer, it was adjusted using de-ionized water, and the dynamic viscosity reading was set to 0% using the dash sign. The viscometer was then prepared for measurement by setting the spindle speed to 100 rpm and ensuring the bubble level was centered (Liyansan *et al*., 2022).
For each trial, 60 mL of oil sample was taken from each fried cycle of the 1st, 3rd, 5th, 7th, and 9th fried cycle of the oil. Before each measurement, the viscometer was turned off, cleaned with distilled water and a soft cloth, and the spindle was turned on. To maintain the acceptable range of percentage value, the spinning speed was adjusted if it fell below 10% by increasing the speed and changing to a larger size spindle, or if it exceeded 100% by decreasing the speed and using a smaller size spindle (Raji *et al*., 2022).

The material contained FHPO & FHPOR with the oil samples carefully positioned below the spindle, which was then immersed deep into the oil. The viscometer was turned on and set to a speed of 100 rpm. After allowing it to rotate in the oil for 2-3 min to achieve stability, the viscosity readings were recorded in triplicate for each sample in centipoises and calculated the kinetic viscosity (Nuru & Getachew, 2021).

3.10. Chemical Parameter Analysis of HPO Using Titration Method

3.10.1. Determination of peroxide value (PV)

Peroxide value was evaluated according to standard methods of AOCS, Mechqoq *et al*., (2021), which was determined by measuring the iodine released from KI, with some modifications. To assess the formation of primary oxidation products, 5 g samples of FHPO and FHPOR were taken from the last frying cycle (1st, 3rd, 5th, 7th, and 9th) and placed in each 250 mL conical flasks. A mixture of acetic acid and chloroform solvent (3:2 ratio) was added to 30 mL of each oil sample and stirred thoroughly for dissolution. Then, 1 mL of KI solution was added to each solution. The solution was kept in a dark room for 1 min, with occasional stirring, followed by the addition of 30 mL of distilled water. The liberated iodine was slowly titrated with 0.01N sodium thiosulfate solution until the yellow color disappeared, shaking vigorously. After that, 1 mL of starch indicator solution was added, and the titration continued by shaking vigorously until the release of all I_2 from the CH_3Cl layer, resulting in a blue color disappearance finally become cloudy solution. This analysis was done in triplicates (Elamin, 2019).

3.10.2. Determination of Iodine Value (IV) using Hanus Method

Iodine value was evaluated according to standard methods of American Oil Chemist's Society (AOCS), Mechqoq *et al*., (2021). A 13.2 g of pure resublimed iodine was added to glacial acetic acid and placed into a 500 mL volumetric flask by warming over a water bath. When the iodine was completely dissolved, the solution was cooled and then about 1.5 mL of pure Br_2 was added to the solution. The solution was diluted into 500 mL with glacial acetic acid. The whole operation was conducted in a fume hood (Fariha, 2020). To determine the degree of modified unsaturation, 5 g of FHPO and FHPOR from the last frying cycle (1st, 3rd, 5th, 7th, and 9th) were weighed separately into 250 mL stoppered conical flasks. Carbon tetrachloride (25 mL) solvent was added to each oil sample and thoroughly mixed to dissolve. Then, the prepared Hanus reagent of 25 mL was added to each solution, mixed well, and kept in a dark place in the vial for 30 min for a complete reaction between iodine and the unsaturated bonds of oils. The flask was covered by aluminum foil to avoid light exposure (Negash *et al*., 2019). After allowing it to stand, KI solution (15 mL), and distilled water (100 mL) were added to the sample solution to transform leftover iodine into iodide. The released iodine was titrated with 0.1 N sodium thiosulfate solution using starch indicator solution (1 mL) until a blue color forms and disappears after thorough stirring. The blank determination was also carried out following the same procedure without the oil. This analysis was repeated three times. The difference between the volumes, in mL, of 0.1 N sodium thiosulfate vs consumed by the blank test and the actual test, multiplied by 126.9 (atomic weight of iodine) and divided by the weight in g of the substance taken for the test was found to be the iodine value. The iodine value of the oil was determined using the formula from the literature as described by (Jurid *et al*., 2020).

3.10.3. Determination of Acid Value (AV)

Acid value (AV) was evaluated according to the standard methods of the American Oil Chemists' Society (AOCS) (Mechqoq *et al*., 2021). To determine the presence of free fatty acids resulting from rancidity or contamination with some modification, 3 g of each cooled oil sample was taken from the last frying cycles of FHPO and FHPOR (1st, 3rd, 5th, 7th, and 9th fried cycles) were weighed and placed into 250 mL conical flasks. Next, 30 mL of newly neutralized ethanol was added, followed by thorough shaking to dissolve the sample (Ameen *et al*., 2023). The sample solution was boiled for approximately 5 min. After the mixture was allowed to cool, and then 1 mL of phenolphthalein indicator was added. Then after, the sample solution was titrated with 1N NaOH solution until a permanent pale pink color appeared. For the blank titration, NaOH (1N) was slowly added to 30 mL of ethanol in the presence of phenolphthalein as an indicator. This analysis was conducted in triplicates (Elamin, 2019).

3.10.4. Determination of Saponification Value (SV)

The saponification value (SV) was obtained according to the American Society for Testing and Materials 464 (ASTMD464) (Mishra *et al*., 2023). The saponification value was determined with some modifications of ASTMD464, and hence, 3 g of FHPO and FHPOR from the last frying cycles (1st, 3rd, 5th, 7th, and 9th) were weighed separately and placed into 250 mL Erlenmeyer flasks. Next, 25 mL of 0.5 N alcoholic KOH solution was added to each flask. A blank determination was also performed following the same procedures as the sample used. The flasks, along with the condenser, were gently boiled in a water bath at regular intervals until saponification was completed until it indicated the absence of oily material and the appearance of a transparent fluid solution. Clarity was achieved after approximately 30 min of boiling. Once the flask and condenser had cooled, the inside of the condenser was washed with approximately 10 mL of ethanol. After that, 1 mL of phenolphthalein indicator was added to the solution and the excess KOH was titrated with 0.5 N HCl until a cloudy solution was formed. This analysis was also repeated three times (Osunrinade *et al*., 2020).

3.11. Characterization of FHPO and FHPOR Samples

3.11.1. Conjugated Di-ene Value Analysis

With minor modifications, a UV-visible spectrophotometric examination was carried out to quantitatively determine the conjugated fatty acid values (diene) of the treated and untreated samples. The measurements were carried out at 230 nm, for the treated FHPOR and untreated FHPO samples (Aly *et al*., 2021). Using AOCS standard procedures, UV absorbance at 230 nm was measured (Mechqoq et al., 2021). Accordingly, a 50 mL volumetric flask was filled with 3 mL of the filtrated, treated, and untreated oil sample from the 1st, 3rd, 5th, 7th, and 9th frying cycles. The oil sample was then dissolved in 30 mL of cyclohexane, using a magnetic stirrer. The resultant organic phase was carefully collected using a decanted after being centrifuged for 5 min at 1,500 rpm to extract the upper layer, which contained cyclohexane (Jiang *et al*., 2020). A UV-visible spectrophotometer was then used to evaluate the absorbance of the samples. Finally, following the procedures described by (Fonseca *et al*., 2021), the conjugated dienes were computed.

3.11.2. Heavy Metal Analysis

3.11.2.1. Sample preparation using digestion methods

To determine the heavy metal content, the treated and untreated samples were subjected to wet acid digestion following the standard methods described on Association of Official Analytical Chemists (AOAC), 2000 protocols (Frances *et al*., 2023). In this process, 1 mL of the sample was accurately weighed and transferred into a digester tube and was digested via a mixture of 10 mL HNO_3 (70%), 4 mL $HClO_4$ (70%), and 4 mL H_2O_2 (30%) at a temperature of 240°C for 2 h in a digestive furnace until all the samples were dissolved completely and also to obtain a clear and colorless solution (Sun *et al*., 2021). After completion of the digestion process, and cooling at room temperature for 30 minutes. After cooling, 50 mL of deionized water was added to dilute the solution (Gebeyehu & Bayissa, 2020).

3.11.2.2. Analysis of heavy metals using AAS

To create standard solutions of Pb, Cd, Cu, Fe, Hg, and As, their corresponding salts of Pb $(NO_3)_2$, Cd $(NO_3)_2$, Fe $(NO_3)_2$, $AsNO_3$, Hg $(NO_3)_2$, and Cu $(NO_3)_2$ were dissolved with de-ionized water to get a 1000 ppm stock solution each salt. The stock solutions were serially diluted to prepare working standards with concentrations of each heavy metal element at 2, 5, and 10 ppm (Frances *et al*., 2023). The analytical wavelengths, energy, lamp current, and slit width for each element were used as per the protocols used and the absorbance of the interest element was measured in replicates. Accordingly, the absorbance of supernatant solutions of the interest of elements was measured at the following operating condition: wavelengths and spectral bandpass for Pb, Cd, Fe, Cu, Hg, and As were, Pb: 228.8 nm (0.5 nm), Cd: 217.0 nm (0.5 nm), Fe: 238.2 nm (0.5 nm), Cu: 324.7 nm (0.5 nm), Hg: 254 nm (0.5 nm), and As: 193.7 nm (0.5 nm). Pb, Cd, Cu, Fe, Hg, and As were determined using a Deuterium arc background correction equipped with a hollow cathode lamp with the flow rate of the nebulizer with 5.0 mL min^{-1}. Finally, the average concentration value of each metal was expressed in mg/g of day weight using the following formula; Heavy metals $\left(\frac{\mathrm{mg}}{\mathrm{100g}}\right) = \frac{\mathrm{C}\ in \left(\frac{\mathrm{mg}}{\mathrm{ml}}\right)\times \mathrm{V\ in\ ml}}{\mathrm{Sample\ mass\ (g)}}$, Where C = Concentration of metal ions (mg/mL), V = Final volume (50 mL) of solution, W= Initial weight (1 g) of the sample measured. Conversion factor 1 ppm or µg/mL = 0.001 mg/g. Where “x” from the calibration curve is in µg/ml is the absorbance reading concentration.

3.11.3. GC-MS Analysis of FHPO and FHPOR

3.11.4.1. Preparation of Fatty Acid Methyl Ester (FAME)

The fatty acid profile was determined using gas chromatography/mass spectrometer after the oil samples were esterified into Fatty Acid Methyl Esters (FAMEs) suitable for analysis. First, 10 mL of extraction solvent was added for every 1 g of sample (10:1 solvent-to-sample ratio). A 1 g portion of the treated and untreated fried samples were weighed and transferred into a 50 mL centrifuge tube. To remove water, 0.5g of Na_2SO_4 and 10 mL of n-hexane were added. After Allowing the mixture to stand for a specific duration of time, the extraction of the target compounds was facilitated into the solvent (Lisa *et al*., 2022), and then the mixture was stirred by a magnetic stirrer for 1 min. After the extraction time was completed, the extract was separated with centrifugation followed by carefully decanting the liquid phase. Next, 5 mL of a 2 M KOH-methanol solution was added to the solution and allowed to stay for the reaction to be taken place for about 5 min (Hee *et al*., 2023), followed by placing a water bath for 2 min at 70°C. After that, a 1 g of Na_2SO_4 was added to neutralize any excess KOH. The centrifuge tube was then rapidly cooled in a desiccator and then add 4 mL of ultrapure water and 5 mL of n-hexane were added. The upper solution was extracted through centrifugation at 9400 rpm for 2 min, and the upper layer, which contained the interest of the analyte/sample in n-hexane, was carefully separated into a vial using a pasture pipette for GC-MS analysis (He *et al*., 2022).

3.11.4.2. Gas Chromatography-Mass spectrometry (GC-MS) Fatty Acid Analysis

The extract of FHPO and FHPOR were concentrated to 1 mL for GC-MS analysis and 1 μL was injected into the GC capillary column, (HP-88 containing 88% cyanopropyl arylpolysiloxane as stationary phase (30m, 0.25mm, 0.25μm film thickness)). The injector and detector temperatures were adjusted to 240^{o}C and 260^{o}C, respectively.

The GC oven's initial temperature was 60^{o}C and maintained for 2 min, then after raised to 230^{o}C at the rate of 8^{o}C/min, kept at 280^{o}C and held for 5 min with a total run time of 34 min. The EI MS parameters included a solvent delay of 3 min and a source temperature of 230 ^{o}C. The split ratio used was 10:1, and helium (purity 99.99%) was used as a carrier gas with a flow rate of 1mL/min in GC separation. The mass spectrometer was operated in the electron impact (EI) mode at 70eV; with an ion source temp: (250^{o}C), a quadruple temp: (150^{o}C), and a translating line temperature of 270°C. The mass scan was found in the range between 50 and 550 m/z with an em voltage, of 1035V. Peak identifications for the FAs in FHPO & FHPOR oil samples were performed by comparison with MS spectra and retention times (Rt) of the standards. Similar procedures were also used for the analysis of the chemical composition of methanolic rosemary extracted (RE).

3.12. Data Analysis

All data values obtained from the physical and chemical analysis of both treated and untreated oils were presented as means ± standard deviation (SD) (Mean ± S.D; N=3) to illustrate the mean difference between FHPO and FHPOR. Statistical analysis was conducted to examine the relationship between fry time (independent variable) and physio-chemical properties (dependent variables) of the oil samples. One-way ANOVA was performed in Excel using data analysis, followed by Turkey's test. Graphical representations of the edible oil parameters were generated using Microsoft Excel 2019 and Origin Pro software 2018 version. A 95% confidence interval was employed with a significance level set at $p < 0.05$.

CHAPTER-FOUR

4. RESULTS AND DISCUSSION

4.1. Extraction Yields of Rosemary

Extraction yields of rosemary (RE) in this study was 16.71% as shown in Figure 10 based on the dry weight of 21.538 g obtained from macerated rosemary leaf powder. This result falls between the 27% yield reported by Tohma *et al.*, (2021), for 18.7 g methanol extracts and the yield found by Chaqroune and Taleb, (2022) for 25 g of rosemary extracted with n-hexane. In Taleb's study, methanol yielded the highest total phenolic content (19.06%), followed by ethanol (13.31%), ethyl acetate (7.62%), and n-hexane (5.14%) over 72 h macerated. Therefore, the present study's yield is within this range, it suggests that the rosemary extract produced here is good quality, with potential applications in chips preparations and health benefits, particularly due to its antioxidant properties.

4.2. Total polyphenol Content in Rosemary

According to, Manzoor *et al*., (2022) the total polyphenol content (TPC) of the macerated rosemary in methanol extract was determined using a spectrophotometer and Gallic acid (GA) as a standard. The concentration of mg GA in the rosemary leaf sample was found to be approximately 0.2597, 8.44, 20.65, 27.143, and 40.65 for standard solutions 10, 20, 30, 40, and 50 µg/mL, respectively. Moreover, the total phenols in the methanolic extract of different rosemary concentrations were quantitatively estimated as mg of gallic acid equivalent (GAE mg / L), N=3) was assessed by the Folin-Ciocâlteu reagent method from calibration line as shown in both Appendix Figure 12 and Table 12 (Mohammed & Saleem, 2023). To calculate the total amount of polyphenols in the rosemary leaf sample, the dilution factor or sample-to-volume ratio (1:10 w/v) used during sample preparation.

The concentration of polyphenols in the sample after dilution was calculated using the following equation:

$$\boxed{\text{X or Concentration}\left(\frac{\mu g}{ml}\right) = \text{Concentration}\left(\frac{\mu g}{ml}\right)\text{x dilution factor}} \qquad \text{Eq. (24)}$$

Thus, the concentration (µg/mL) after applying the dilution factor were as follows: 2.597, 84.4, 206.5, 271.43, and 406.5 µg/mL, respectively. The TPC from the sample volumes used in serial dilution law (10, 20, 30, 40, and 50) $\frac{\mu g}{ml}$, were taken as 1 mL, 2 mL, 3 mL, 4 mL, and 5 mL, respectively. The resulting TPC values were as 0.02597, 1.688, 6.195, 13.572, 20.325 $\frac{mg}{g}$ correspondingly 10g of rosemary extract had the highest TPC (41.81 mg GAE/g), and this result agree with a previous study by Bianchin *et al*., (2020), who measured 45.67 mg GAE/g) for the lyophilized rosemary ethanolic extracted.

4.3. Effect of Rosemary on Repeatedly Deep-Fried Cycles of HPO

Hayat palm oil (HPO) contains relatively balanced unsaturated and saturated fatty acids. This allowed for use for repeated frying for a specific number of cycles. For this reason, HPO was chosen for the deep-frying experiment (Nduka *et al*., 2021). As shown in Figure 11, the pale-yellow color of fried HPO without any addition of rosemary in the 1st cycle oil changed to deep brown by the 9th cycle. Similar results were observed in a Yılmaz *et al*., (2023) study where potatoes fried in palm oil, showed a distinct color change from golden yellow to brown after the 8th frying. According to Wang *et al*., (2023), this progressive increase in color intensity indicates the decomposition of unsaturated triglycerides, and free fatty acids (FFAs), which leads to the formation of harmful compounds. In addition to Nanayakkara *et al*., (2020) study, the oxidation of soybean oil with 10% rosemary extract dissolved in ethanol was found to be lower than that of oils treated with the maximum legally permitted level of butylated hydroxy anisole (BHA). Rosemary extract enhances the oxidative stability of frying oils and reduces the dark coloration of potato chips during frying by inhibiting the Maillard reaction and controlling polymerization reactions.

4.4. Measurement of Physico-chemical parameters of HPO

The quality of Hayat palm oil was analyzed by determining the physicochemical properties such as moisture content, specific gravity, viscosity, pH value, refractive index, peroxide value, iodine value, acid value, and saponification values were tested for FHPO and FHPOR as shown from Appendix Table 13 to 17.

4.4.1. Physical parameters of fried HPO

The physical parameters (moisture content, specific gravity, refractive index, pH value and viscosity) of FHPO and FHPOR were investigated before and after the addition of rosemary leaf powder Table 4.

Table 4: Result analysis of physical parameters of FHPO and FHPOR.

Para mete	**FHPO**					**Standard**	**Reference**
	1st	**3rd**	**5th**	**7th**	**9th**		
MC	0.738 ± 0.01	0.740 ± 0.11	0.770 ± 0.05	0.790 ± 1.09	1.231 ± 0.04	0.2%	(Hishamuddin *et al*, 2020; Negash, *et al.*, 2019; Purnama, *et al.*, 2020 ; Edo *et al.*, 2022; Adelagun *et al.*, 2023)
SG	0.9156 ± 0.02	0.9066 ± 0.01	0.9192 ± 0.02	0.9156 ± 0.01	0.9159 ± 0.03	0.895	
RI	1.459 ± 0.01	1.478 ± 0.02	1.489 ± 0.01	1.502 ± 0.03	1.546 ± 0.01	1.455	
pH	4.54 ± 0.03	4.42 ± 0.05	4.43 ± 0.01	4.17 ± 0.01	4.07 ± 0.02	5-7	
V	4.73 ± 1.09	77.03 ± 0.11	79.27 ± 1.21	85.35 ± 0.45	88.02 ± 0.39	50-60	
Para mete	**FHPOR**					**Standard**	
	1st	**3rd**	**5th**	**7th**	**9th**		
MC	0.220 ± 0.03	0.540 ± 0.36	0.180 ± 0.03	0.270 ± 0.11	0.130 ± 0.02	0.2%	
SG	0.9091 ± 0.01	0.9016 ± 0.02	0.893 ± 0.02	0.9007 ±0. 03	0.9083 ± 0.01	0.895	
RI	1.459 ± 0.02	1.459 ± 0.01	1.454 ± 0.02	1.459 ± 0.01	1.459 ± 0.01	1.455	
pH	4.69 ± 0.01	5.79 ± 0.02	5.54 ± 0.02	5.24 ± 0.04	4.73 ± 0.01	5-7	
V	64.84 ± 1.09	59.45 ± 0.11	55.27 ± 0.11	52.2 ± 1.32	49.02 ± 0.81	50-60	

N.B. MC = moisture content in %, SG=specific gravity, RI=refractive index, pH, and V=viscosity, were calculated as (Mean ± Standard deviation, N = 3) are significantly different $p < 0.05$.

Moisture transferred from food to oil, during frying, resulting in water loss from the food and an increase in the oil's MC, affects various physicochemical properties (Liyansan *et al*.2022; Yildiz *et al.*, 2024). An analysis of the MC of frying oils over multiple cycles showed that FHPO samples had values, all exceeding the international organization for standardization (ISO 662) and American oil chemists society (AOCS) limits, 0.2% (Begum *et al.*, 2024). This aligns with Anwar *et al.*, (2024), who noted an increase in palm oil MC from (0.08%) before frying to 0.19%, 0.29%, and 0.61% after the 1st, 2nd, and 3rd frying cycles, respectively, due to moisture transfer from the potato chips to the oil. Continued frying raises MC, this is due to oxygen exposure and excess water transfer from potatoes to oil, potentially leading to hydrolytic rancidity (Moufakkir *et al.*, 2023). Previous studies have linked high moisture levels to chemical reactions such as polymerization, oxidation, and hydrolysis (Banchode *et al*., 2021), with excessive moisture accelerating degradation and increase the formation of fatty acids (de Alzaa *et al*., 2021; Dodoo *et al*., 2022).

In contrast, FHPOR samples showed MC values, remaining near the recommended value, during the 1st fry but increased in the 3rd and 7th cycles, due to excess water from potatoes or washing. However, adding rosemary, achieving reductions of MC across the cycles. This effect is attributed to the phenolic compounds in rosemary, which have protective properties. One-way ANOVA analysis p (9.88×10^{-5}) < 0.05 and t-cal (4.535) > t-critical (1.701) confirmed significant differences between FHPO and FHPOR, highlighting the effectiveness of rosemary leaf powder in preserving optimal frying conditions and enhancing the safety and quality of fried oils by reducing MC.

The quality and purity of edible oils are significantly influenced by their specific gravity (Ahmed *et al*., 2021). According to Negash *et al*., (2019), FHPO continuously exceeded the permissible standard range of 0.891 to 0.899, after multiple frying cycles, suggesting potential deterioration and increased toxicants. This aligns with findings by Mishra *et al*., (2023) who noted that soybean oil's specific gravity increased from fresh oil value (0.911 to 0.920), 5th (0.914 to 0.922), 10th (0.916 to 0.923), suggesting that frying cycle contributes the accumulation of aromatic compounds. While FHPOR exhibited a relative decrease in SG compared to FHPO, values remained above the recommended range for all cycles except the 5th fried cycle.

The concentration of toxicants in repeatedly deep-fried HPO decreased significantly over cycles. Repeated frying leads to hydrolysis, oxidation, and polymerization, which alter oil density and specific content, which was mitigated by the antioxidant properties of rosemary leaf powder (Mishra *et al*., 2023). One-way ANOVA p (0.00078) < 0.05 and t-cal (3.768) > t-critical (1.701) indicated significant differences between FHPO and FHPOR. The efficiency of rosemary leaf powder in preserving frying quality and safety by reducing specific gravity.

Refractive index (RI) is a physical property that indicates how light passes through a material, providing insights into its chemical composition, making it crucial for assessing oil quality during multiple frying cycles (Ahmed *et al*., 2021). FHPO exhibits a higher increase in RI compared to FHPOR, attributed to the accumulation of conjugated fatty acids formed during thermal degradation, indicating greater autoxidation in FHPO (Ahmed *et al*., 2021). This aligns with Gautam, (2024), who reported that the RI of palm oil increased from 1.459 to 1.461 after frying the 5th frying cycle, suggesting that frequent frying leads to oil rancidity and discourages the reuse of vegetable oil. The addition of rosemary powder decreased the RI, indicating lower thermal degradation and suggesting that rosemary stabilizes the oil's chemical characteristics. However, the RI in FHPOR varied, notably decreasing from the 1st to 5th fry cycle due to rosemary's presence, while subsequent cycles from the 5th to 7th showed an increase, likely due to the degradation of rosemary's antioxidant properties. The stabilization of RI From the 7th to 9th cycle suggests a reached equilibrium in oil degradation. The percentage of reduced toxicants was noted, particularly at the 5th cycle with 200 mg/kg of rosemary, aligning closely with standard RI of edible Hayat palm oil 1.455 (Begum *et al.*, 2024).

One-way ANOVA analysis p (8.85×10^{-5}) < 0.05 and t-cal (4.575) > t-critical (1.70) showed significant differences between FHPO and FHPOR, this indicates the usefulness of rosemary leaf powder in maintaining optimal frying conditions and improving the safety and quality of fried oils by lowering refractive index.

The pH value, typically ranges for HPO from 5 to 7 (Edo *et al*., 2022). In this study, the pH values of fried oils were assessed, revealing that FHPO's values fell below this range. The higher acidity in FHPO suggests a significant breakdown of fatty acids during frying, which aligns with findings by Benmeziane *et al*., (2024), who reported pH decreases values in soybean and corn oil due to free fatty acid, released during repeated frying (Jaffar *et al*.,2024). This decline was catalyzed by vapors, oxygen, and water from the fried potato.

The addition of rosemary in FHPOR initially raised the pH from the 1st to 3rd cycle, though a slight decline occurred by the 9th cycle, likely due to, rosemary's ability to inhabit oil decomposition. Among all cycles, the pH in the 5th frying cycle with 200 mg/kg of rosemary remained within the standard limit. Additionally, the toxicant levels decreased over the cycles for 1st (3.2%), 3rd (23.8%), 5th (20.11 %), 7th (20.9%), and 9th (13.84%), indicating that rosemary powdered contributes to maintaining oil quality and safety by mitigating acidity and reducing toxicants.

One-way ANOVA p (1.7×10^{-7}) < 0.05 and t-cal (2.048) > t-critical (1.701) confirmed significant differences between FHPO and FHPOR, highlighting the efficiency of rosemary leaf powder in preserving conditions and improving fried oil quality.

Viscosity represents the resistance of a liquid to flow (Duguma & Abebaw, 2020). FHPO's Viscosity increased from the 1st fried 74.73 to 88.02 cP, consistently exceeding the recommended maximum range of 50–60 cP (Adelagun *et al*., 2023). This increase aligns with findings by Kung

& Hsieh, (2021), who observed that the viscosity of palm oil rises due to the formation of dimer and polymeric compounds through polymerization, resulting in carbon-carbon or carbon-oxygen–carbon linkages between fatty acids. Similarly, for the Fresh palm oil starts at 55.23 to 75.80 cP after 24th. With frying cycles, indicating oil degradation as unsaturation decreases and C=C bonds break (Ahmed *et al*., 2021). This suggests that as frying continues, FHPO gets thicker and more viscous (Ooi *et al*., 2024).

In contrast to this previous study, FHPOR maintained viscosity values decreasing from 64.838 to 49.02 cP. The lower viscosity, particularly in the 5th frying cycle with 200 mg/kg rosemary leaf powder mitigates the viscosity decrease and inhibits the formation of high molecular weight of oil toxicant effect. Rosemary's antioxidant properties may further delay oxidative polymerization, thus reducing viscosity changes (Wang *et al*., 2023). Additionally, toxicant levels decreased with rosemary, ranging from13.23 to 44.31%, indicating a positive impact in oil quality and safety.

One-way ANOVA p (8.84×10^{-13}) < 0.05 and t-cal (12.268) > t-critical (1.701) showed significant differences between FHPO and FHPOR, demonstrating the effectiveness of rosemary leaf powder in preserving optimal frying conditions and is essential for improving the safety and quality of fried oils by lowering viscosity.

4.4.2. Chemical Parameter of Fried HPO

The chemical parameters of fried Hayat palm oil (FHPO) and fried Hayat palm oil with rosemary (FHPOR) were extensively investigated before and after the addition of rosemary leaf powder as shown from Appendix Table 18 to 21. Table 5 presents the data on peroxide value, iodine value, acid value, and saponification value for both oil samples.

Table 5: Result analysis of chemical parameters of FHPO and FHPOR.

Paramete	**FHPO**					**Standard**	**Reference**
	1st	**3rd**	**5th**	**7th**	**9th**		
PV	10.82 ± 0.65	10.87 ± 1.97	11.84 ± 1.96	11.73 ± 1.86	12.57 ± 2.01	< 10	(Hishamuddin *et al*, 2020; MacArthur, *et al.*, 2021; Purnama, *et al.*, 2020)
IV	55.98 ± 1.36	55.83 ± 0.16	55.42 ± 0.43	55.24 ± 0.27	54.71 ± 1.17	45-55	
AV	3.74 ± 1.87	3.43 ± 1.08	1.87 ± 0.94	1.87 ± 0.94	1.87 ± 0.94	0.6	
SV	205.08 ± 0.54	206.01 ± 0.54	207.57 ± 0.94	207.54 ± 0.54	207.57 ± 0.94	195-205	
Paramete	**FHPOR**					**Standard**	
	1st	**3rd**	**5th**	**7th**	**9th**		
PV	8.97 ± 0.83	8.50 ± 1.48	8.01 ± 0.49	6.97 ± 0.72	6.87 ± 0.40	< 10	
IV	46.07 ± 0.52	47.35 ± 0.21	49.50 ± 0.97	48.34 ± 1.46	48.25 ± 0.17	45-55	
AV	0.743 ± 0.05	0.704 ± 0.01	0.556 ± 0.19	0.426 ± 0.12	0.374 ± 0.19	0.6	
SV	158.54 ± 1.41	194.98 ± 1.40	202.17 ± 1.81	197.31 ± 0.91	183.26 ± 1.43	195-205	

N.B. PV = peroxide value, IV = iodine value, AV = Acid value, and SV = Saponification value, were calculated as (Mean ± SD, N = 3) are significantly different $p < 0.05$.

Peroxides and hydroperoxides are the initial oxidation products of oils, characterized as unstable, odorless, and colorless (Mansour *et al*., 2022). The peroxide value (PV) quantifies the dissolved oxygen in oil serving as an indicator of oxidative degradation, freshness, rancidity, shelf life, and overall oil quality (Habarakada *et al*., 2021). In this study, the PV of FHPO increased steadily over multiple frying cycles, ranging from 10.82 to 12.57 meq O_2/kg oil, surpassing the standard limit of 10 meq O_2/kg oil (Begum *et al*., 2024). This trend indicates increase is indicative of increased rancidity, and oxidative degradation (Habarakada *et al*., 2021). At 5th and 7th fry PV decreases from 11.84 to 11.73, potentially due to variations in oxygen exposure affecting oxidation rates (Yılmaz *et al*., 2023). In contrast, the PV for frying oil with rosemary (FHPOR) ranging from 8.97 to 6.87 meq O_2/kg oil, demonstrating that lower PV correlates with better oil quality. So, in PV in FHPOR in terms of quality the nearest to the standard is the best oil quality (Moufakkir *et al*., 2022). For comparison, untreated sunflower oil reached 23 meq O_2 /Kg after 30 frying cycles, while rosemary-treated oil decreased to 9 meqO_2 /Kg, highlighting the antioxidant properties of rosemary effectively delayed oxidation and inhibited formation of excess peroxides.

Additionally, the percentage of reduced toxicants improved significantly from 17.1 to 45.4%. Moreover, the results of analysis using one-way ANOVA p (4.92×10^{-8}) < 0.05 and t-cal (7.378) > t-critical (1.701) confirmed significant differences between FHPO and FHPOR, underscoring the effectiveness of rosemary leaf powder in enhancing frying oil quality and safety by lowering peroxide values.

The iodine value (IV) measures the degree of unsaturation in fats and oils, specifically the concentration of carbon-carbon double bonds. Higher iodine values indicate greater unsaturation, making the oil susceptible to oxidation and rancidity (MacArthur *et al*., 2021; Omara *et al*., 2019). In this study, the IV of FHPO decreased from 55.98 to 54.71 g of I_2 /100g oil, were above standard range of 45 to 55g of I_2 /100g oil for HPO (Purnama *et al*., 2020). This decline suggests a loss of unsaturated bonds due to oxidation and polymerization, leading to degradation and reduced nutritional value (Omara *et al*., 2019). Gautam, (2024), also observed similar study, the reduction in IV indicates a loss of unsaturated bonds, but formed saturated compounds. The increased oxidation also raised the oil's viscosity, making the oil thicker and less fluid or high viscosity (Waqar *et al*., 2023). Therefore, the last 9st cycle, for FHPO becomes more saturated or rancid.

However, the IV of FHPOR was initially increase from 1st to 5th cycle which means, this high value of IV is due to a high content of unsaturated fatty acids essentially due to the abundance of oleic and linoleic acids, remain the oil undecomposed (Ahmed *et al*., 2024). However, the subsequent decrease from the 5th to 9th cycle suggests that rosemary's antioxidant properties reduce during further oxidation reactions. While the IV values of both oils remained within acceptable limits, FHPOR exhibited better quality due to lower levels of unsaturated and associated toxicants, which decreased percentage lowered from 11.6 to 15.8 %.

One-way ANOVA analysis p (7.85×10^{-17}) < 0.05 and t-cal (17.848) > t-critical (1.701) showed significant differences between FHPO and FHPOR. This also showed the usefulness of rosemary leaf powder in preserving ideal frying conditions and is essential for improving the safety and quality of fried oils by increasing the iodine value.

The acid value (AV) quantifies free fatty acids present in fats and oils, indicating the level of hydrolytic in rancidity and overall oil quality (Frances *et al*., 2023). Higher AV signals increased hydrolysis and reduced quality (Mansour *et al*., 2022).

In this study, the AV of FHPO decreased from 3.74 to 1.87 mg KOH/g. This decrease contrasts with findings by Chu, *et al*., (2024), which reported an increase in AV for 1st frying oils increased, indicating that oil degradation, and produce free fatty acids (Dodoo *et al*., 2022). But, after the 3rd cycle, AV decreased to the 5th cycle, due to high thermal degradation, and oxidative reach to the maximum. After the 5th cycle, the AV remains constant due to the degradation of oil to produce free fatty acids (Habarakada *et al*., 2021).

For FHPOR, the AV ranged from 0.37 to 0.74 mg KOH/g, indicating that rosemary's antioxidants properties effectively reduced free fatty acids and inhabited the lipid hydrolysis resulting in better overall quality (Banchode *et al*., 2021). But 1st and 3rd fried cycles are still above the maximum permissible value, confirming that insufficient antioxidants for detoxification. In contrast, FHPO's AV exceeded the standard for HPO (0.6 mg KOH/g) and was considered unsuitable for further frying (Begum *et al.*, 2024). Notably, the AV of FHPOR at the 5th cycle was nearly the same as the standard value. The reduction in toxicants across cycles was evident, with percentages decreasing from 70.3 to 80.13%. One-way ANOVA analysis p (4.19×10^{-6}) < 0.05 and t-cal (5.69) $>$ t-critical (1.701) confirmed significant differences between FHPO and FHPOR, indicating the effectiveness of rosemary leaf powder in enhancing frying oil safety and quality by lowering acid values.

The saponification value (SV) measures the amount of potassium hydroxide (KOH) needed to saponify one gram of the sample, reflecting the average molecular weight of fatty acids in fats and oils. This value provides insights into the oil composition and quality, indicating the presence of fatty acids with varying chain lengths (Frances *et al*., 2023). The results for FHPO showed SV increasing from 205.08 to 207.59 mg KOH/g. Similar results were reported by Gautam, (2024), who observed the SV of fresh palm oil increase from an initial 200.5 mg KOH/g to 214. 55 mg KOH/g by the 5th frying cycle, this attributed to the formation of secondary oxidation products, such as carbonyl compounds. The increases in SV for FHPO from the 1st to 9th cycles, due to the breakdown of triglycerides into free fatty acids resulted in decrease in unsaturated fatty acid composition and produce secondary compounds.

In contrast, FHPOR showed values increase from 158.54 to 202.17 mg KOH/g and then decrease from 197.31 to 183.26 mg KOH/g for the same cycles. For FHPOR, the initial increase in SV from the 1st to 5th cycles was followed by a decrease, likely from cycle 5th to 9th, this may be due to the antioxidant properties of rosemary leaf powder, which helped stabilize the fatty acid profile and reduce oxidative degradation. A high SV in FHPOR typically indicates shorter-chain fatty acids that are more easily digested, and nutritionally valuable (Banchode *et al*., 2021). While FHPO generally exceeds the standard SV of 195 to 205mg KOH/g, FHPOR values remain below this range, indicating that the molecular weight of fatty acids is affected by the addition of rosemary leaf powder (Begum *et al*., 2024). The best outcomes occurred at the 5th frying cycle with a rosemary dose of 200 mg/kg, which significantly reduced toxicants in the oil and was close to the standard.

One-way ANOVA analysis p (0.0001×10^{-8}) < 0.05 and t-cal (4.526) > t-critical (1.701) confirmed significant differences between FHPO and FHPOR, highlighting the efficacy of rosemary leaf powder in preserving ideal frying conditions and improving the safety and quality of fried oils by lowering saponification value.

4.5. Characterization of Fried Hayat Palm Oil

4.5.1. Conjugated diene value Analysis using UV-visible

The conjugated diene value (CDV) is an important measure for evaluating the stability and quality of edible oils, reflecting the extent of oxidative breakdown and free radical production due to the arrangement of double bonds in unsaturated fatty acids. Conjugated dienes, are more reactive and prone to oxidation than isolated double bonds (Kaseke *et al*., 2021). In Appendix Table 22, CDV was measured for FHPO and FHPOR during the 1st, 3rd, 5th, 7th, and 9th frying cycles. The % CDV for FHPO, in Table 6 was increase from 3.18 to 4.03 %, and then decrease from 4.03 to 3.30 %, all exceeding the standard value of 2.5 % (Chbani *et al*., 2023). The increase in CDV during the initial frying cycles (1st to 7th) can be attributed to oxidation and isomerization of linoleic fatty acids due to frequent frying and oxygen exposure (Ahmed *et al*., 2024). CDV generally rises with repeated frying but decreases at the 9th cycle due to maximum oil decomposition (Wann *et al*., 2021). A similar study by Saleh *et al*., (2021), found that fresh oil samples had CDV of 0.34 to1.01%, while in-use frying oil from restaurants ranged from 0.52 to 2.97%. This increase is linked to higher polyunsaturated fatty acids, particularly linoleic acid, and the number of frying cycles, leading to increased rancidity.

In contrast, FHPOR showed significantly lower CDV values from 0.29 to 0.64 %, indicating reduced oxidative degradation. Adding rosemary can reduce CDV by neutralizing free radicals (Nanayakkara *et al*., 2020). FHPOR showed consistency with lower CDV than FHPO, indicating reduced oxidative degradation. This is supported by Kumari *et al*., (2024), who reported a 5.2-fold increase in CDV for oils without antioxidants after 30 days, compared to a lower 3.25-fold increase with rosemary extract, which reduced by approximately 27%. Related to this present study, toxicant levels decreased across the frying cycles from 90.97 to78.4%. One-way ANOVA analysis p (7.42 X 10^{-23}) < 0.05 and t-cal (4.53) > t-critical (1.701) confirmed significant differences between FHPO and FHPOR, confirming the effectiveness of rosemary in maintaining optimal frying conditions and improving the safety and quality of fried oils.

Table 6: Result analysis of the CDV of FHPO and FHPOR using a UV-visible spectrometer.

Parameter	**FHPO**					**Standard**	**Reference**
	1st	**3rd**	**5th**	**7th**	**9th**		
CDV	3.18 ± 0.09	3.34 ± 0.09	3.45 ± 0.15	4.03 ± 0.34	3.30 ± 0.33	< 2.5 %	(Chbani, *et al.*, 2023)
Parameter	**FHPOR**					**Standard**	
	1st	**3rd**	**5th**	**7th**	**9th**		
CDV	0.29 ± 0.01	0.39 ± 0.02	0.48 ± 0.03	0.50 ± 0.02	0.64 ± 0.01	< 2.5 %	

N.B. CDV = Conjugated diene value was calculated as (Mean ± SD, N = 3) are significantly different p < 0.05.

4.5.2. Chemical Composition of Rosemary

The volatile components of rosemary leaf extracts, obtained using 99.8% methanol at room temperature and under reflux conditions, were analyzed using GC-MS with Electron Impact (EI). The data, compared to the National Institute of Standards and Technology (NIST) database, identified 19 major compounds *(*Jeruto *et al.*, 2024*)*. These compounds were calculated their percentage composition by dividing each peak area to the total peak area as follows:-

$$\boxed{\%\ \text{chemical composition} = \frac{\text{each peak area}}{\Sigma\ \text{total peak area}}\ \text{X}\ 100\ \%}$$ (Korede *et al.*, 2024).

Table 7: The chemical composition of methanolic extract of rosemary leaves powder analyzed by GC-MS.

peak №	**compound name**	**common name**	**RT**	**Peak area**	**% Peak area**
1	$C_9H_{10}O$	2-Methylenebicyclo [4.2.0] oct- 4-en-7-one	3.472	44704	0.714
2	C_8H_{10}	Methyl laurate	4.91	220815	3.525
3	C_8H_8	Benzene, ethenyl- (Styrene)	5.409	107734	1.72
4	C_8H_{10}	m-xylene and p-xylene	5.447	174855	2.79
5	$C_6H_{10}O_4$	Butane dioic acid, dimethyl ester	7.812	30697	0.49
6	$C_{14}H_{22}O$	2,4-Di-tert-butylphenol	14.683	146178	2.33
7	$C_{12}H_{14}O_4$	1,2-Benzenedicarboxylic acid, diethyl ester	15.711	536957	8.57
8	$C_{15}H_{30}O_2$	Tridecanoic acid, 12-methyl-, methyl ester	17.093	16398	0.262
9	$C_{17}H_{34}O_2$	Hexadecenoic acid, methyl ester	19.193	820800	13.102
10	$C_{16}H_{32}O_2$	Palmitic acid P639	19.534	331995	5.3
11	$C_{19}H_{34}O_2$	Methyl linoleate	20.84	723701	11.55
12	$C_{19}H_{36}O_2$	13-Octadecenoic acid, methyl ester	20.897	1581820	25.25
13	$C_{19}H_{38}O_2$	Methyl stearate	21.111	280610	4.48
14	$C_{18}H_{34}O_2$	oleic acid	21.237	323529	5.16
15	$C_{18}H_{36}O_2$	Stearic acid P80616	21.427	115363	1.84
16	$C_{18}H_{32}O_2$	Linoleic acid @P785	21.994	26820	0.43
17	$C_{15}H_{24}O_2$	Santalcamphor	22.493	29489	0.471
18	$C_{19}H_{36}O_3$	Methyl ricinoleate	22.606	709071	11.32
19	$C_{18}H_{34}O_2$	Methyl palmitoleate	22.859	43162	0.689

N.B.17)(2R,3R,4aR,5S,8aS)-2-Hydroxy-4a,5-dimethyl-3-(prop-1-en-2-yl) octahydronaphthalen1(2H)-one 18) 9-Octadecenoic acid, 12- hydroxy-, methyl ester, [R- (Z)]- The chemical composition of methanolic extracted rosemary leaves, summarized in Table 7 and Appendix Figure 13, reveals a different bioactive compound. The prominent among them are 13-octadecenoic acid, (25.25%; $C_{19}H_{36}O_2$), which exhibits anti-inflammatory, hepatoprotective, anti-androgenic, nematicide, and anti-arthritic properties (Ayoola *et al.*, 2020). Hexadecanoic Acid (13.102%: $C_{17}H_{34}O_2$), detected at 19.193 min known for anti-inflammatory, anti-bacterial, anti-oxidant, and blood cholesterol-lowering properties (Tulandi *et al.*, 2021). Additionally, 2,4-di-tert-butyl-phenol or 2,4-DTBP (2.33%; $C_{14}H_{22}O$) detected at 14.683 min has Ms ions m/z 253 $[M]^+$ is good agreement with 2,4-Bis (1,1-dimethyl ethyl)-phenol) phenolic compound exhibit anti-fungal, anti-bacterial, herbicide, food additives (antioxidant), anticancer (cytotoxic), anti-inflammatory, antiviral, phytotoxic, and nematoidal properties (F. Zhao *et al*., 2020) and Santalcamphor (0.471%; $C_{15}H_{24}O_2$), is a terpenoid compound well-known for having antioxidant qualities, detected at 22.493 min with Ms ions m/z 279.1 $[M]^+$ in Figure 14 (Candra *et al*., 2023), which is good agreement with a common name Santalcamphor contain specific hydroxyl group (-OH). These isolated through GC-MS analysis, demonstrate significant antioxidant potential, helping to scavenge free radicals, reducing oxidative stress, and potentially delaying aging processes (Zhao *et al*., 2023). Thus, these phenols can prevent several chronic diseases, including diabetes, cancer, and cardiovascular disease (Chraibi *et al*., 2020). Other notable compounds include Methyl 10-trans,12-cis-octadecadienoate or methyl linoleate (11.55%; $C_{19}H_{34}O_2$) detected at 20.84 min. This fatty acid ester has been linked to anti-cancer, anti-microbial, and anti-oxidant properties (Shahin *et al*., 2022). Rosemary extract also contains 9-Octadecenoic acid, 12-hydroxy-methyl ester, [R-(Z)]- or methyl ricinoleate (11.32%; $C_{19}H_{36}O_3$) detected at 22.61 min which have antioxidant and anti-cancer properties (Tulandi *et al.*, 2021), along with 1,2-Benzene dicarboxylic acid, diethyl ester or phthalate ester (8.57%; $C_{12}H_{14}O_4$) detected at 15.711 min, which has anti-viral, anti-inflammatory, antioxidant, and antibacterial properties and Oleic acid (5.16%; $C_{18}H_{34}O_2$) with peak 21.237 min known for its antibacterial, anti-inflammatory, and anti-cancer qualities (Lamloum *et al*., 2023; Perera *et al*., 2021).

overall, the GC-MS analysis highlights the high prevalence of fatty acids and phenolic compounds in rosemary, underscoring its potential as a functional ingredient with significant health benefits, particularly due to its antioxidant and anti-inflammatory properties.

4.5.3. Chemical Composition of Fatty Acid in Fried Hayat Palm Oil

The study investigated the impact of rosemary leaf powder on the chemical profile and toxicants in repeatedly deep-fried HPO using GC-MS analysis. Fatty acids were expressed as % of total fatty acids. $\boxed{\%\ \text{fatty acid} = \frac{\text{each peak area}}{\Sigma\ \text{total peak area}}\ \text{X}\ 100\ \%}$ (Korede *et al*., 2024).

Table 8: Summarizes the percentage peak areas and retention times for the total fatty acid result from GC-MS (FHPOR).

peak №	**Formula**	**types of fatty acid methyl ester**	**RT**	**Area**	**% Peak area**
1	$C_{13}H_{26}O_2$	Lauric acid	14.777	3019244	0.561
2	$C_{15}H_{30}O_2$	Myristic acid	17.118	14920663	2.77
3	$C_{17}H_{32}O_2$	Methyl palmitoleate	19.01	3085233	0.573
4	$C_{17}H_{34}O_2$	Palmitic acid	19.351	189998786	35.279
5	$C_{18}H_{36}O_2$	Heptadecanoic acid	20.203	2243129	0.417
6	$C_{19}H_{36}O_2$	13-Octadecenoic acid	21.061	259976671	48.272
7	$C_{19}H_{38}O_2$	Methyl stearate	21.294	43707047	8.115
8	$C_{19}H_{36}O_2$	Oleic acid	21.338	2457239	0.4563
9	$C_{20}H_{38}O_2$	(E)-9-Octadecenoic acid ethyl ester	21.559	1512822	0.281
10	$C_{21}H_{40}O_2$	cis-13-Eicosenoic acid	22.688	4272561	0.793
11	$C_{21}H_{42}O_2$	Eicosanoic acid	22.897	9441326	1.753
12	$C_{23}H_{46}O_2$	Methyl 20-methyl-heneicosanoate	24.499	1799182	0.334
13	$C_{25}H_{50}O_2$	Tetracosanoic acid	26.001	2132952	0.396

In the above Table 8 and Appendix Figure 15, thirteen fatty acids were detected in each of the examined FHPOR samples. Among these, the most dominant peaks were 13-octadecanoic acid, which accounted for 48.272% of the total percentage area and was detected (molecular formula: $C_{19}H_{36}O_2$), and palmitic acid, with a percentage area 35.279% (molecular formula: $C_{17}H_{34}O_2$).

Additionally, methyl stearate was identified, with a peak area of 8.115% (molecular formula: $C_{19}H_{38}O_2$). Other identified fatty acids such as myristic acid, which had a peak area of 2.77% (molecular formula: $C_{15}H_{30}O_2$), as well as eicosanoic acid indicates a peak area of 1.753% (molecular formula: $C_{21}H_{42}O_2$). Lastly, lauric acid was detected with a peak area of 0.561% (molecular formula: $C_{13}H_{26}O_2$). The presence of oleic acids ($C_{19}H_{36}O_2$; 0.4563 %) in FHPOR, enhanced by the addition of rosemary, indicates that this oil retains its beneficial properties without decomposition at 21.338 min. Oleic fatty acids, in palm oil may help lower bad cholesterol and reduce heart disease (Stavila *et al*., 2023).

Table 9: Summarizes the percentage peak areas and retention times for the total fatty acid result from GC-MS (FHPO).

peak №	**Formula**	**types of Fatty acid methyl esters**	**RT**	**Area**	**% Peak Area**
1	$C_{13}H_{26}O_2$	Lauric acid	14.777	1902349	0.529867
2	$C_{15}H_{30}O_2$	Myristic acid	17.105	8381588	2.33455
3	$C_{17}H_{32}O_2$	Methyl palmitoleate	19.011	1928451	0.537137
4	$C_{17}H_{34}O_2$	Palmitic acid	19.345	1.28E+08	35.68191
5	$C_{18}H_{36}O_2$	Heptadecanoic acid	20.184	1116381	0.310949
6	$C_{19}H_{36}O_2$	13-Octadecenoic acid	21.061	1.73E+08	48.31474
7	$C_{19}H_{38}O_2$	Methyl stearate	21.206	28929275	8.057761
8	$C_{19}H_{36}O_2$	9-Octadecenoic acid (Z)-	21.275	911178	0.253793
9	$C_{19}H_{34}O_2$	Methyl 10-trans,12-cis-octadecadienoate	21.32	1006704	0.2804
10	$C_{19}H_{36}O_3$	Oxirane octanoic acid, 3-octyl-	22.506	1090903	0.303853
11	$C_{21}H_{40}O_2$	cis-13-Eicosenoic acid	22.682	2153457	0.599809
12	$C_{19}H_{36}O_3$	Octadecanoic acid, 10-oxo-	22.72	1626129	0.452931
13	$C_{21}H_{42}O_2$	Eicosanoic acid ME P1072	22.884	5347137	1.489355
14	$C_{19}H_{38}O_4$	Octadecanoic acid, 9,10-dihydroxy-	24.234	963030	0.268236
15	$C_{23}H_{46}O_2$	Behenic acid	24.493	997263	0.277771
16	$C_{25}H_{50}O_2$	Tetracosanoic acid	26.001	1101977	0.306937

The GC-MS analysis of FHPO samples, detailed in Table 9 and Appendix Figure 16, identified 16 different fatty acid methyl esters. In the sample without rosemary, predominant fatty acids included 13-octadecenoic acid ($C_{19}H_{36}O_2$; 48.315 %), and palmitic acid ($C_{17}H_{34}O_2$; 35.68%). Additionally, fatty acids detected such as myristic acid ($C_{15}H_{30}O_2$; 2.335%) eicosanoic acid (1.489% peak area, at 22.884-minute, $C_{21}H_{42}O_2$), lauric acid (0.52987% peak area, at 14.777-minute, $C_{13}H_{26}O_2$). Moreover, the FHPO sample showed new peaks potentially harmful secondary compounds: an epoxide (3-Octyl-2,3-epoxyoctanoate; $C_{19}H_{36}O_3$), an alcohol (Methyl 9,10-dihydroxystearate; $C_{19}H_{36}O_3$), a ketone (Methyl 10-oxostearate; $C_{19}H_{38}O_4$).

These compounds are associated with serious health risks, such as cardiovascular diseases, diabetes, colon cancer, neurodegenerative diseases, and aging (Nid *et al*., 2024). Additionally, this study, identified Methyl 10-trans,12-cis-octadecadienoate ($C_{19}H_{34}O_2$; 0.2804%), a conjugated diene of linoleic acid with a 0.2804%. Research by Mechqoq *et al*.,(2021), indicates that repeated frying palm oil results in the formation of hydro-peroxides from the breakdown of omeg-6 essential fatty acids (Shahidi & Yeo, 2020). Consuming deep-fried foods, like potato chips, can generate harmful byproducts including peroxides, Ketones, aldehydes, alcohols, free radicals, and epoxide which can lead to rancid tastes and odors from oxidation at n-6 double bonds (Ujong *et al*.,2023; Mohammadi *et al*., 2021).

However, the addition of rosemary led to a significant reduction in the concentrations of several fatty acids and complete removal of some toxic substances with 200 mg/kg of rosemary leaf powdered effectively preventing the formation of epoxides, alcohols, ketones and conjugated diene of linoleic fatty acids were missing in FHPOR, but present oleic acid. The presence of polyphenol antioxidants like 2,4-DTBP and Santalcamphor in rosemary is likely responsible for this inhibition (Kedir *et al*.,2023). Overall, incorporating rosemary leaf powder into repeatedly deep-fried Hayat palm oil enhances its chemical profile, reducing harmful compounds and supporting healthier cooking practices through the use of natural antioxidants.

4.5.4. Heavy Metal Content in Fried Hayat Palm Oil

This study evaluates the impact of rosemary leaf powder 200mg/kg at 5th fried on heavy metal contamination in HPO subjected to repeated deep frying. The analysis revealed concerning levels of heavy metals in both the control (FHPO) and rosemary-treated (FHPOR) palm oil samples from Appendix Table 23 and Figure 17 calibration curves were calculated for Pb, Fe, Cu, Cd, As, and Hg. Vegetable oils may contain heavy metals from a variety of sources, such as environmental pollution, and contamination during extraction and storage (Ntube *et al*., 2024).

Table 10: Result analysis of some selected heavy metals of FHPO and FHPOR using atomic absorption spectroscopy (AAS).

Heavy metals	**FHPO (mg/100g)**	**FHPOR (mg/100g)**	**Standard (mg/100g)**	**Reference**
Lead (Pb)	0.10	0.01	0.05	(Lin *et al*., 2024)
Iron (Fe)	0.02	0.10	1.50	(Al-Akayleh *et al*., 2024)
Copper (Cu)	0.11	0.10	0.10	
Cadmium (Cd)	0.12	0.01	0.05	(Wathum, 2021)
Arsenic (As)	0.11	0.01	0.01	(Enemuor *et al*.,2021)
Mercury (Hg)	0.10	0.01	0.05	(Code, 2021)

In Table 10, FHPO exhibited higher concentrations of Pb (0.10mg/100g), Fe (0.02 mg/100g), Cu (0.11 mg/100g), Cd (0.12 mg/100g), As (0.11 mg/100g), and Hg (0.10 mg/100g) while FHPOR showed much lower values: Pb (0.01 mg/100g), Fe (0.10 mg/100g), Cu (0.10 mg/100g), Cd (0.01 mg/100g), As (0.01 mg/100g), and Hg (0.01 mg/100g). This suggests that rosemary leaf powder significantly reduces heavy metal contamination. For example, the Lead (Pb) concentration in FHPO (0.10 mg/100g) exceeded the WHO/FAO standard of 0.05 mg/g, while FHPOR achieved an 88.7% reduction to 0.01 mg/100g. The neurological and carcinogenic risks associated with elevated lead levels have been well documented (Gungshik *et al*.,2023).

Similarly, while Iron (Fe) levels in FHPO (0.02 mg/100g) were below the 1.50 mg/g WHO/FAO standard (Blessing, *et al*., 2024), it increased to 0.10 mg/100g in FHPOR, remaining within safe limits. This slight increase may be attributed to the rosemary leaf content Makhamra, (2023), although Fe was below the standard, the formation of free radicals and accelerated oxidation processes (Ghosh *et al*., 2020). The copper (Cu) concentration in FHPO (0.11 mg/100g) exceeded the WHO/FAO limit of 0.10 mg/g, while FHPOR showed a minimal reduction (3.85%) to 0.10 mg/g, in line with safety guidelines. Excess copper intake has been linked to neurological disorders (Blessing *et al*., 2024). Cadmium (Cd) levels in FHPO (0.12 mg/100g) increased the 0.05 mg/g limit with implications for serious health problems, such as carcinogenicity, kidneys, lungs, bones, stomach, and prostate (Adeyeye *et al*., 2022; Ali *et al*., 2023). But, after adding rosemary Cd level decreased to 0.01 mg/100g in FHPOR was markedly lower a reduction of 93.75%. Similarly, the Arsenic (As) concentration in FHPO (0.11 mg/100g) exceeded the WHO/FAO limit of 0.01 mg/g, but decreased by 95.5% to 0.01 mg/100g in FHPOR, reducing risks associated with As level can cause health problems including illnesses, neurological problems, gastrointestinal, hematological, renal, hepatic, and reproductive issues as well as being carcinogenic and mutagenic (Isiodu *et al*., 2024). Mercury (Hg) concentration in FHPO (0.10 mg/100g) was also above the 0.05 mg/g WHO/FAO limit with potential neurological consequences and carcinogenic risks (Mallongi *et al*., 2023). But, after the rosemary addition, the mercury level was decreased by 90.72% to 0.01 mg/100g in FHPOR. Statistical analysis using one-way ANOVA p (0.45) > 0.05 and t-cal (-0.79) < t-critical (2.23) showed insignificant differences between FHPO and FHPOR. However, the addition of rosemary significantly reduced heavy metal concentration to 61.3%. This reduction is attributed to the presence of 2,4-DTBPa and Santalcamphor in rosemary, which possesses antioxidant and metal-chelating properties effectively binding and sequestering heavy metals.

Table 11: Method Validation Parameters for heavy metals in FHPO and FHPOR Using AAS

Heavy metal	**Permissible limit (mg/100g)**	**FHPO (µg/ml)**		**FHPOR (µg/ml)**		**Linearity ($R^2 > 0.95$)**	
		LOD	**LOQ**	**LOD**	**LOQ**	**FHPO**	**FHPOR**
Pb	0.05	2.14	7.14	2.63	8.75	0.9983	0.9948
Fe	1.50	2.53	8.42	2.50	8.33	0.9991	0.9643
Cu	0.10	2.33	7.78	2.47	8.22	0.9959	0.9564
Cd	0.05	2.57	8.57	2.40	8.00	0.9735	0.9868
As	0.01	2.24	7.46	3.00	10.0	0.9891	0.9423
Hg	0.05	1.10	3.67	2.00	6.67	0.9973	0.9643

In the above Table 11, the R^2 values for most metals in FHPO and FHPOR range from 0.9564 to 0.9991, indicating strong linearity and a reliable, consistent relationship between metal concentration and absorbance. This suggests that the FAAS method is accurate and precise, allowing for reliable quantification of metal concentrations across a wide range. However, the R^2 value for arsenic in FHPOR which is 0. 9423, the lowest in the dataset, indicates weaker linearity and less consistency in measurement. This may be due to interference from rosemary or other compounds in FHPOR that affect arsenic's absorbance at the measured wavelength, making arsenic less reliable quantified in FHPOR compared to FHPO.

Limits of Detection (LOD) and Limits of Quantification (LOQ): assess the sensitivity of the method for detecting and quantifying low metal concentrations. In FHPO, Hg (LOD =1.1 µg/ml) and Pb (LOD =2.1 µg/ml) have low LODs, indicating high sensitivity and precise detection at trace levels, which is ideal for identifying contaminations in food products. Similarly, Fe and Cu also show low LODs and LOQs, suggesting the method's overall good sensitivity in FHPO. In contrast, FHPOR shows higher LOD and LOQ, especially for As (3.0 µg/ml and 10.0 µg/ml respectively), indicating that As is harder to detect in FHPOR, likely due to interference from rosemary or other matrix components. Rosemary compounds may bind to metals, reducing their availability for absorption and lowering sensitivity. Therefore, the AAS method performs better in FHPO, where the simpler matrix results in lower LODs and stronger linearity, while in FHPOR, the complex matrix introduces interference that impacts the detection and quantification of metals, especially arsenic. Generally, the AAS instrument is sensitive enough to reliably detect the above heavy metals, as their LOD and LOQ values are below acceptable limits.

CHAPTER-FIVE

5. CONCLUSION AND RECOMMENDATION

5.1. CONCLUSION

This study optimized by incorporating powdered rosemary leaves into repeatedly deep-fried Hayat palm oil significantly improves oil quality and safety. A study found that adding 200 mg/kg of rosemary enhances key physicochemical properties, resulting in more stable and less hazardous oil. The FHPOR exhibited positive changes ($p < 0.05$) in moisture content, specific gravity, pH value, refractive index, viscosity, peroxide value, iodine value, acid value, and saponification value, along with increased oxidative stability. The conjugated diene value demonstrated that rosemary addition improved oil stability, achieving in removal efficacy of 86.214%.

Using the Folin-Ciocâlteu reagent method, the total polyphenol content (TPC) reached 41.81 mg GAE/g. GC-MS analysis identified significant antioxidants in the methanolic rosemary extract, such as 2,4-DTBP, and Santalcamphor, which effectively reduced their oxidative degradation in FHPOR. This reduction is evidenced by decreased harmful carbonyl compounds including ketones, alcohol, epoxides, and conjugated diene value of linoleic acid (CDV), and improved fatty acid profiles. Also, oleic acid in FHPOR confirms that the oil fried at 200mg/kg of rosemary has not decomposed. The addition of rosemary leaf powder significantly reduces heavy metal contamination in FHPO, making FHPOR a safer product for consumption. While FHPO exhibited elevated concentration and all except Fe, exceeding permissible limits and posing health risks, FHPOR showed much lower levels, within safety guidelines. Notably, rosemary reduced copper by 3.85%, lead by 88.7%, cadmium by 93.75%, arsenic by 95.5 %, and mercury by 90.72%. This reduction is attributed to the metal-chelating and antioxidant properties of rosemary, resulting in a total reduction of heavy metals to 61.3%. Overall, the findings support using powdered rosemary leaves as a natural additive to frying oils, enhancing oil stability and promoting healthier cooking practices. This sustainable option benefits the food industry by advancing safer food preparation techniques and contributing to healthier fried food products.

5.2. RECOMMENDATION

Many women in Tigrai use Hayat palm oil to fry foods like chips, to mitigate health risks, it is recommended to add 200mg/kg of rosemary leaf powder to 2 L of fresh HPO can be fry the oil up to the 5th fry cycle. This natural antioxidant helps prevent lipid degradation and improve food safety. Public awareness campaigns should educate food vendors and consumers on the benefits of rosemary as a natural antioxidant, promoting healthier cooking and eating habits. Future research should explore the effect of rosemary leaf powder on a wider range of frying oils and cooking environments. Investigation of additional parameters related to frying oil safety and nutritional quality can significantly improve public health outcomes in the region. Expanding the study to include various oils will enhance the generalizability of the findings and provide deeper insights into rosemary leaf powder’s role in promoting safer, healthier cooking practices.

REFERENCE

Abdullahi, N., Umar, N., Tsoho, A., Sani, A., Yazeed, Z., Tsangaya, M., Abdullahi, U. (2023). Nigerian Palm Oil: Quality Disparity, Contamination and Processing Wastes Handling. FUDMA Journal of Sciences, 7(1), 126-135.

Abed, S. M., Mohammad, S. M., Hassan, Z., Muhammad, A., & Rajamanickam, S. (2023). Fabrication of UV zno NRS photodetector based on seeded silicon substrate via the drop-casting technique. Microelectronics International, 40(1), 35-45.

Abeshu, Y. (2023). Review on deep fat-fried food products safety and its implication for consumer healthiness. Agriculture and Food Sciences Research, 10(2), 14-27.

Abiodun, A. J., Alamu, G. A., Daramola, O. O., Adedokun, O., & Sanusi, Y. K. (2024). A Green Synthesis of Copper Oxide Nanoparticles for Improved Performance in Monolithic Dye Sensitized Solar Cells. Fountain Journal of Natural and Applied Sciences, 13(2).

Abiodun, G. W., Kolade, R. A., & Adeyinka, O. J. (2020). Comparative analysis of the effects of domestic frying and storage on some selected oil samples from local and commercial sources. Earthline Journal of Chemical Sciences, 3(1), 17-34.

Adelagun, R., Berezi, E., Fagbemi, J., Igbaro, O., Aihkoje, F., Ngana, O., & Garba, M. (2023). Evaluation of level of rancidity of edible oil in some fried snacks food. Journal of Chemical Society of Nigeria, 48(1).

Adeyeye, E., Akinyeye, R., & Adesina, A. (2022). Concentration Of Trace Metals In The Fresh And Fried Edible Vegetable Oils Used In The Production Of Plantain Chips In Ekiti State: Health Implications. J Traditional Med Applications, 1 (1), 31-39. In: EI Adeyeye, Department of Chemistry, Faculty of Science, Ekiti State ….

Ahmed, I., Farooq, M. F., Rani, I., Zulfiqar, H., Hussain, I., Zulfiqar, H., & Jan, A. (2023). Unraveling the Challenges of Oxidative Stability and Methods for Assessing Oxidation of Commercial Oils: A Review. Journal of Chemistry and Environment, 52-97.

Ahmed, M. N., Abourat, K., Gagour, J., Majourhat, K., Koubachi, J., & Gharby, S. (2024). Valorization of saffron (Crocus sativus L.) Stigma as a potential natural antioxidant for soybean (Glycine max L.) Oil stabilization. Heliyon, 10(4).

Ahmed, W., Shabbir, M. A., Aadil, R. M., & Zia, M. A. (2021). Quality assessment of used edible fats and oils by local vendors of Faisalabad. Pakistan Journal Of Agricultural Sciences, 58(6).

Al-Akayleh, F., Abu-Nameh, E., Qutishat, S., Ahmad, R., & Agha, A. (2024). Determination of Heavy Metal Concentrations in Commercial Edible Vegetable Oil Sold in the Jordanian Market by Inductively Coupled Plasma Optical Emission Spectrometry. Jordan Journal of Chemistry (JJC), 19(1), 19-24.

Alexandre, E. M., Saraiva, J. M., & Pintado, M. (2022). Technologies to Recover Polyphenols from agrofood By-Products and Wastes: Academic Press.

Ali, A., Bashmil, Y. M., Cottrell, J. J., Suleria, H. A., & Dunshea, F. R. (2021). Lc-ms/ms-qtof screening and identification of phenolic compounds from australian grown herbs and their antioxidant potential. Antioxidants, 10(11), 1770.

Ali, W., Bian, Y., Zhang, H., Qazi, I. H., Zou, H., Zhu, J., & Liu, Z. (2023). Effect of cadmium exposure during and after pregnancy of female. Environmental Pollutants and Bioavailability, 35(1), 2181124.

Aly, A., Ali, H., & Abdeldaiem, M. (2021). Improvement of the sunflower oil stability by blending with moringa or sesame oils. Slovak Journal of Food Sciences, 15.

Amalraj, A., Kuttappan, S., AC, K. V., & Matharu, A. (2022). Herbs, Spices and Their Roles in Nutraceuticals and Functional Foods: Elsevier.

Ameen, M., Zafar, M., Ahmad, M., Munir, M., Abid, I., Mustafa, A. E.-Z. M.,Yuldashev, A. (2023). Cleaner biofuel production via process parametric optimization of nonedible feedstock in a membrane reactor using a titania-based heterogeneous nanocatalyst: an aid to sustainable energy development. Membranes, 13(12), 889.

Amran, N. A., Bello, U., & Ruslan, M. S. H. (2022). The role of antioxidants in improving biodiesel's oxidative stability, poor cold flow properties, and the effects of the duo on engine performance: A review. Heliyon, 8(7).

Amsalu, H., Wondimnew, T., Mateos, T., Fekadie, M., & Bogale, G. (2020). The effect of palm oil-fried street kokor on liver and kidney biomarkers of Swiss albino mice. Journal of lipids, 2020(1), 8819749.

Anwar, H., Hussain, A., Samin, G., Kausar, T., Rehman, A., Sharif, M. A., Nisar, R. (2024). Evaluation of Quality and Sensory Attributes of Potato Chips Fried in Different Oils and

Their Blends, and Chemical Changes Occurred in Oils During Different Frying Counts. CHEMICA: Jurnal Teknik Kimia, 11(1).

Arce-Saldaña, L., Soto, G., Herrera, J. R., Simakov, A., & Flores, U. C. (2023). Compact device for in situ ultraviolet–visible spectrophotometric measurement of photocatalytic kinetics. Review of Scientific Instruments, 94(8).

Aslam, F., Iqbal, S., Imran, M., Rebezov, M., Chumakov, V., Kenijz, N., & Shariati, M. A. (2021). Physicochemical properties of chemically interesterified vegetable oils. Journal of microbiology, biotechnology and food sciences, 10(5), e4291-e4291.

Asouzu, N. C., Ifunanya, O. A., Aja, P. M., Ben, O. M., Asouzu, N. C., Lucy, A., Chinaza, A. G. (2023). Physicochemical and Fat-Soluble Vitamins Constituents of Fresh and Reused Vegetable Oil from Abakaliki Metropolis, Ebonyi State. Jurnal Multidisiplin Madani, 3(9), 1986-1998.

Asrade, B., & Ketema, G. (2023). Determination of the selected heavy metal content and its associated health risks in selected vegetables marketed in Bahir Dar town, Northwest Ethiopia. Journal of Food Quality, 2023(1), 7370171.

Assefa, D., Dessalegn, E., & Abegaz, K. (2024). Effect of kesse, koseret, and tosign extract treatments on the oxidative stability of oil during the repeated frying of potato chips. Heliyon, 10(17).

Ayoola, A., Ekunseitan, D., Muhammad, S., Oguntoye, M., & Adejola, Y. (2020). Phytochemicals analysis and GC-MS determination of ethanolic extracts of Azadirachta indica and Mangifera indica stem bark and their biological potentials. The Pac J Sci Technol, 21(1), 219-222.

Ayouaz, S., Bensadia, D., Hamitri-Guerfi, F., Muhammad, D. R. A., Mouhoubi, K., Arab, R., . . . Madani, K. (2022). Impact of incorporating sesame oil (Sesamum indicum L.) In an Algerian frying oil and margarine formulation. The North African Journal of Food and Nutrition Research, 6(14), 165-177.

Bajo-Fernández, M., Montero, G., Alonso-Herranz, V., Barbas, C., Rey-Stolle, F., & García, A. (2024). Structural elucidation of derivatives of polyfunctional metabolites after methyl chloroformate derivatization by high-resolution mass spectrometry gas chromatography. Application to microbiota metabolites. Journal of Chromatography A, 1717, 464656.

Banchode, R., Bhallamudi, S. P., & Kanchana, S. (2021). Evaluation of the Quality of Commonly Used Edible Oils and The Effects of Frying. The Scientific Temper, 12(1&2), .-.

Beals, K. A. (2019). Potatoes, nutrition and health. American journal of potato research, 96(2), 102-110.

Begum, R., Hasan, M., Akter, S., & Rahman, M. (2024). Fortified edible oils in Bangladesh: A study on vitamin A fortification and physicochemical properties. Heliyon, 10(3).

Benmeziane, F., Araba, K., & Belahcene, A. (2024). Impact of deep-fat frying cycles on the physicochemical characteristics of two edible vegetable oils marketed in Algeria. The North African Journal of Food and Nutrition Research, 8(17), 21-31.

Berger, T., & Trunschke, A. (2021). Optical Properties: UV/Vis Diffuse Reflectance Spectroscopy and Photoluminescence. Metal Oxide Nanoparticles: Formation, Functional Properties, and Interfaces, 2, 435-482.

Beya, M. M., Netzel, M. E., Sultanbawa, Y., Smyth, H., & Hoffman, L. C. (2021). Plant-based phenolic molecules as natural preservatives in comminuted meats: A review. Antioxidants, 10(2), 263.

Bianchin, M., Pereira, D., Almeida, J. D. F., Moura, C. D., Pinheiro, R. S., Heldt, L. F. S., . . . Carpes, S. T. (2020). Antioxidant properties of lyophilized rosemary and sage extracts and its effect to prevent lipid oxidation in poultry pátê. Molecules, 25(21), 5160.

Bikila, A. M., Tola, Y., Esho, T. B., & Forsido, S. F. (2020). Effect of predrying treatment and drying temperature on proximate composition, mineral contents, and thermophysical properties of anchote (Coccinia abyssinica (Lam.) Cogn.) Flour. Food science & nutrition, 8(10), 5532-5544.

Blessing, O.-O. M., Vera, I. C., & Eka, E. B. (2024). Polycyclic Aromatic Hydrocarbons Contamination and Quality of Locally Produced Crude Palm Oil in South-South Zone, Nigeria. European Journal of Nutrition & Food Safety, 16(5), 159-174.

Borsato, d., Spacino, K. R., Angilelli, K. B., Gonçales Filho, J., Marcheafave, G. G., & Mantovani, A. C. G. (2020). The effect of Cr3+, Co2+, Fe2+ and Fe3+ ions on the oxidative stability and kinetics of biodiesel oxidation reaction with and without the addition of rosemary extract. Revista Virtual de Química, 12(4).

Bouizgma, k., abourriche, a., rabbah, n., & zakari, a. (2023). Food strategy: Antioxidants Synergistic effect of natural plant extracts. Journal of Analytical Sciences and Applied Biotechnology, 5(1).

Candra, R. M., Isnindar, I., & Luliana, S. (2023). Isolasi Dan Identifikasi Terpenoid Fraksi Heksan Daun Premna serratifolia L. Menggunakan GC-MS. Journal Syifa Sciences and Clinical Research (JSSCR), 5(2).

Carpentieri, M. A., & Domenici, V. (2024). Introducing UV–visible spectroscopy at high school level following the historical evolution of spectroscopic instruments: a proposal for chemistry teachers. Foundations of Chemistry, 26(1), 115-139.

Cavalcanti, R., Koshima, C., Forster-Carneiro, T., Gomes, M., Rostagno, M., Prado, J., & Meireles, M. (2022). Uses and applications of extracts from natural sources.

Ceylan, M. M., & Baştürk, A. (2023). Thermal oxidation, 3-MCPD and glycidyl esters formation in hazelnut oil enriched with natural extracts during French fries production. Journal of Food Measurement and Characterization, 17(1), 33-45.

Chaqroune, A., & Taleb, M. (2022). Effects of extraction technique and solvent on phytochemicals, antioxidant, and antimicrobial activities of cultivated and wild rosemary (Rosmarinus officinalis L.) From Taounate region. Biointerface Res. Appl. Chem, 12, 8441-8452.

Chathiran, W., On-nom, N., Somsong, P., Tiyayon, P., Niranjan, K., & Srichamnong, W. (2024). The efficacy and lipid degradation properties resulting from corncob biochar treatment for acrylamide reduction in reused palm oil. LWT, 192, 115720.

Chbani, M., El Harkaoui, S., Willenberg, I., & Matthäus, B. (2023). Analytical extraction methods, physicochemical properties and chemical composition of cactus (Opuntia ficus-indica) seed oil and its biological activity. Food Reviews International, 39(7), 4496-4512.

Cheng, X., Zang, M., Wang, S., Zhao, X., Zhai, G., Wang, L., Yue, Y. (2022). Physicochemical and Antioxidant Properties of Nanoliposomes Loaded with Rosemary Oleoresin and Their Oxidative Stability Application in Dried Oysters. Bioengineering, 9(12), 818.

Chew, C. L. (2021). Quality Improvement of Crude Palm Oil via in situ Washing with Treated Aerobic Liquor: Process Development and Product Evaluation. Monash University, Chowdhury, S. R. (2023). The Study of Physicochemical Properties of Edible Oil and Heated Oil and Evaluation of The Changes of Oil Characteristics After Reheating. Chattogram Veterinary & Animal Sciences University, Khulshi, Chattogram,

Chraibi, M., Farah, A., Elamin, O., Iraqui, H. M., & Fikri-Benbrahim, K. (2020). Characterization, antioxidant, antimycobacterial, antimicrobial effcts of Moroccan rosemary essential oil, and its synergistic antimicrobial potential with carvacrol. Journal of advanced pharmaceutical technology & research, 11(1), 25-29.

Christodoulou, M. C., Orellana Palacios, J. C., Hesami, G., Jafarzadeh, S., Lorenzo, J. M., Domínguez, R.,Hadidi, M. (2022). Spectrophotometric methods for measurement of antioxidant activity in food and pharmaceuticals. Antioxidants, 11(11), 2213.

Chu, M., Noh, E., & Lee, K.-G. (2024). Analysis of oxidation products and toxic compounds in edible and blended oil during the deep-frying of french fries. Food Science and Biotechnology, 1-13.

Code, q. (2021). Health risk assessment of heavy metals in commonly consumed cooking oils in ibadan metropolis. Int. J of Forensic Med Invest.| Vol, 7(1), 30.

Conrad, J. K., Rollins, H. W., Peterman, D. R., & Fox, R. V. (2024). Design of a high-temperature cell for cobalt-60 irradiations of aqueous solutions with in situ UV–visible spectroscopy. Review of Scientific Instruments, 95(2).

Dangal, A., Tahergorabi, R., Acharya, D., Timsina, P., Rai, K., Dahal, S.,Giuffrè, A. M. (2024). Review on deep-fat fried foods: physical and chemical attributes, and consequences of high consumption. European Food Research and Technology, 250(6), 1537-1550.

Daniel, T., Eriba-Idoko, F., Tsor, J., Kungur, S., Enokela, E., Gbaorun, F., Ushie, P. (2021). Effects of Repeated Frying on Physical Properties of Cooking Oil obtained from Local Markets in Makurdi Metropolis, Benue State, Nigeria. Journal of the Nigerian Society of Physical Sciences, 469-476.

De Alzaa, F., Guillaume, C., & Ravetti, L. (2021). Evaluation of Chemical and Nutritional Changes in Chips, Chicken Nuggets, and Broccoli after Deep-Frying with Extra Virgin Olive Oil, Canola, and Grapeseed Oils. Journal of Food Quality, 2021(1), 7319013.

Demgne Loungaing, V., Tonfack Djikeng, F., Boungo Teboukeu, G., Njike Ngamga, F. H., & Womeni, H. M. (2023). The effect of soursop-flower-enriched fried palm olein on some biochemical and hematological parameters of rats. Food science & nutrition, 11(6), 2798-2810.

Dodoo, D., Adjei, F., Tulashie, S. K., Adukpoh, K. E., Agbolegbe, R. K., Gawou, K., & Manu, G. P. (2022). Quality evaluation of different repeatedly heated vegetable oils for deep-frying of yam fries. Measurement: Food, 7, 100035.

Duguma, S., & Abebaw, G. (2020). Quality assessment of oil used for frying of potato chips: In the case of Wolkite University community. American Journal of Bioscience and Bioengineering, 8(5), 92-98.

Edo, G. I., Makinde, M. G., Nwosu, L. C., Ozgor, E., & Akhayere, E. (2022). Physicochemical and pharmacological properties of palm oil: an approach for quality, safety, and nutrition evaluation of palm oil. Food Analytical Methods, 15(8), 2290-2305.

El Maouardi, M., Kharbach, M., Cherrah, Y., De Braekeleer, K., Bouklouze, A., & Vander Heyden, Y. (2023). Quality control and authentication of Argan oils: Application of advanced analytical techniques. Molecules, 28(4), 1818.

Elamin, N. Y. (2019). Investigation of Physicochemical, Spectroscopic Characteristics and the Concentration of Some Metals in Canola Oil. International Research Journal of Pure and Applied Chemistry, 17(4), 1-7.

Enemuor, S., Adige, A., & Okechukwu, V. (2021). Heavy metals and microbial contamination of palm oil produced and sold at some markets in Kogi East Area, Kogi State, Nigeria. African Journal of Microbiology Research, 15(8), 454-460.

Erickson, M. D., Yevtushenko, D. P., & Lu, Z.-X. (2023). Oxidation and thermal degradation of oil during frying: A review of natural antioxidant use. Food Reviews International, 39(7), 4665-4696.

Esfarjani, F., Khoshtinat, K., Zargaraan, A., Mohammadi-Nasrabadi, F., Salmani, Y., Saghafi, Z., . . . Bahmaei, M. (2019). Evaluating the rancidity and quality of discarded oils in fast food restaurants. Food science & nutrition, 7(7), 2302-2311.

Fabjanowicz, M., Różańska, A., Abdelwahab, N. S., Pereira-Coelho, M., da Silva Haas, I. C., dos Santos Madureira, L. A., & Płotka-Wasylka, J. (2024). An analytical approach to determine the health benefits and health risks of consuming berry juices. Food Chemistry, 432, 137219.

Fajriati, I., Aji, T., Dhemi, P., Kumalawati, D. A., & Puspitaningrum, R. (2023). Purification of used cooking oil of shredded chicken using activated carbon from coconut shell. Paper presented at the AIP Conference Proceedings.

Fariha, T. T. (2020). formulation and quality evaluation of baked tortilla chips supplemented with pumpkin seed flour. Chattogram Veterinary and Animal Sciences University Chattogram-4225, Bangladesh,

Fatima, S., Kumar, V., Bhadauria, G., & Verma, H. (2023). Quality indicators based rapid test kits for detection of frying oil quality: A review. Food Chemistry Advances, 2, 100305.

Ferraz-Almeida, R., Spokas, K. A., & De Oliveira, R. C. (2020). Columns and detectors recommended in gas chromatography to measure greenhouse emission and O2 uptake in soil: A review. Communications in Soil Science and Plant Analysis, 51(5), 582-594.

Flores, M., Avendaño, V., Bravo, J., Valdés, C., Forero-Doria, O., Quitral, V., Ortiz-Viedma, J. (2021). Edible oil parameters during deterioration processes. International Journal of Food Science, 2021(1), 7105170.

Fonseca, H. M., Santos, C. O., Cruz, L. P. A., Arthur, V., Freitas, B. C. B., Souza, A. R. M., & Martins, G. A. D. S. (2021). The effects of microwave application on the physicochemical properties of bacaba (Oenocarpus bacaba Mart.) Oil. Acta Scientiarum Polonorum Technologia Alimentaria, 20(2), 189-196.

Fotiadou, R., Vougiouklaki, D., Houhoula, D., & Stamatis, H. (2024). Improvement of the oxidative stability of edible oils through enzymatic esterification with hydroxytyrosol-rich extract. European Journal of Lipid Science and Technology, 2400014.

Frances, E. C., Johnson, O. O., Enoch, N. N., Eziamaka, A.-E. C., & Ann, M. O. (2023). Determination of Heavy Metals in Edible Palm Oil Adultrated with Plant Dye: Experimental Investigation. Asian Journal of Research in Agriculture and Forestry, 9(3), 1-12.

Gao, H. X., Chen, N., He, Q., Shi, B., Yu, Z. L., & Zeng, W. C. (2022). Effects of Ligustrum robustum (Rxob.) Blume extract on the quality of peanut and palm oils during storage and frying process. Journal of Food Science, 87(10), 4504-4521.

Gautam, N. (2024). Thermal Degradation of Soybean and Palm Olein during Deep Fat Frying. EC Nutrition, 19, 01-09.

Gebeyehu, H. R., & Bayissa, L. D. (2020). Levels of heavy metals in soil and vegetables and associated health risks in Mojo area, Ethiopia. Plos One, 15(1), e0227883.

Ghosh, G. C., Khan, M. J. H., Chakraborty, T. K., Zaman, S., Kabir, A. E., & Tanaka, H. (2020). Human health risk assessment of elevated and variable iron and manganese intake with arsenic-safe groundwater in Jashore, Bangladesh. Scientific reports, 10(1), 5206.

Ginsburg, S. R., & Maleky, F. (2020). Extraction of lipid-soluble antioxidants from rosemary leaves using vegetable oils. International Journal of Food Science & Technology, 55(9), 3135-3144.

Girish, Y. R., Sharath Kumar, K. S., Prashantha, K., Rangappa, S., & Sudhanva, M. S. (2023). Significance of antioxidants and methods to evaluate their potency. Materials Chemistry Horizons, 2(2), 93-112.

González-Benjumea, A., Marques, G., Herold-Majumdar, O. M., Kiebist, J., Scheibner, K., Del Río, J. C., Gutiérrez, A. (2021). High epoxidation yields of vegetable oil hydrolyzates and methyl esters by selected fungal peroxygenases. Frontiers in bioengineering and biotechnology, 8, 605854.

Grootveld, M. (2022). Evidence-based challenges to the continued recommendation and use of peroxidatively-susceptible polyunsaturated fatty acid-rich culinary oils for high-temperature frying practises: Experimental revelations focused on toxic aldehydic lipid oxidation products. Frontiers in Nutrition, 8, 711640.

Gu, H., Huang, X., Chen, Q., & Sun, Y. (2020). Rapid assessment of total polar material in used frying oils using manganese tetraphenylporphyrin fluorescent sensor with enhanced sensitivity. Food Analytical Methods, 13, 2080-2086.

Gungshik, J., Ibrahim, M., Onyemowo, O., & Rabiat, L. (2023). Comparative Analysis of the Physico-Chemical Properties and Trace Metal Content of Palm Oil, from Selected Markets in Jos South and Jos North LGA, Plateau State, Nigeria. Nigerian Journal of Chemical Research, 28(2), 100-111.

Guo, M., Yang, L., Li, X., Tang, H., Li, X., Xue, Y., & Duan, Z. (2023). Antioxidant efficacy of rosemary extract in improving the oxidative stability of rapeseed oil during storage. Foods, 12(19), 3583.

Guo, Y., Liu, C., Ye, R., & Duan, Q. (2020). Advances on water quality detection by uv-vis spectroscopy. Applied Sciences, 10(19), 6874.

Habarakada, A., Perumpuli, P., Thathsaranee, W., & Wanninaika, I. (2021). Physical, chemical, and nutritional quality parameters of three different types of oil: Determination of their reusability in deep frying.

Haider, S., Akhtar, A., & Khalid, N. (2023). Quality Assessment of Fried Oils from Different Street Food Vendors and Restaurants in Different Areas of Gilgit, Pakistan: Cooking Oil Quality in Northern Areas of Pakistan. Proceedings of the Pakistan Academy of Sciences: B. Life and Environmental Sciences, 60(1), 71-82.

Hasanah, N. N., Asyrul-Izhar, A. B., Faridah, M. R., Kumar, P., & Ismail-Fitry, M. R. (2024). Effect of Red Palm Olein and Glutinous Rice Flour Mixture as Fat Replacers on the Physicochemical, Rheological, and Microstructural Properties of Buffalo Meat Emulsion. Pertanika J. Trop. Agric. Sci, 47(1), 41-56.

He, X., Li, B., Yu, X., Zhuang, Y., Li, C., Dong, L.,Wang, S. (2022). Inhibiting effects of ginger and rosemary on the formation of heterocyclic amines, polycyclic aromatic hydrocarbons, and trans fatty acids in fried pork balls. Foods, 11(23), 3767.

Hee, P.-T. E., Liang, Z., Zhang, P., & Fang, Z. (2023). Formation mechanisms, detection methods and mitigation strategies of acrylamide, polycyclic aromatic hydrocarbons and heterocyclic amines in food products. Food Control, 110236.

Heshmati, A., Mehri, F., Karami-Momtaz, J., & Khaneghah, A. M. (2020). The concentration and health risk of potentially toxic elements in black and green tea—both bagged and loose-leaf. Quality Assurance and Safety of Crops & Foods, 12(3), 140-150.

Hishamuddin, E., Sulaiman, N., Bustamam, F. A., & Beng, Y. C. (2020). Recent updates on the Codex standard for named vegetable oils (CXS 210-1999) in relation to palm oil and palm kernel oil. Palm Oil Developments, 72, 34-41.

Hussain, A. (2020). A preliminary up-to-date review on Pakistani medicinal plants with potential antioxidant activity. RADS Journal of Biological Research & Applied Sciences, 11(1), 61-88.

Hussein, S. A., Abo Zaid, O. R., Abdelmaksoud, H. F., Ismael, T. F., Amin, A., Lawaty, A., & Fathy, G. (2022). The role of hesperidin and rosemary leaves extract on myocardium glucose transporter 4 pathway for attenuation of diabetic cardiomyopathy. Benha Veterinary Medical Journal, 42(2), 57-63.

Iloamaeke, I. M., Unoka, E. C., Ikezuagu, B. C., & Simon, C. J. (2024). Quality Assessment of Selected Brands of Vegetable Oil Sold at Relief Market Onitsha, Anambra State of Nigeria.

Irfan, U. B., Pui, L. P., & Solihin, M. I. (2020). Feasibility study of detecting palm oil adulteration with recycled cooking oil using a handheld NIR spectroscopy. Paper presented at the AIP Conference Proceedings.

Isiodu, V. C., Onyegeme-Okerenta, B. M., & Essien, E. B. (2024). Dietary exposure and risk characterization of selected toxic metals in crude palm oil (Elaeis guineensis Jacq) from six states in Niger Delta, Nigeria. Magna Scientia Advanced Research and Reviews, 10(1), 025-037.

Jadhav, H. B., Gogate, P. R., Waghmare, J. T., & Annapure, U. S. (2022). Comparative assessment of thermo-oxidative stability of palm oil designer lipid and palm oil blends as frying medium. Applied Food Research, 2(1), 100039.

Jaffar, S. S., Saallah, S., Misson, M., Siddique, S., Roslan, J., & Lenggoro, W. (2024). Green synthesis, characterization and antimicrobial efficacy of silver nanoparticles from Kappaphycus alvarezii extract. Research on Chemical Intermediates, 1-18.

Jeruto, R. D., Onyango, L. A., Nakhumicha, A., & Omwoma, S. (2024). Comparing Synthetic and Natural Antioxidants in Vegetable Oils: Effects on Oxidation and Oil Quality. Asian Journal of Applied Chemistry Research, 15(4), 119-137.

Jiang, H., Chen, W., Jia, Z., & Tao, F. (2020). Physiochemical properties of short-term frying oil for chicken wing and its oxidative stability in an oil-in-water emulsion. Food science & nutrition, 8(1), 668-674.

Joia, R., & Muhammad, H. (2023). advancement of gas chromatography in quantitative analysis. Chemical-Biological Series, 18.

Jurid, L. S., Zubairi, S. I., Kasim, Z. M., & Ab Kadir, I. A. (2020). The effect of repetitive frying on physicochemical properties of refined, bleached and deodorized Malaysian tenera palm olein during deep-fat frying. Arabian Journal of Chemistry, 13(7), 6149-6160.

Kaisan, M. U., Abubakar, S., Ashok, B., Balasubramanian, D., Narayan, S., Grujic, I., & Stojanovic, N. (2021). Comparative analyses of biodiesel produced from jatropha and neem seed oil using a gas chromatography–mass spectroscopy technique. Biofuels.

Kamanula, M., Yangontha Munthali, C., & Finias Kamanula, J. (2022). Yield and physicochemical properties of marula (Sclerocarya birrea) seed oils among nine international provenances tested in Malawi. International Journal of Agronomy, 2022(1), 7145113.

Kaseke, T., Opara, U. L., & Fawole, O. A. (2021). Novel seeds pretreatment techniques: Effect on oil quality and antioxidant properties: A review. Journal of Food Science and Technology, 1-14.

Kedir, W. M., Geletu, A. K., Weldegirum, G. S., & Sima, M. F. (2023). Antioxidant activity of selected plants extract for palm oil stability via accelerated and deep frying study. Heliyon, 9(7).

Korede, A., Adeboyejo, F., Fapojuwo, O., & Ogunwole, O. (2024). Quality variation in shea butter and olein from Irepodun Local Government Area, Oyo State, Nigeria.

Kung, Y., & Hsieh, B.-C. (2021). Quality Assessment of Deep-Frying Palm Oil by Impedimetric Sensing with a Simple and Economic Electrochemical Cell. Sensors, 21(21), 7093.

Lamloum, N. S., Soliman, H. A., Ahmed, R. R., Ahmed, O. M., Abdel-Maksoud, M. A., Kotob, M. H., & Zaky, M. Y. (2023). Improvement effects of green tea and pumpkin oils on myelin oligodendrocyte glycoprotein-induced Multiple sclerosis in rats. Journal of Functional Foods, 111, 105876.

Lee, S. Y., Kim, O. Y., Kang, H. J., Kim, H. S., & Hur, S. J. (2020). Overview of studies on the use of natural antioxidative materials in meat products. Food Science of Animal Resources, 40(6), 863.

Li, J., Yuan, F., Teng, J., Li, F., Zhou, P., & Bi, Y. (2023). Effects of tea polyphenols and tertiary butylhydroquinone on quality of palm oils and losses of endogenous vitamin E during batch frying and oxidative stability of fried instant noodles. Food Chemistry: X, 20, 101049.

Lin, S. T., Liao, K. W., Xuan, T. C., Chiou, T. Y., Lin, Z. E., & Lee, W. J. (2024). Determination, distribution, and health risk assessment of 12 heavy metals in various edible oils in Taiwan. JSFA Reports, 4(3), 175-183.

Lisa, S., Kabir, M., Rahman, M., & Rahman, S. (2022). Qualitative changes of different vegetable oils during repeated deep frying. Bangladesh Journal of Scientific and Industrial Research, 57(1), 49-60.

Liu, X. (2020). Modeling Analysis on Deterioration Characteristics of Frying Oil Using Metabolomics Approach.

Liyansan, S. M., Fatunsin, O. T., & Olayinka, K. O. (2022). Evaluation of Physicochemical Parameters of Unbranded Palm Oil Samples Purchased from Important Markets in Lagos, Nigeria.

Lozano-Castellon, J., de Alvarenga, J. F. R., Vallverdu-Queralt, A., & Lamuela-Raventos, R. M. (2022). Cooking with extra-virgin olive oil: A mixture of food components to prevent oxidation and degradation. Trends in Food Science & Technology, 123, 28-36.

Macarthur, R., Teye, E., & Darkwa, S. (2021). Quality and safety evaluation of important parameters in palm oil from major cities in Ghana. Scientific African, 13, e00860.

Madhujith, T., & Sivakanthan, S. (2019). Oxidative stability of edible plants oils. In: Springer Nature.

Maduako, M. C., Amaefule, K. I., & Ifemeje, J. C. (2022). Comparative Study of Physiochemical Properties of Different Brands of Vegetable Oil Sold in Ihiala Market of Anambra State. Asian Journal of Biochemistry, Genetics and Molecular Biology, 12(3), 8-13.

Mahiran, S. N. S. N., Abd Kadir, N. H., Maulidiani, M., Mohamad, T. R. T., Gooderham, N. J., & Alam, M. (2023). Multivariate modelling analysis for prediction of glycidyl esters and 3-monochloropropane-1, 2-diol (3-MCPD) formation in periodically heated palm oil. Heliyon, 9(10).

Mahmud, N., Islam, J., Oyom, W., Adrah, K., Adegoke, S. C., & Tahergorabi, R. (2023). A review of different frying oils and oleogels as alternative frying media for fat-uptake reduction in deep-fat fried foods. Heliyon.

Makhamra, J. M. (2023). Biological Activities and Nutritional Composition of Essential Oil from Rosmarinus officinalis L. Leaves.

Mallongi, A., Rauf, A., Astuti, R., Palutturi, S., & Ishak, H. (2023). Ecological and human health implications of mercury contamination in the coastal water. Global Journal of Environmental Science and Management, 9(2), 261-274.

Mansour, H. M., El-Sohaimy, S. A., Zeitoun, A. M., & Abdo, E. M. (2022). Effect of natural antioxidants from fruit leaves on the oxidative stability of soybean oil during accelerated storage. Antioxidants, 11(9), 1691.

Manzoor, S., Masoodi, F., Rashid, R., & Dar, M. (2022). Effect of Apple Pomace-Based Antioxidants on the Stability of Mustard Oil During Deep Frying of French Fries. LWT. 163: 113576. In.

Manzoor, S., Masoodi, F., Rashid, R., & Dar, M. M. (2022). Effect of apple pomace-based antioxidants on the stability of mustard oil during deep frying of French fries. LWT, 163, 113576.

Mathew, M. (2021). Cyclic fatty acid monomers of alpha-linolenic acid: isolation and separation of isomers, and effects of structural parameters on their oxidation.

Mechqoq, H., El Yaagoubi, M., Momchilova, S., Msanda, F., & El Aouad, N. (2021). Comparative study on yields and quality parameters of argan oils extracted by conventional and green extraction techniques. Grain & Oil Science and Technology, 4(3), 125-130.

Mishra, S., Firdaus, M., Patel, M., & Pandey, G. (2023). A study on the effect of repeated heating on the physicochemical and antioxidant properties of cooking oils used by fried food vendors of Lucknow city. Discover Food, 3(1), 7.

Miyuranga, K. V., Arachchige, U. S., Marso, T., & Samarakoon, G. (2023). Biodiesel production through the transesterification of waste cooking oil over typical heterogeneous base or acid catalysts. Catalysts, 13(3), 546.

Mohammadi-Nasrabadi, F., Zargaraan, A., Salmani, Y., Abedi, A., Shoaie, E., & Esfarjani, F. (2021). Analysis of fat, fatty acid profile, and salt content of Iranian restaurant foods during the COVID-19 pandemic: Strengths, weaknesses, opportunities, and threats analysis. Food science & nutrition, 9(11), 6120-6130.

Mohammed, i. A., & saleem, p. H. (2023). Development method for the determination of cr, cd and pb in edible sunflower oil using emulsion extraction-faas. Journal of Duhok University, 26(1), 198-210.

Moufakkir, C., Kharbach, Y., Tanghort, M., Dassouli, A., & Remmal, A. (2022). Antioxidant effect of natural rosemary on the oxidation of mid-oleic sunflower frying oil on chicken wings. Food Science and Technology, 42, e70122.

Moufakkir, C., Kharbach, Y., Tanghort, M., Dassouli, A., & Remmal, A. (2023). Preserving soybean oil for the frying of breaded butterfly shrimp using natural rosemary antioxidant. International Journal of Food Science, 2023(1), 5984636.

Multari, S., Marsol-Vall, A., Heponiemi, P., Suomela, J.-P., & Yang, B. (2019). Changes in the volatile profile, fatty acid composition and other markers of lipid oxidation of six different vegetable oils during short-term deep-frying. Food Research International, 122, 318-329.

Munir, M., Ahmad, M., Rehan, M., Saeed, M., Lam, S. S., Nizami, A.,Zafar, M. (2021). Production of high quality biodiesel from novel non-edible Raphnus raphanistrum L. Seed oil using copper modified montmorillonite clay catalyst. Environmental research, 193, 110398.

Nanayakkara, T., Wijelath, W., & Marso, T. (2020). Deep-fat Frying of Vegetable Oils: Major Chemical Reactions and Effect of Natural Extracts on Oxidative Stability-A Review.

Nandiyanto, A. B. D., Ragadhita, R., & Aziz, M. (2023). How to calculate and measure solution concentration using UV-vis spectrum analysis: Supporting measurement in the chemical decomposition, photocatalysis, phytoremediation, and adsorption process. Indonesian Journal of Science and Technology, 8(2), 345-362.

Nduka, J. K. C., Omozuwa, P. O., & Imanah, O. E. (2021). Effect of heating time on the physicochemical properties of selected vegetable oils. Arabian Journal of Chemistry, 14(4), 103063.

Negash, Y. A., Amare, D. E., Bitew, B. D., & Dagne, H. (2019). Assessment of quality of edible vegetable oils accessed in Gondar City, Northwest Ethiopia. BMC research notes, 12, 1-5.

Nhivekar, G. S., Jagdale, S. R., Kamble, S. B., Jadhav, B. T., Kamat, R. K., & Dongale, T. D. (2022). Versatile Three-in-One Single Beam Visible Colorimeter for Undergraduate Chemistry Laboratories. In: ACS Publications.

Nid Ahmed, M., Gagour, J., Asbbane, A., Hallouch, O., Atrach, L., Giuffrè, A. M., Gharby, S. (2024). Advances in the Use of Four Synthetic Antioxidants as Food Additives for Enhancing the Oxidative Stability of Refined Sunflower Oil (Helianthus annuus L.). Analytica, 5(2), 273-294.

Nieto, G., Martínez-Zamora, L., Peñalver, R., Marín-Iniesta, F., Taboada-Rodríguez, A., López-Gómez, A., & Martínez-Hernández, G. B. (2023). Applications of plant bioactive compounds as replacers of synthetic additives in the food industry. Foods, 13(1), 47.

Nik Ibrahim, N. A., Ahmad Tarmizi, A. H., Selvaduray, K. R., & Kuntom, A. (2022). Sustainability and Traceability in the Malaysian Oil Palm Industry. In Recent Advances in Edible Fats and Oils Technology: Processing, Health Implications, Economic and Environmental Impact (pp. 425-461): Springer.

Nizam, A. F. A., & Mahmud, M. S. (2021). Food quality assurance of crude palm oil: a review on toxic ester feedstock. OCL, 28, 23.

Ntube, N. E. E., Tiencheu, B., Dibanda, R. F., Eboue, F. L. E., Djikeng, F. T., & Moses, C. M. (2024). Evaluation of Chemical Composition, Physicochemical and Anti-nutritional Properties of Giant Yellow Mulberry Fruit (Myrianthus arboreus). European Journal of Nutrition & Food Safety, 16(5), 48-65.

Nuru, Z., & Getachew, P. (2021). Improving the quality of used frying niger seed oil with adsorbent treatment. Heliyon, 7(4).

Okoro, C., Olawuni, A., & Elemuo, G. (2023). Evaluation of the Physicochemical Properties of Re-used Frying Oils Treated with Natural Antioxidating Materials; Onion, Ginger, Turmeric and Carrot.

Omara, T., Kigenyi, E., Laker, F., Adokorach, M., Otim, G., Kalukusu, R., Victoria Nakabuye, B. (2019). Effects of continuous deep-fat frying on the physicochemical properties of assorted brands of edible cooking oils sold in Greater Metropolitan Kampala. Asian Journal of Applied Chemistry Research, 3(2), 1-13.

Omojola, A., Freddie, I., & Idoko, O. E. (2020). Effect of usage on the fatty acid composition and properties of neat palm oil, waste palm oil, and waste palm oil methyl ester. International Journal of Engineering & Technology, 9(1), 110-117.

Omozuwa, P., Nduka, J., Kelle, H., Aghedo, O., & Idemudia, S. (2023). analysis of fuel properties of biodiesels prepared from selected vegetable oils (virgin oils and their waste). Nigerian Journal of Science and Environment, 21(2).

Ondo-Azi, A. S., Missang, C. E., & Silou, T. (2021). Physicochemical Properties and Antioxidant Activity of Mixed Oil of Safou (Dacryodes edulis (G. Don) HJ Lam) from Several Trees. Journal of Food Research, 9(4), 1-50.

Ooi, E. Z. H., Ab Karim, N. A., Chan, E. S., Wang, Y., Tang, T. K., Tong, S. C., Lee, Y. Y. (2024). Underutilised palm stearin as hard stock for deep-frying medium and its performance for oil uptake in instant noodles. Journal of the Science of Food and Agriculture, 104(7), 3958-3970.

Osunrinade, O., Jimoh, K., & Babalola, J. (2020). Chemical changes associated with repetitive re-use of vegetable oil during deep frying of bean cake, plantain and yam. J Food Technol, 7(1), 1-8.

Pasias, I. N., Rousis, N. I., Psoma, A. K., & Thomaidis, N. S. (2021). Simultaneous or sequential multi-element graphite furnace atomic absorption spectrometry techniques: Advances within the last 20 years. Atom. Spectrosc, 42(6), 310-327.

Pathmasiri, T., & Perera, G. (2020). Potential of using polyethylene as viscosity enhancer of palm oil to use as a lubricating oil. Advances in Mechanical Engineering, 12(11), 1687814020970745.

Patil, R. S., Waghmare, J., & Annapure, U. (2023). Comparative assessment of the frying performance of palm olein and sunflower oil during deep-fat frying of Indian battered food products. Journal of Agriculture and Food Research, 14, 100778.

Pereira, J. C., Sivakanthan, S., & Vasantharuba, S. (2020). Effect of Star Fruit (Averrhoa carambola L.) By-product on Oxidative Stability of Sesame (Sesamum indicum) Oil under Accelerated Oven Storage and during Frying. Journal of Oleo Science, 69(8), 837-849.

Perera, M. P. J., Binuwangi, A. K. D. M., Silva, A. A. G., Attanayake, R. N., Wickramarachchi, S. R., & Rajapakse, C. S. K. (2021). Antioxidant activity and chemical constituents of methanolic extract of Durio zibethinus Murr.(durian) peels. medicinal plants-international journal of phytomedicines and related industries, 13(2), 275-282.

Pirzadah, T. B., Malik, B., & Dar, F. A. (2019). Phytoremediation potential of aromatic and medicinal plants: A way forward for green economy. Journal of Stress Physiology & Biochemistry, 15(3), 62-75.

Plaskova, A., & Mlcek, J. (2023). New insights of the application of water or ethanol-water plant extract rich in active compounds in food. Frontiers in Nutrition, 10, 1118761.

Poh, A. H., Adikan, F. R. M., & Moghavvemi, M. (2020). The past, present, and prospective on UV–VIS–NIR skin photonics and spectroscopya wavelength guide. Medical & Biological Engineering & Computing, 58, 1159-1175.

Pontillo, A. R. N., Papakosta-Tsigkri, L., Lymperopoulou, T., Mamma, D., Kekos, D., & Detsi, A. (2021). Conventional and enzyme-assisted extraction of rosemary leaves (Rosmarinus officinalis L.): Toward a greener approach to high added-value extracts. Applied Sciences, 11(8), 3724.

Pougoue Ngueukam, A. A., Klang, M. J., Zokou, R., Teboukeu Boungo, G., Djikeng Tonfack, F., Azeez, B. K.,Tsopmo, A. (2023). Peptidomics Analysis of Soy Protein Hydrolysates—

Antioxidant Properties and Mechanism of their Inhibition of the Oxidation of Palm Olein during Frying Cycles. Foods, 12(18), 3498.

Pulassery, S., Abraham, B., Ajikumar, N., Munnilath, A., & Yoosaf, K. (2022). Rapid iodine value estimation using a handheld Raman spectrometer for on-site, reagent-free authentication of edible oils. ACS omega, 7(11), 9164-9171.

Purnama, K. O., Setyaningsih, D., Hambali, E., & Taniwiryono, D. (2020). Processing, characteristics, and potential application of red palm oil-A review. International Journal of Oil Palm, 3(2), 40-55.

Rahman, N., Hashem, S., Akther, S., & Jothi, J. S. (2023). Impact of various extraction methods on fatty acid profile, physicochemical properties, and nutritional quality index of Pangus fish oil. Food science & nutrition, 11(8), 4688-4699.

Raji, R. O., Inengite, A. K., Godwin, J., & Ajibesin, K. K. (2022). Assessment of proximate and physicochemical properties of crude palm oil from south-west and South-south Nigeria. African Journal of Pure and Applied Chemistry, 16(2), 40-56.

Redzuan, N. Q., Halid, I., & Hamdan, S. H. (2023). analysing the lubricant rheology-pressure relation for biodiesel derived waste palm cooking oil (wpco). Journal of Transport System Engineering, 1-7.

Salama, M. A., El Harkaoui, S., Nounah, I., Sakr, H., Abdin, M., Owon, M.,Matthäus, B. (2020). Oxidative stability of Opuntia ficus-indica seeds oil blending with Moringa oleifera seeds oil☆. OCL, 27, 53.

Saleh, F. A., Al-Otaibi, M. M., & Al-Zoraky, N. S. (2021). Quality Assessment of Frying Oil from some Restaurants in Al-Ahsa City, Saudi Arabia.

Sarmah, R., Kanta Bhagabati, S., Dutta, R., Nath, D., Pokhrel, H., Mudoi, L. P.,Jyoti Nath, R. (2020). Toxicity of a synthetic phenolic antioxidant, butyl hydroxytoluene (BHT), in vertebrate model zebrafish embryo (Danio rerio). Aquaculture Research, 51(9), 3839-3846.

Sevillano-Morales, J., Sevillano-Caño, J., Amaro-López, M., & Cámara-Martos, F. (2023). Probabilistic Assessment of the Intake of Trace Elements by Consumption of Red Deer (Cervus elaphus) and Wild Boar (Sus scrofa) Meat. Applied Sciences, 13(24), 13263.

Shahidi, F., & Yeo, J. (2020). Should the in vitro colorimetric assays in antioxidant and lipid oxidation evaluation be abandoned?: A critical review focusing on bioactive molecule screening assays in in vitro and in vivo models. Journal of Food Bioactives, 9.

Shahin, A., Nabil-Adam, A., Elnagar, K., Osman, H., & Shreadah, M. A. (2022). Bioactivity and metabolomics fingerprinting characterization of different organic solvents extracts of Padina pavonica collected from Abu Qir Bay, Egypt. Egyptian Journal of Chemistry, 65(12), 207-225.

Shotts, M.-L., Plans, M., Wong, K., Milligan, A. M., Aykas, D. P., & Rodriguez-Saona, L. E. (2021). Application of mid-infrared portable spectrometer for the rapid determination of trans-fatty acid content in lipid extracts of snack and bakery products. Journal of AOAC International, 104(1), 29-38.

Sikdar, P., Sree, K. R., Pravallika, G. S., Sudha, K. G., Ajitha, S., Kumar, K. D., & Rushitha, K. (2021). Comparitative study of different crude and refined reheatededible oils available in Tirupati.

Slota, A., Svoboda, M., Suchopár, V., & Kratzer, J. (2023). Determination of Germanium species by hydride generation atomic absorption spectrometry: Comparison of atomizers based on diffusion Flame, heated quartz tube, and dielectric barrier discharge plasma. Atomic Spectroscopy, 44(4), 207-218.

Stavila, E., Yuliati, F., Adharis, A., Laksmono, J. A., & Iqbal, M. (2023). Recent advances in synthesis of polymers based on palm oil and its fatty acids. RSC advances, 13(22), 14747-14775.

Sulthana, S. F., Iqbal, U. M., Suseela, S. B., Anbazhagan, R., Chinthaginjala, R., Chitathuru, D., . . . Kim, T.-h. (2024). Electrochemical Sensors for Heavy Metal Ion Detection in Aqueous Medium: A Systematic Review. ACS omega, 9(24), 25493-25512.

Sun, T., Zhang, J., Zhang, Q., Li, X., Li, M., Yang, Y.,Zhou, B. (2021). Transcriptome and metabolome analyses revealed the response mechanism of apple to different phosphorus stresses. Plant Physiology and Biochemistry, 167, 639-650.

Tan, S. L., Suhaimy, M., Hanani, S., & Abd Samad, N. A. (2022). Evaluation of fresh palm oil adulteration with recycled cooking oil using GC-MS and ATR-FTIR spectroscopy: A review. Czech Journal of Food Sciences, 40(1).

Tanwar, S. N., Parauha, Y. R., There, Y., Swart, H. C., & Dhoble, S. J. (2024). Plant-Based Biosynthesis of Metal and Metal Oxide Nanoparticles: An Update on Antimicrobial and Anticancer Activity. Chembioeng Reviews, e202400012.

Tek, P. P. Y., & Ng, C. C. (2024). Accumulation of potentially toxic elements in fourfinger threadfin (Eleutheronema tetradactylum) and black pomfret (Parastromateus niger) from Selangor, Malaysia. Environmental Monitoring and Assessment, 196(4), 382.

Tohma, S., Günal-Köroğlu, D., Turan, S., & Ramadan, M. F. (2021). Efficacy of rosemary (Rosmarinus officinalis L.) Powder and extracts in the protection of refined and stripped hazelnut oil. Rendiconti Lincei. Scienze Fisiche e Naturali, 32(3), 585-598.

Tolessa, E. S., Weldegiorigis, G., & Chindi, A. (2019). Traditional Potato Food Types Preparation Practices and Farmer Reaction in Welmera and Ada Berga District, West Shewa, Ethiopia. History, 6(1), 127-133.

Tulandi, S. M., Tanzil, L., & Ulfa, D. M. (2021). Analysis of Bioactive compounds from methanol extract of Diadema setosum sea urchin gonads using gas Chromatography-mass spectrometry. Research Journal of Pharmacy and Technology, 14(3), 1629-1634.

Ujong, A., Emelike, N., Owuno, F., & Okiyi, P. (2023). Effect of frying cycles on the physical, chemical and antioxidant properties of selected plant oils during deep-fat frying of potato chips. Food Chemistry Advances, 3, 100338.

Ukwo, S. P. (2024). Heavy Metal Residues and Bacterial Pathogens of Food Safety Significance in Edible Crustacean from Crude-Oil-Impacted Niger Delta, Nigeria. Journal of Aquatic Food Product Technology, 33(6), 469-483.

Vallbona, B. F., Kajtazi, A., Shahtahmassebi, G., & Hanley, Q. (2024). Raw Data and Noise in Spectrophotometry.

Valle, C., Echeverría, F., Chávez, V., Valenzuela, R., & Bustamante, A. (2024). Deep-frying impact on food and oil chemical composition: Strategies to reduce oil absorption in the final product. Food Safety and Health.

Vella, F. M., & Laratta, B. (2023). Rosemary Essential Oil Extraction and Residue Valorization by Means of Polyphenol Recovery. Paper presented at the Biology and Life Sciences Forum.

Viana da Silva, M., Santos, M. R. C., Alves Silva, I. R., Macedo Viana, E. B., Dos Anjos, D. A., Santos, I. A., Lannes, S. C. D. S. (2022). Synthetic and natural antioxidants used in the oxidative stability of edible oils: An overview. Food Reviews International, 38(sup1), 349-372.

Voss, K., Holzbeck, P., Pfeilsticker, K., Kleinschek, R., Wetzel, G., Fuentes Andrade, B.,Butz, A. (2024). A novel, balloon-borne UV/visible spectrometer for direct sun measurements of stratospheric bromine. Egusphere, 2024, 1-33.

Wang, D., Xiao, H., Lyu, X., Chen, H., & Wei, F. (2023). Lipid oxidation in food science and nutritional health: A comprehensive review. Oil Crop Science, 8(1), 35-44.

Wang, F., Sun, Y., Li, S., Yan, J., Qin, W., Saleh, A. S., & Zhang, Q. (2023). Plant phenolic extracts for the quality protection of frying oil during deep frying: Sources, effects, and mechanisms. Grain & Oil Science and Technology.

Waqar, M., Ahmad, A., Qaisar, W., Basri, R., & Aziz, H. (2023). Influence of Phenolic Antioxidants on Changes in Quality Characteristics of Palm Olein during Intermittent Frying of Potato Chips. Jammu Kashmir Journal of Agriculture, 3(2), 79-88.

Wathum, J. (2021). Fatty acids, heavy metal concentration, and characteristics of selected oil seeds grown in west Nile, Uganda. Kyambogo University,

Williams, C., Mbuyane, L. L., Bauer, F. F., Mokwena, L., Divol, B., & Buica, A. (2021). A gas chromatography-mass spectrometry method for the determination of fatty acids and sterols in yeast and grape juice. Applied Sciences, 11(11), 5152.

Yadav, D. K., Kadam, P., Wadikar, D., Kannan, V., & Semwal, A. (2023). Changes in the Quality Attributes of Edible Vegetable Oils During Deep Frying Concerning Defence Ration.

Yaghi, M. M., Elsherif, K. M., & El-Shawish, A. A. (2022). Assessment of some Heavy Metals in Potato and Corn Chips available in Libyan Market. Arabian Journal of Chemical and Environmental Research, 9(1), 122-135.

Yildiz, A. Y., Echegaray, N., Öztekin, S., & Lorenzo, J. M. (2024). Quality and stability of frying oils and fried foods in ultrasound and microwave–assisted frying processes and hybrid technologies. Comprehensive Reviews in Food Science and Food Safety, 23(4), e13405.

Yılmaz, B., Şahin, T. Ö., & Ağagündüz, D. (2023). Oxidative Changes in Ten Vegetable Oils Caused by the Deep-Frying Process of Potato. Journal of Food Biochemistry, 2023(1), 6598528.

Yusof, N. D. M., & Mohamad, W. A. F. W. (2019). Differences in total yield and physicochemical attributes of virgin coconut oil from coconut milk demulsification using direct heating and microwave heating. Journal of Agrobiotechnology, 10(1S), 35-45.

Zaghi, A. N., Barbalho, S. M., Guiguer, E. L., & Otoboni, A. M. (2019). Frying process: From conventional to air frying technology. Food Reviews International, 35(8), 763-777.

Zeraat Pisheh, F., Falah, F., Sanaei, F., Vasiee, A., Zanganeh, H., Tabatabaee Yazdi, F., & Ibrahim, S. A. (2023). The Effect of Plasma-Activated Water Combined with Rosemary Extract (Rosmarinus officinalis L.) On the Physicochemical Properties of Frankfurter Sausage during Storage. Foods, 12(21), 4022.

Zhang, M., Wang, C., Xie, Z., Gao, B., & Yu, L. (2024). Chemical structures, analytical approaches and toxicological effects of oxidative derivatives of triglycerides as potential hazards in lipid thermal processing: A review. Grain & Oil Science and Technology.

Zhao, F., Wang, P., Lucardi, R. D., Su, Z., & Li, S. (2020). Natural sources and bioactivities of 2, 4-di-tert-butylphenol and its analogs. Toxins, 12(1), 35.

Zhao, W., Whelton, H. L., Blong, J. C., Shillito, L.-M., Jenkins, D. L., & Bull, I. D. (2023). Volatile organic compounds (vocs) as a rapid means for assessing the source of coprolites. Iscience, 26(6).

Zheng, Q., Li, W., Lv, Z., & Fan, J. (2019). Study on Extraction Method of rosemary antioxidant. Paper presented at the IOP Conference Series: Earth and Environmental Science.

Zhou, W., Peng, Y., Wu, Z., Zhang, W., & Cong, Y. (2024). Study on the Frying Performance Evaluation of Refined Soybean Oil after PLC Enzymatic Degumming. Foods, 13(2), 275.

Appendix

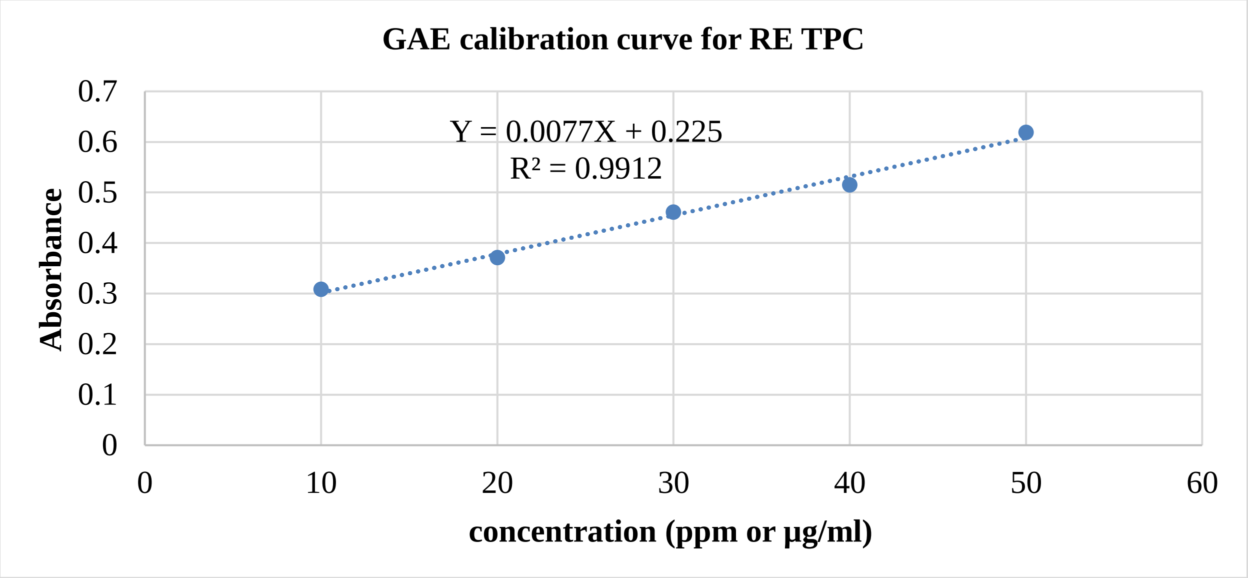

Figure 12: GAE calibration curve for determination of total polyphenol content in RE.

Table 12: Calculation on total amount of polyphenol from gallic acid calibration line

conc.(ppm)	**triai-1**	**trial-2**	**trial-3**	**Sum**	**Mean**	**SD**	**Mean ± SD**
sample-10	0.307	0.308	0.309	0.924	0.308	0.001	0.308 ± 0.001
sample-20	0.37	0.371	0.372	1.113	0.371	0.001	0.371 ± 0.001
sample-30	0.46	0.461	0.462	1.383	0.461	0.001	0.461 ± 0.001
sample-40	0.514	0.515	0.516	1.545	0.515	0.001	0.515 ± 0.001
sample-50	0.618	0.619	0.62	1.857	0.619	0.001	0.619 ± 0.001
Blank	0.08	0.081	0.082	0.243	0.081	0.001	0.081 ± 0.001

Calculation on physical properties for FHPO & FHPOR

Table 13: Moisture content data record using dry digital oven method for FHPO & FHPOR

FHPO	WSBD	WED	WSAD	% MC	Sum	Average
1st	19.98g	11.336g	19.92g	0.742	2.213	0.738
	20.35g	11.612g	20.285g	0.748		
	19.42g	10.6g	19.398g	0.723		
3rd	19.853g	11.37g	19.793g	0.711	2.231	0.744
	20.31g	11.65g	20.252g	0.65		
	19.323g	10.65g	19.25g	0.87		
5th	20.003g	11.371g	19.941g	0.722	2.31	0.77
	20.36g	11.65g	20.29g	0.82		
	20.36g	10.66g	20.284g	0.765		
7th	19.89g	11.37g	19.88g	0.176	2.38	0.79
	20.26g	11.66g	20.25g	0.151		
	19.297g	10.66g	19.12g	2.05		
9th	19.997g	11.378g	19.89g	1.267	3.684	1.228
	20.42g	11.66g	20.312g	1.194		
	19.174	10.66g	19.07g	1.223		
FHPOR	**WSBD**	**WED**	**WSAD**	**% MC**	**Sum**	**Average**
1st	19.924g	11.377g	19.903g	0.246	0.66	0.22
	20.113g	11.66g	20.097g	0.189		
	19.11g	10.66g	19.09g	0.225		
3rd	19.988g	11.38g	19.95g	0.488	1.614	0.538
	20.28g	11.38g	20.262g	0.202		
	19.42g	10.66g	19.339g	0.924		
5th	20.122g	11.377g	20.104g	0.2058	0.525	0.175
	20.194g	11.66g	20.182g	0.1406		
	19.076g	10.66g	19.061g	0.1781		
7th	19.88g	11.378g	19.843g	0.388	0.804	0.268
	20.191g	11.66g	20.176g	0.176		
	19.39g	10.66g	19.369g	0.24		
9th	19.914g	11.378g	19.901g	0.152	0.375	0.125
	20.133g	11.66g	20.124g	0.106		
	19.201g	10.66g	19.191g	0.117		

To calculate % moisture content value using the following equations example for 1st FHPO:

$\%\ \mathrm{Moisture\ ontent} = (\frac{(\mathrm{WSBD}-\mathrm{WED})-(\mathrm{WSAD}-\mathrm{WED}}{\mathrm{WSBD}-\mathrm{WED}})\ \mathrm{X}\ 100\ \%$ where, WSBD = weight of the sample before dry, WED = weight of empty dish, WSAD = weight of sample after dry, give the result as the above in table 13 for 1st FHPO, % moisture content = 0.742, 0.748, & 0.723.

FHPO	**trial-1**	**trial-2**	**trial-3**	**Sum**	**Mean**	**SD**	**Mean ± SD**	**Standard**
1st	0.742	0.748	0.723	2.213	0.73767	0.013051	0.738 ± 0.01	0.2% max
3rd	0.7108	0.6501	0.8676	2.2285	0.74283	0.112233	0.74 ± 0.11	
5th	0.7224	0.8202	0.7654	2.308	0.76933	0.049018	0.77 ± 0.05	
7th	0.176	0.151	2.05	2.377	0.79233	1.089243	0.79 ±1.089	
9th	1.267	1.194	1.223	3.684	1.228	0.036756	1.228 ± 0.037	
FHPOR	**trial-1**	**trial-2**	**trial-3**	**Sum**	**Mean**	**SD**	**Mean ± SD**	**Standard**
1st	0.246	0.1893	0.225	0.6603	0.2201	0.028666	0.220± 0.03	0.2% max
3rd	0.488	0.202	0.924	1.614	0.538	0.363588	0.538± 0.363	
5th	0.2058	0.1406	0.1781	0.5245	0.17483	0.032723	0.174± 0.033	
7th	0.388	0.176	0.24	0.804	0.268	0.108738	0.268± 0.1087	
9th	0.1522	0.1062	0.117	0.3754	0.12513	0.024054	0.12513± 0.02	

To calculate standard deviation, standard deviation is the square root of the variance. $\mathrm{Variance}\ (\mathrm{V})^2 = \frac{\sum_{\mathbf{i=1}}^{\mathbf{n=3}}(\mathbf{x_i}-\bar{\mathbf{x}})^{\mathbf{2}}}{\cap-\perp}$, & $\mathrm{SD} = \sqrt{(\mathbf{v^2})}$ = 0.013051. This calculation can be applied to the other samples in the same manner.

Table 14: Specific gravity data record using pycnometer for FHPO & FHPOR

FHPO	**W_{Oil} in g**	**Wp in g**	**W_{H2O} in g**	**SG**	**Sum**	**Average**
1st	50.223	27.391	52.179	0.9211	2.7469	0.9156
	50.047	27.333	52.105	0.9169		
	50.127	27.565	52.387	0.9089		
3rd	50.287	27.463	52.179	0.9235	2.7199	0.9066
	49.71	27.669	52.398	0.8913		
	50.015	27.398	52.387	0.9051		
5th	50.139	27.402	52.172	0.9179	2.7575	0.9192
	50.373	27.652	52.441	0.9166		
	50.322	27.462	52.228	0.923		
7th	50.01	27.623	52.173	0.9119	2.7467	0.9156
	50.317	26.832	52.44	0.9171		
	50.068	25.999	52.226	0.9177		
9th	50.1	27.033	52.245	0.9149	2.7477	0.9159
	50.364	27.034	52.5	0.9161		
	50.222	27.436	52.292	0.9167		
FHPOR	**W_{Oil} in g**	**Wp in g**	**W_{H2O} in g**	**SG**	**Sum**	**Average**
1st	49.913	27.519	52.246	0.90565	2.7272	0.9091
	50.215	27.727	52.397	0.9116		
	50.11	27.572	52.343	0.9099		
3rd	50.13	27.519	52.244	0.9145	2.7048	0.9016
	49.463	27.727	52.395	0.8811		
	50.093	27.571	52.342	0.9092		
5th	49.5	27.519	52.234	0.8894	2.6783	0.893
	49.4	27.725	52.393	0.8895		
	49.7	27.57	52.341	0.8994		
7th	50.195	27.519	52.242	0.9002	2.7021	0.9007
	50.276	27.725	52.393	0.9012		
	50.179	27.571	52.342	0.9007		
9th	49.957	27.52	52.242	0.9076	2.7249	0.9083
	50.139	27.724	52.393	0.9086		
	50.08	27.571	52.342	0.9087		

To calculate the specific gravity using the following equations, for example, for the 1st FHPO: Specific gravity $= \frac{\mathrm{WOil\_Wp}}{\mathrm{WH2O\_WP}}$, where, W_{Oil} = weight of oil, Wp = weight of pycnometer, W_{H2O} =

weight of oil distilled water, give the result as the above in table 14 for 1st FHPO, specific gravity = 0.9211, 0.9169, and 0.9089.

FHPO	**trial-1**	**trial-2**	**trial-3**	**Sum**	**Mean**	**SD**	**Mean ± SD**	**Standard**
1st	0.9211	0.9169	0.9089	2.7469	0.91563	0.0062	0.9156 ± 0.006	0.891-0.899
3rd	0.9235	0.8913	0.9051	2.7199	0.90663	0.01615	0.9066 ± 0.016	
5th	0.9179	0.9166	0.923	2.7575	0.91917	0.00338	0.9192 ± 0.0034	
7th	0.9119	0.9171	0.9177	2.7467	0.91557	0.00319	0.9156 ± 0.0032	
9th	0.9149	0.9161	0.9167	2.7477	0.9159	0.00092	0.9159 ± 0.0009	
FHPOR	**trial-1**	**trial-2**	**trial-3**	**Sum**	**Mean**	**SD**	**Mean ± SD**	**Standard**
1st	0.90565	0.9116	0.9099	2.72715	0.90905	0.00306	0.9091 ± 0.003	0.891-0.899
3rd	0.9145	0.8811	0.9092	2.7048	0.9016	0.01795	0.9016 ± 0.018	
5th	0.8894	0.8895	0.8994	2.6783	0.89277	0.00574	0.8928 ± 0.006	
7th	0.9002	0.9012	0.9007	2.7021	0.9007	0.0005	0.9007 ± 0.0005	
9th	0.9076	0.9086	0.9087	2.7249	0.9083	0.00061	0.9083 ± 0.0006	

To calculate standard deviation, standard deviation is the square root of the variance. Variance $(\mathrm{V})^2 = \frac{\sum_{\mathbf{i=1}}^{\mathbf{n=3}} (\mathbf{x_i} - \bar{\mathbf{x}})^2}{\cap - \perp}$, & SD $= \sqrt{(\mathbf{v^2})}$ = 0.00617. This calculation can be applied to the other samples in the same manner.

Table 15: Refractive index value data record using refractometer for FHPO & FHPOR

FHPO	**trial-1**	**trial-2**	**trial-3**	**FHPOR**	**trial-1**	**trial-2**	**trial-3**
1st	1.4648	1.4648	1.4648	1st	1.4649	1.4644	1.4647
3rd	1.4649	1.465	1.465	3rd	1.4645	1.4643	1.4646
5th	1.465	1.465	1.465	5th	1.4646	1.4647	1.4647
7th	1.4654	1.4654	1.4655	7th	1.4647	1.4648	1.4647
9th	1.4658	1.4658	1.4659	9th	1.4647	1.4647	1.4647

To calculate refractive index using the following equations example for 1st FHPO: $\mathrm{R} = \mathrm{R}^1 + \mathrm{K}(\mathrm{T}^1 — \mathrm{T})$, for example, R^1= (1.4648, 1.4648, 1.4648), k for Hayat palm oil = 0.000385, T^1 temperature record oil was at 25 ^{0}C & T = 40 ^{0}C, give the result as the above in table 15 for 1st FHPO, refractive index = 1.4590, 1.4590, and 1.4590 respectively.

FHPO	trial-1	trial-2	trial-3	Sum	Mean	SD	Mean ± SD	Standard
1st	1.459	1.459	1.459	4.377	1.459	2.71948E-16	1.459 ± 0.00	1.454- 1.456
3rd	1.477	1.478	1.479	4.434	1.478	0.001	1.478 ± 0.001	
5th	1.481	1.492	1.493	4.466	1.4887	0.0067	1.489 ± 0.007	
7th	1.501	1.502	1.503	4.506	1.502	0.001	1.502 ± 0.001	
9th	1.545	1.546	1.547	4.638	1.546	0.001	1.546 ± 0.001	
FHPOR	**trial-1**	**trial-2**	**trial-3**	**Sum**	**Mean**	**SD**	**Mean ± SD**	**Standard**
1st	1.459	1.4586	1.4589	4.3766	1.4589	0.000252	1.4589 ± 0.02	1.454- 1.456
3rd	1.4587	1.4585	1.4588	4.376	1.4587	0.000153	1.4587 ± 0.01	
5th	1.453	1.454	1.455	4.362	1.454	0.001	1.454 ± 0.00	
7th	1.4589	1.459	1.4589	4.3768	1.459	5.7735E-05	1.459 ± 0.00	
9th	1.4589	1.4589	1.4589	4.3767	1.459	0.01	1.459 ±0.01	

To calculate standard deviation, standard deviation is the square root of the variance. Variance $(V)^2 = \frac{\sum_{i=1}^{n=3}(x_i - \bar{x})^2}{\cap - \perp}$, & SD $= \sqrt{(v^2)}$ = 0.00443. This calculation can be applied to the other samples in the same manner.

Table 16: pH value data record using digital PH meter for FHPO & FHPOR

FHPO	trial-1	trial-2	trial-3	Sum	Mean	SD	Mean ± SD	Standard
1st	4.51	4.54	4.57	13.62	4.54	0.03	4.54 ± 0.03	5-6.4
3rd	4.44	4.36	4.45	13.25	4.42	0.049	4.417 ± 0.05	
5th	4.44	4.43	4.42	13.29	4.43	0.01	4.43 ± 0.01	
7th	4.17	4.16	4.18	12.51	4.17	0.01	4.17 ± 0.01	
9th	4.06	4.09	4.07	12.22	4.07333	0.0153	4.073 ± 0.015	
FHPOR	**trial-1**	**trial-2**	**trial-3**	**Sum**	**Mean**	**SD**	**Mean ± SD**	**Standard**
1st	4.68	4.69	4.7	14.07	4.69	0.01	4.69 ± 0.01	5-6.4
3rd	5.77	5.8	5.81	17.38	5.793	0.0208	5.793±0.021	
5th	5.53	5.54	5.56	16.63	5.543	0.0153	5.543±0.015	
7th	5.29	5.22	5.21	15.72	5.24	0.04359	5.24±0.0435	
9th	4.74	4.72	4.72	14.18	4.72667	0.01155	4.727±0.012	

To calculate pH of 1st FHPO using HNNA digital pH-meter, the result in the above table 16 gives as fellow 4.51, 4.54, and 4.57. To calculate standard deviation, standard deviation is the square root of the variance. Variance $(V)^2 = \frac{\sum_{i=1}^{n=3}(x_i - \bar{x})^2}{\cap - \perp}$, & SD $= \sqrt{(v^2)}$ = 0.03. This calculation can be applied to the other samples in the same manner.

Table 17: Viscosity data record using digital viscometer for FHPO & FHPOR

FHPO	trial-1	trial-2	trial-3	FHPOR	trial-1	trial-2	trial-3
1st	67	68	69	1st	60	59	58
3rd	70	70.1	70.2	3rd	54.1	54.2	54.3
5th	71.1	72.3	73.4	5th	50.2	50.3	50.4
7th	77.2	78.1	77.9	7th	48.7	47.5	46.3
9th	79.9	80.1	80.5	9th	45.2	44.8	43.9

To calculate kinematic viscosity using the following equations for example of 1st FHPO: Kinematic Viscosity of oil $(v) = \frac{\eta oil}{\rho oil}$, while ρ_{oil} is density(g/ml) at room temperature (0.889-0.92 which is average density 0.91g/ml), the result gives 73.63, 74.73, and 75.82 mm^2/second. respectively.

FHPO	trial-1	trial-2	trial-3	Sum	Mean	SD	Mean ± SD	Standard
1st	73.63	74.73	75.82	224.18	74.7267	1.095	74.73 ± 1.095	50-60 cP
3rd	76.92	77.03	77.14	231.09	77.03	0.11	77.03 ± 0.11	
5th	78.02	79.34	80.44	237.8	79.2667	1.21167	79.267 ± 1.211	
7th	84.84	85.71	85.5	256.05	85.35	0.45398	85.35 ± 0.454	
9th	87.7	87.91	88.46	264.07	88.0233	0.39247	88.023 ± 0.392	
FHPOR	**trial-1**	**trial-2**	**trial-3**	**Sum**	**Mean**	**SD**	**Mean ± SD**	**Standard**
1st	65.934	64.84	63.74	194.514	64.838	1.097	64.838 ±1.097	50-60 cP
3rd	59.34	59.45	59.56	178.35	59.45	0.11	59.45 ± 0.11	
5th	55.16	55.27	55.38	165.81	55.27	0.11	55.27 ± 0.11	
7th	53.51	52.198	50.88	156.588	52.196	1.315	52.196 ± 1.315	
9th	49.7	49.23	48.13	147.06	49.02	0.80579	49.02 ± 0.806	

To calculate standard deviation, standard deviation is the square root of the variance. Variance $(V)^2 = \frac{\sum_{i=1}^{n=3}(x_i - \bar{x})^2}{\cap - \perp}$, & SD $= \sqrt{(v^2)}$ = 1.095. This calculation can be applied to the other samples in the same manner.

Calculation on chemical properties for FHPO & FHPOR.

Table 18: Peroxide value data record using titration methods for FHPO & FHPOR

FHPO	trial-1	trial-2	trial-3	N $Na_2S_2O_3$	Woil in g	FHPOR	trial-1	trial-2	trial-3
1st	0.51 ml	0.54 ml	0.6 ml	0.1 N	5	1st	0.473 ml	0.46 ml	1 ml
3rd	0.45 ml	0.53 ml	0.65 ml	0.1 N	5	3rd	0.473 ml	0.46 ml	0.33 ml
5th	0.51 ml	0.54 ml	0.71 ml	0.1 N	5	5th	0.385 ml	0.43 ml	0.39 ml
7th	0.71 ml	0.56 ml	0.74 ml	0.1 N	5	7th	0.324 ml	0.33 ml	0.39 ml
9th	0.55 ml	0.6 ml	0.74 ml	0.1 N	5	9th	0.34 ml	0.37 ml	0.33 ml

To calculate peroxide value using the following equations for example, for 1st FHPO: $PV = \frac{\text{Vs x N x 1000}}{\text{Weight of sample (g)}}$, the result gives 10.2, 10.75, and 11.5.

FHPO	trial-1	trial-2	trial-3	Sum	Mean	SD	Mean ± SD	Standard
1st	10.2	10.75	11.5	32.45	10.8167	0.65256	10.8167 ± 0.65	0.1-10
3rd	9.02	10.65	12.95	32.62	10.8733	1.9745	10.8733 ± 1.974	
5th	10.63	10.8	14.1	35.53	11.8433	1.95618	11.8433 ± 1.956	
7th	10.8	11.2	13.8	35.2	11.7333	1.85831	11.733 ± 1.858	
9th	10.9	12	14.8	37.7	12.5667	2.0108	12.567 ± 2.011	
FHPOR	**trial-1**	**trial-2**	**trial-3**	**Sum**	**Mean**	**SD**	**Mean ± SD**	**Standard**
1st	9.9	8.3	8.7	26.9	8.96667	0.83267	8.967 ± 0.833	0.1-10
3rd	9.45	9.2	6.78	25.43	8.47667	1.47466	8.477 ± 1.475	
5th	7.7	8.57	7.75	24.02	8.00667	0.4885	8.0067 ± 0.489	
7th	6.47	6.65	7.8	20.92	6.97333	0.72155	6.9733 ± 0.722	
9th	6.8	7.3	6.5	20.6	6.86667	0.40415	6.867 ± 0.4042	

To calculate standard deviation, standard deviation is the square root of the variance. $\text{Variance } (V)^2 = \frac{\sum_{i=1}^{n=3}(x_i - \bar{x})^2}{\cap - \perp}$, & $SD = \sqrt{(v^2)}$ = 0.65256. This calculation can be applied to the other samples in the same manner.

Table 19: Iodine value data record using titration methods for FHPO & FHPOR

	Volume of blank in ml			Volume of sample in ml				
FHPO	**Vs_1**	**Vs_2**	**Vs_3**	**Vb_1**	**Vb_2**	**Vb_3**	**N of $Na_2S_2O_3$**	**Woil in g**
1st	169	169	172	40.5	41.5	40	0.1N	3g
3rd	175	176	170	45.28	40	39		
5th	170	171	170.5	39.6	39.7	40.5		
7th	172	171	172.5	39.6	39.34	40.57		
9th	172.5	169	171.9	41.5	39.5	39.87		
FHPOR	**Vs_1**	**Vs_2**	**Vs_3**	**Vb_1**	**Vb_2**	**Vb_3**	**N of $Na_2S_2O_3$**	**Woil in g**
1st	175	177	179	60	60.5	59.5	0.1N	3g
3rd	181.5	182.6	183.7	70	69.5	65.5		
5th	188.7	189.5	192	75	76	77.5		
7th	167	168.8	169.5	57	56.5	57.9		
9th	152.7	165.5	162.5	44.5	55.2	54.3		

To calculate Iodine value using the following equations for example of 1st FHPO: $IV = \frac{12.69 \text{ x N x } (V_s - V_b)}{W}$, the result gives 54.99, 57.53, and 55.41.

FHPO	trial-1	trial-2	trial-3	Sum	Mean	SD	Mean ± SD	Standard
1st	54.99	57.53	55.41	167.93	55.9767	1.36152	55.98 ± 1.36	45-55
3rd	56	55.69	55.81	167.5	55.8333	0.15631	55.83 ± 0.156	
5th	55.41	54.99	55.85	166.25	55.4167	0.43004	55.42 ± 0.43	
7th	55.2	55.54	54.99	165.73	55.2433	0.27755	55.24 ± 0.27	
9th	53.51	54.78	55.84	164.13	54.71	1.16658	54.71 ± 1.166	
FHPOR	**trial-1**	**trial-2**	**trial-3**	**Sum**	**Mean**	**SD**	**Mean ± SD**	**Standard**
1st	45.77	46.67	45.77	138.21	46.07	0.51962	46.07 ± 0.52	45-55
3rd	46.53	47.5	47.2	94.7	47.35	0.21213	47.35 ± 0.212	
5th	48.65	49.3	50.55	148.5	49.5	0.96566	49.5 ± 0.965	
7th	47.2	47.84	49.99	145.03	48.3433	1.46152	48.34 ± 1.461	
9th	48.1	48.22	48.434	144.754	48.2513	0.16919	48.25 ± 0.169	

To calculate standard deviation, standard deviation is the square root of the variance. $\text{Variance } (V)^2 = \frac{\sum_{i=1}^{n=3} (x_i - \bar{x})^2}{\cap - \perp}$, & $SD = \sqrt{(v^2)}$ = 0.65256. This calculation can be applied to the other samples in the same manner.

Table 20: Acid value data record using titration methods for FHPO & FHPOR

FHPO	Volume of blank in ml			Volume of sample in ml			N of KOH	Woil in g
	Vs_1	Vs_2	Vs_3	Vb_1	Vb_2	Vb_3		
1st	13	14	15	12	12	12	0.1N	3g
3rd	15.5	16.5	16.5	14	14	15		
5th	19.5	19	24	18	18	22.5		
7th	22.5	23.5	24.2	22	22.5	22.7		
9th	24.7	25.5	26.5	24.2	24.5	25		
FHPOR	Vs_1	Vs_2	Vs_3	Vb_1	Vb_2	Vb_3	**N of KOH**	**Woil in g**
1st	1.4	1.32	1.31	1	0.9	0.9	0.1N	3g
3rd	0.98	1.3	1.4	0.6	0.9	1		
5th	1	1.3	1.3	0.8	0.9	1		
7th	1.1	1.2	1	0.9	0.9	0.8		
9th	1.5	1.3	1.4	1.3	1.2	1.1		

To calculate Acid value using the following equations for example of 1st FHPO: Acid value $\left(\mathrm{mg}\frac{\mathrm{KOH}}{\mathrm{g}}\right) = \frac{\mathrm{Mx\ 56.1\ x\ (Vs-Vb)}}{\mathrm{w}}$, the result gives 1.87, 3.74, and 5.61.

FHPO	trial-1	trial-2	trial-3	Sum	Mean	SD	Mean ± SD	Standard
1st	1.87	3.74	5.61	11.22	3.74	1.87	3.74 ± 1.87	0.6mg
3rd	2.805	4.675	2.805	10.285	3.42833	1.07965	3.43 ± 1.08	
5th	0.935	1.87	2.805	5.61	1.87	0.935	1.87 ± 0.935	
7th	0.935	1.87	2.805	5.61	1.87	0.935	1.87 ± 0.935	
9th	0.935	1.87	2.805	5.61	1.87	0.935	1.87 ± 0.935	
FHPOR	**trial-1**	**trial-2**	**trial-3**	**Sum**	**Mean**	**SD**	**Mean ± SD**	**Standard**
1st	0.687	0.778	0.765	2.23	0.74333	0.04922	0.743 ± 0.0492	0.6mg
3rd	0.711	0.701	0.699	2.111	0.70367	0.00643	0.7036 ± 0.006	
5th	0.374	0.748	0.547	1.669	0.55633	0.18717	0.5563 ± 0.187	
7th	0.374	0.561	0.342	1.2773	0.42577	0.11818	0.426 ± 0.12	
9th	0.374	0.186	0.561	1.121	0.37367	0.1875	0.374 ± 0.188	

To calculate standard deviation, standard deviation is the square root of the variance. Variance $(\mathrm{V})^2 = \frac{\sum_{\mathbf{i=1}}^{\mathbf{n=3}}(\mathbf{x_i}-\bar{\mathbf{x}})^2}{\cap-\perp}$, & SD $= \sqrt{(\mathbf{v^2})}$ = 1.87. This calculation can be applied to the other samples in the same manner.

Table 21: Saponification value data record using titration methods for FHPO & FHPOR

FHPO	Volume of blank in ml			Volume of sample in ml			N of HCl	Woil in g
	Vs_1	Vs_2	Vs_3	Vb_1	Vb_2	Vb_3		
1st	46.4	46.6	47.4	24.5	24.6	25.2	0.5N	3g
3rd	44	42.9	41.5	20.5	20.9	19.5		
5th	45.7	46.2	45.8	23.5	24	23.5		
7th	45.1	45	45.3	23.1	23.1	23.3		
9th	47.02	47	47.1	25	24.9	22.8		
FHPOR	Vs_1	Vs_2	Vs_3	Vb_1	Vb_2	Vb_3	**N of HCl**	**Woil in g**
1st	32.5	31.9	32.6	15.7	14.9	15.5	0.5N	3g
3rd	33.66	32.5	33.5	12.8	11.8	12.5		
5th	37.5	37.46	36.9	15.8	15.7	15.5		
7th	35	36	35.1	14	14.9	13.9		
9th	35.8	36	35.9	16	16.5	16.4		

To calculate saponification value using the following equations for example of 1st FHPO: $SV = \frac{56.1 \ \mathrm{x}\ 0.5\mathrm{NHCl}\ (\mathrm{Vs}-\mathrm{Vb})}{\mathrm{w}}$, the result gives 204.8, 205.7, and 204.8.

FHPO	trial-1	trial-2	trial-3	Sum	Mean	SD	Mean ± SD	Standard
1st	204.77	205.7	204.77	615.24	205.08	0.53694	205.08 ± 0.5369	195-205
3rd	206.64	205.7	205.7	618.04	206.013	0.54271	206.013 ± 0.543	
5th	206.64	207.57	208.51	622.72	207.573	0.935	207.573 ± 0.935	
7th	205.7	204.77	205.7	616.17	205.39	0.53694	205.39 ± 0.54	
9th	207.57	206.64	208.51	622.72	207.573	0.935	207.573 ± 0.935	
FHPOR	**trial-1**	**trial-2**	**trial-3**	**Sum**	**Mean**	**SD**	**Mean ± SD**	**Standard**
1st	157.08	159.89	158.64	475.61	158.537	1.40785	158.537 ± 1.408	195-205
3rd	195.041	193.55	196.35	584.941	194.98	1.40099	194.98 ± 1.401	
5th	202.9	203.5	200.1	606.5	202.167	1.81475	202.167 ± 1.81	
7th	196.4	197.3	198.22	591.92	197.307	0.91002	197.307 ± 0.91	
9th	185.13	182.325	183.26	550.715	183.572	1.42824	183.26 ± 1.43	

To calculate standard deviation, standard deviation is the square root of the variance. $\mathrm{Variance}\ (\mathrm{V})^2 = \frac{\sum_{\mathbf{i=1}}^{\mathbf{n=3}} (\mathbf{x_i} - \bar{\mathbf{x}})^2}{\cap - \perp}$, & $\mathrm{SD} = \sqrt{(\mathbf{v^2})}$ = 1.3706. This calculation can be applied to the other samples in the same manner.

Table 22: Result analysis of CDV for FHPO & FHPOR using UV-Visible spectrometer.

FHPO	trial-1	trial-2	trial-3	Sum	Mean	SD	Mean ± SD	Standard
1st	3.1604	3.0884	3.283	9.5318	3.17727	0.09839	3.1773 ± 0.0984	< 2.25%
3rd	3.2332	3.3708	3.4031	10.0071	3.3357	0.09022	3.3357 ± 0.0902	
5th	3.421	3.315	3.6126	10.3486	3.44953	0.15084	3.44953 ± 0.1508	
7th	4.1538	4.2945	3.6418	12.0901	4.03003	0.3435	4.0300 ± 0.3435	
9th	3.111	3.1051	3.6821	9.8982	3.2994	0.33144	3.2994 ± 0.3314	
FHPOR	**trial-1**	**trial-2**	**trial-3**	**Sum**	**Mean**	**SD**	**Mean ± SD**	**Standard**
1st	0.2867	0.2865	0.2866	0.8598	0.2866	0.0001	0.2866 ± 0.0001	< 2.25%
3rd	0.3942	0.394	0.3943	1.1825	0.39417	0.00015	0.39417 ± 0.0002	
5th	0.483	0.4832	0.4832	1.4494	0.48313	0.00012	0.48313 ± 0.000	
7th	0.5041	0.5043	0.5042	1.5126	0.5042	1E-04	0.5042 ± 0.000	
9th	0.6424	0.6424	0.6427	1.9275	0.6425	0.00017	0.6425 ± 0.0002	

To calculate CDs value using the following equations for 1st FHPO: $\mathrm{CDs} = [\frac{A\lambda_s 230}{bc}]$, where c or concentration of sample =1mL and b or path length of cuvette =1cm, the result gives 3.1604, 3.0884, and 3.283. To calculate standard deviation, standard deviation is the square root of the variance. $\text{Variance } (V)^2 = \frac{\sum_{i=1}^{n=3}(x_i-\bar{x})^2}{\cap-\perp}$, & $SD = \sqrt{(v^2)}$ = 0.09839. This calculation can be applied to the other samples in the same manner.

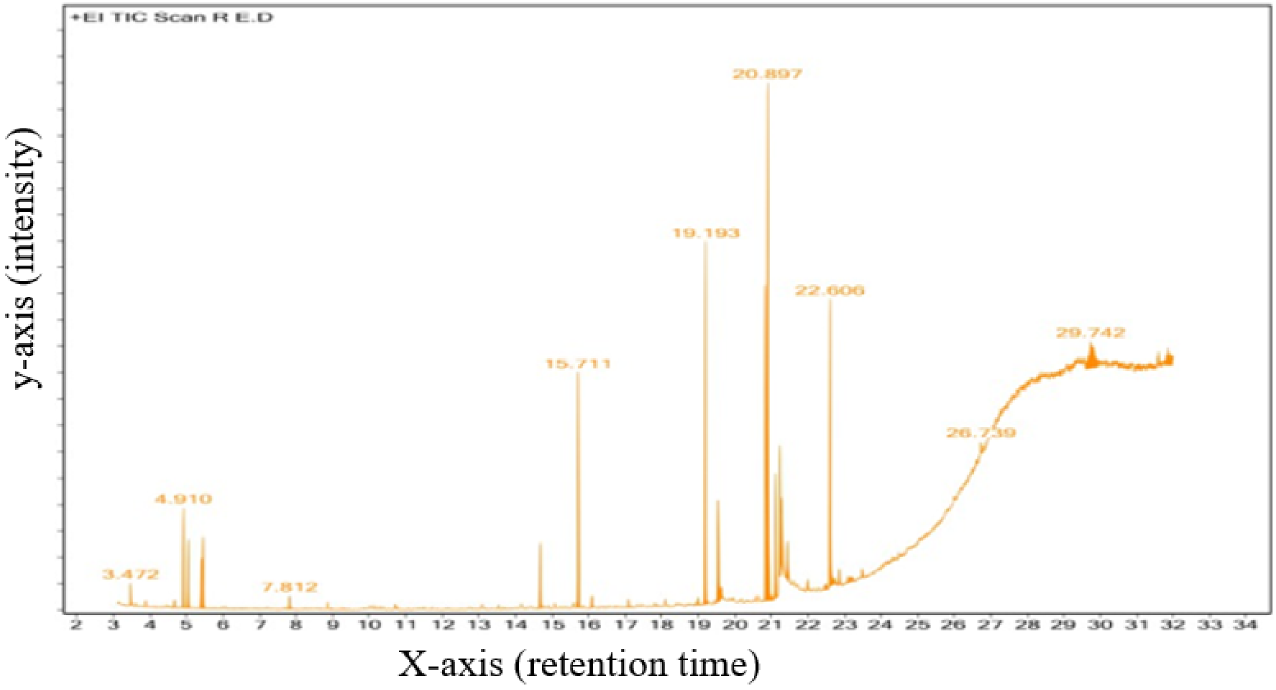

Figure 13: Typical GC-MS total ion mass chromatograms showing the volatile chemicals found in the 99.8% methanolic extracts for extracted rosemary leaves at room temperature.

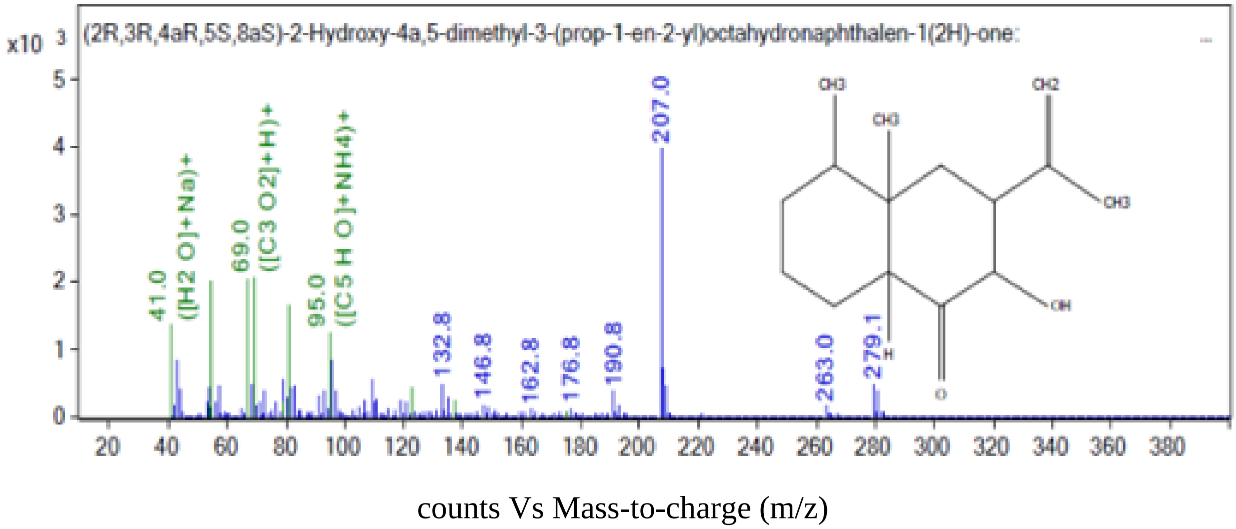

Figure 14: MS (m/z) ratio fragment for (2R,3R,4aR,5S,8aS)-2-Hydroxy-4a,5-dimethyl-3-(prop-1-en-2-yl) octahydronaphthalen-1(2H)-one($C15H24O2$) Compound.

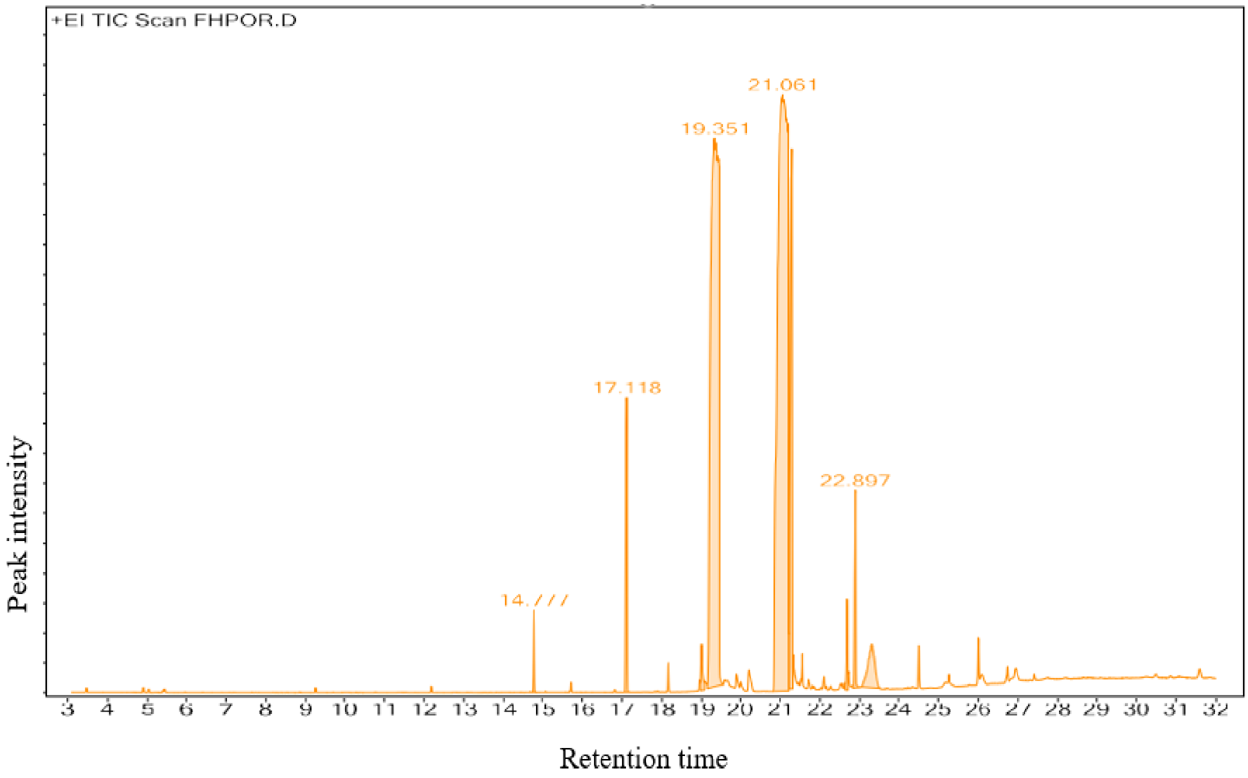

Figure 15: Typical GC-MS total ion mass chromatograms showing the volatile chemicals found in FHPOR at room temperature.

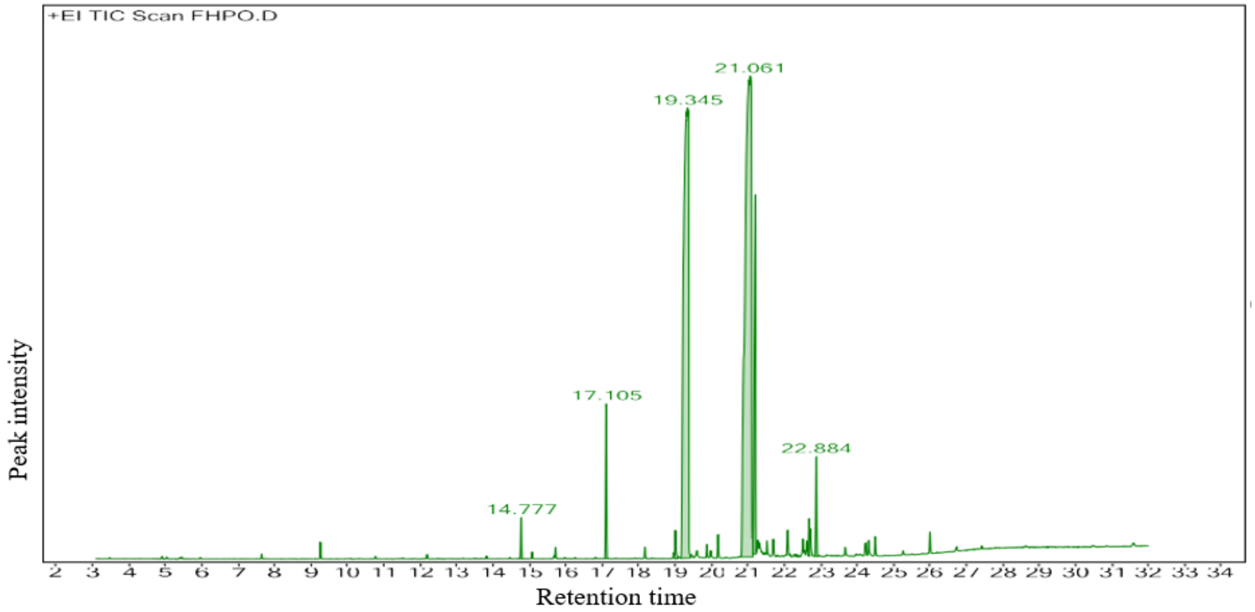

Figure 16: Typical GC-MS total ion mass chromatograms showing the volatile chemicals found in FHPO at room temperature.

Table 23: Result of heavy metals for FHPO & FHPOR using AAS spectrometer.

Fried Hayat palm oil (FHPO)

№	Concentration in ppm	2ppm	5ppm	10ppm	Sum	Mean	SD	Mean ± SD	Standard
1	Lead (µg/ml Pb)	0.07	0.085	0.098	0.253	0.084	0.01	0.084 ± 0.01	0.05
2	Iron (µg/ml Fe)	1.85	1.95	2.04	5.84	1.95	0.08	1.95 ± 0.08	1.5
3	Copper (µg/ml Cu)	0.14	0.15	0.158	0.448	0.15	0.007	0.15 ± 0.007	0.1
4	Cadmium (µg/ml Cd)	0.12	0.129	0.134	0.383	0.13	0.006	0.13 ± 0.006	0.05
5	Arsenic (µg/ml As)	0.55	0.65	0.75	1.95	0.65	0.082	0.65 ± 0.082	0.01
6	Mercury (µg/ml Hg)	0.1	0.15	0.21	0.46	0.15	0.045	0.15 ± 0.045	0.05

Fried Hayat palm oil with rosemary leaf powder (FHPOR)

№	Concentration in ppm	2ppm	5ppm	10ppm	Sum	Mean	SD	Mean ± SD	Standard
1	Lead (µg/ml Pb)	0.04	0.047	0.056	0.143	0.048	0.007	0.048 ± 0.007	0.05
2	Iron (µg/ml Fe)	1.1	1.2	1.4	3.7	1.23	0.125	1.23 ± 0.125	1.5
3	Copper (µg/ml Cu)	0.067	0.09	0.14	0.297	0.099	0.031	0.099 ± 0.03	0.1
4	Cadmium (µg/ml Cd)	0.01	0.02	0.035	0.065	0.022	0.01	0.022 ± 0.01	0.05
5	Arsenic (µg/ml As)	0.006	0.0065	0.0067	0.0192	0.006	0.0003	0.006 ± 0.0003	0.01
6	Mercury (µg/ml Hg)	0.01	0.011	0.013	0.034	0.011	0.001	0.011 ± 0.001	0.05

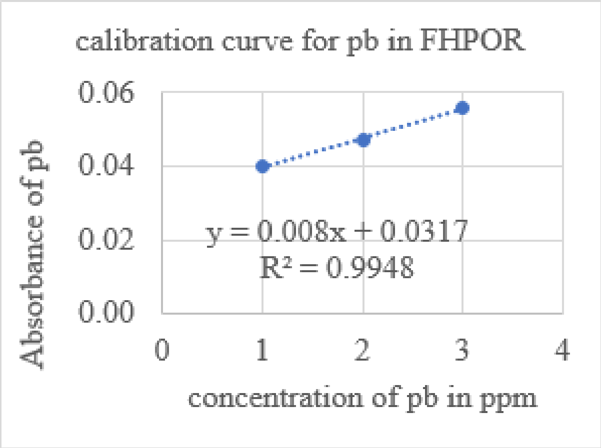
calibration curve for pb in FHPOR
Absorbance of pb
0.06
0.04
0.02
0.00
0
1
2
3
4
y = 0.008x + 0.0317
R² = 0.9948
concentration of pb in ppm

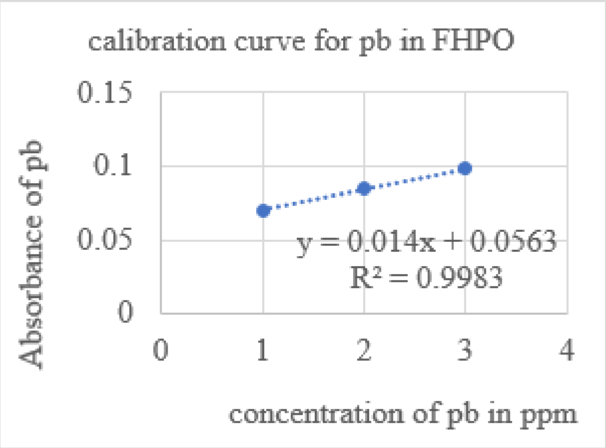
calibration curve for pb in FHPO
Absorbance of pb
0.15
0.1
0.05
0
0
1
2
3
4
y = 0.014x + 0.0563
R² = 0.9983
concentration of pb in ppm

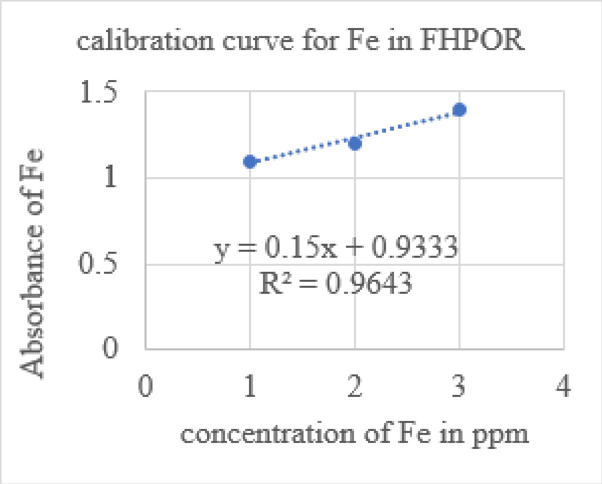
calibration curve for Fe in FHPOR
Absorbance of Fe
1.5
1
0.5
0
0
1
2
3
4
y = 0.15x + 0.9333
R² = 0.9643
concentration of Fe in ppm

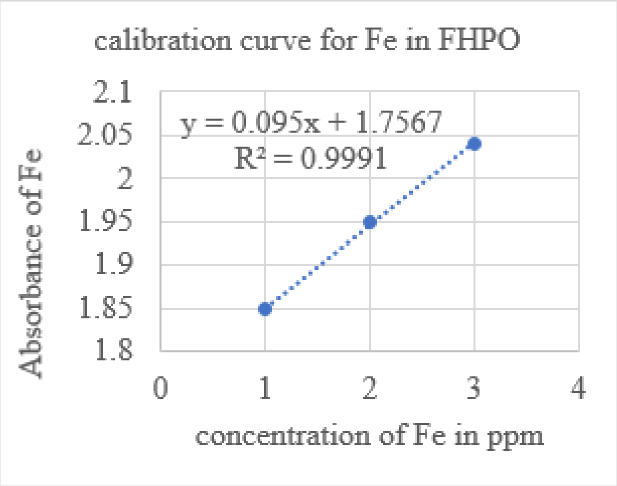
calibration curve for Fe in FHPO
Absorbance of Fe
2.1
2.05
2
1.95
1.9
1.85
1.8
0
1
2
3
4
y = 0.095x + 1.7567
R² = 0.9991
concentration of Fe in ppm

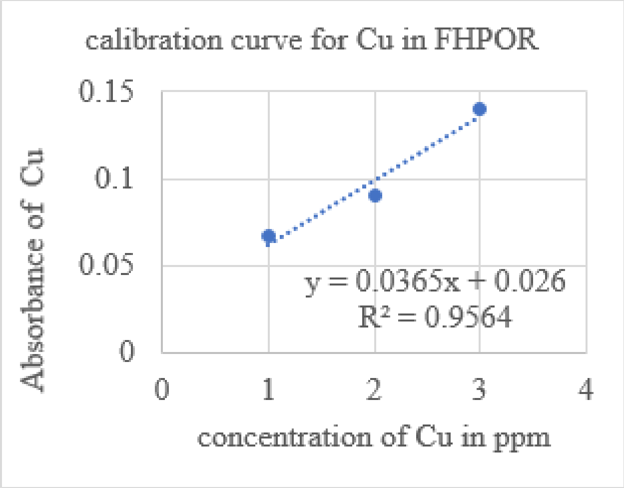
calibration curve for Cu in FHPOR
Absorbance of Cu
0.15
0.1
0.05
0
0
1
2
3
4
y = 0.0365x + 0.026
R² = 0.9564
concentration of Cu in ppm

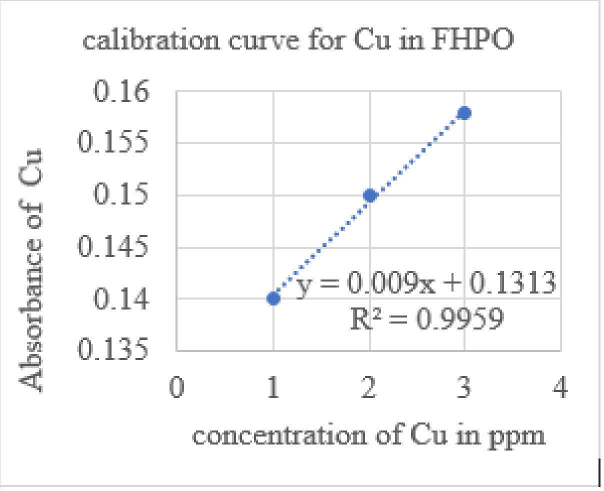
calibration curve for Cu in FHPO
Absorbance of Cu
0.16
0.155
0.15
0.145
0.14
0.135
0
1
2
3
4
y = 0.009x + 0.1313
R² = 0.9959
concentration of Cu in ppm

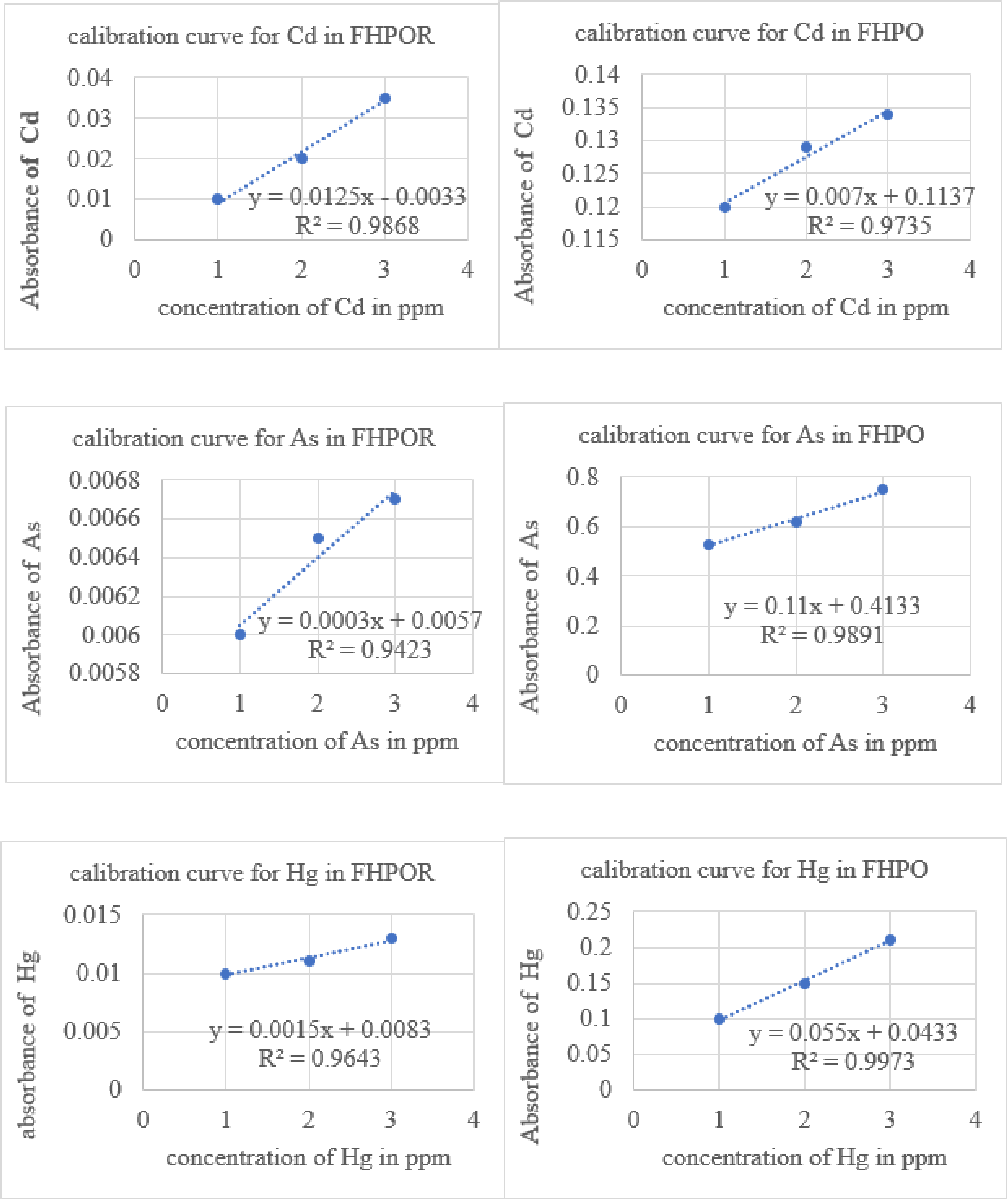

Figure 17: Calibration graphs for all six heavy metals analyzed by AAS.